Regulation of tissue oxygen levels in the ocular lens

Richard McNulty
University of Wollongong

Regulation of Tissue

Oxygen Levels in the Ocular Lens

A thesis submitted in partial fulfilment of the

requirements for the award of the degree of

Doctor of Philosophy

from

University of Wollongong

by

Dr Richard McNulty

B.A., M.B., B.S. (Syd.)

Department of Chemistry

2004

The only use discovered of this work was that

it may help to make a vain man humble

-after Benjamin Franklin

Certification

I, Richard McNulty, declare that this thesis, submitted in partial fulfilment of the requirements for the award of Doctor of Philosophy, in the Department of Chemistry, University of Wollongong, is wholly my own work unless otherwise referenced or acknowledged. The document has not been submitted for qualifications at any other academic institution.

Richard McNulty

6 August 2004

Table of Contents

List of Figures and Tables

Acknowledgements

Thanks to my family for long distance encouragement and support. During this thesis I learnt the true meaning of the phrase "the scientific community." As such, I feel sole authorship is a generous and misleading interpretation of this PhD and I have many people to thank. Numerous colleagues have contributed in various ways to the realization of experiments: Beryl Ortwerth helped with HPLC ascorbate measurements, Richard Mathias and Huan Wang collaborated on the mathematical model, Frank Giblin, Alec Salt and Shane Hale provided guinea pigs, and David Beebe donated human lenses. Helpful advice came from Joseph Bonanno, James Dillon, Tony Hulbert, Ying Bo Shui and Abraham Spector. The Heartland Lion's Eyebank team, especially Kelly Green-O'Neal are thanked for special effort (and cake). Thanks to the team at Trenton Processing, Illinois, for more eyeballs than I can count. Stephen Turney assisted with 2-photon microscopy. Thanks to my lab mum Peggy Winzenburger and to Anna Zandy, my favourite American.

Special thanks must go to Roger Truscott, my long suffering and long distance supervisor. And lastly, but most importantly, to Steven Bassnett, my mentor, friend and stylist, who took a gamble and ensured that the limiting factor in this work was not lack of opportunity or resources: to you, Sire, my humble thanks[1].

---

[1]However, late night deliveries of fish and chips were somewhat lacking.

Publications

Sections of the work described in this thesis have been reported in the following publications:

1. S Bassnett and R McNulty (2003). The effect of elevated intraocular oxygen on organelle degradation in the embryonic chicken lens. J Exp Biol 206, 4353-4361.

2. Richard McNulty, Huan Wang, Richard T Mathias, Beryl J Ortwerth, Roger J W Truscott and Steven Bassnett. Regulation of tissue oxygen levels in the mammalian lens. J Physiol, 2004 (*in press published online July 22, 2004 as 10.1113/jphysiol.2004.068619*).

Abstract

Age-related nuclear cataract is a major cause of blindness and is thought to result from oxidation of key cellular components. Molecular oxygen (O_2) is a possible oxidant in this process. The aim of this thesis was to investigate the regulation of tissue O_2 levels in the ocular lens. We mapped the distribution of O_2 within isolated lenses using a fluorescent optode. All lenses examined (bovine, rabbit and human) showed U-shaped Po_2 profiles across both the optic and equatorial axes resulting in core hypoxia. When equilibrated in physiological conditions (Po_2 environment of 36mmHg), the lens nucleus Po_2 was 1.6 ± 0.5 mmHg (n=6), 12.5 ± 2.5 mmHg (n=6), and 13.8 ± 7.6 mmHg (n=24 pairs) in the bovine, rabbit and human lens, respectively.

We examined a possible role of Po_2 gradients on the development of the embryonic chicken lens. The lens contains two populations of fibre cells, differentiating fibers (DF) in the outer cortex that contain a full complement of organelles (including mitochondria), and mature fibers (MF) in the lens core that do not. Incubating chicken embryos in hyperoxic conditions resulted in larger lenses and an increase in the depth of the DF population compared to lenses from embryos raised in normoxia. This is consistent with the hypothesis that hypoxia triggers the elimination of organelles from the lens.

The consumption of O_2 by the lens was region-dependent. Both respirometric measurements (performed on dissected regions of the bovine lens) and a diffusion/consumption mathematical model showed that approximately 90% of O_2 consumption occurred in the cortex, the remainder occurring in the core which contains only MF. The distribution of mitochondria in the DF layer was mapped using 2-photon or confocal microscopy on living lenses treated with mitochondria-specific dyes (rhodamine

123 or Mito Tracker) and in fixed tissue by immunofluorecence using an antibody to cytochrome *c*-oxidase. The depth of the mitochondria-containing cell layer varied in different species, being 500-760 μm in the bovine lens and 50-100 μm in the human. The Po_2 gradients in the lens extended beyond the boundaries of the mitochondria-containing DF layer, consistent with a role for non-mitochondrial O_2 consumption (albeit a minor one) in the MF region in the intact lens. We therefore examined both mitochondrial and non-mitochondrial processes which may be responsible for modulating lens O_2 levels. Mitochondria-inhibition studies showed that the contribution of oxidative phosphorylation to bovine lens QO_2 was approximately 90%. Interestingly, mitochondria-inhibiting drugs and age had an insignificant effect on human lens QO_2. Ascorbate, found in high levels in the lens, was investigated as an O_2 consumer. Bovine and human lens core O_2 consumption could be induced by metals and inhibited by the metal-chelator DETAPAC, characteristics which are consistent with ascorbate-dependent O_2 consumption. We found no evidence for a role for a trans-plasma membrane oxido-reductase system or photo-oxidation as non-mitochondrial O_2 consumers.

The movement of O_2 through the lens tissue was studied by decreasing lens QO_2. Sub-physiological temperatures resulted in a marked decrease in lens QO_2 and a concomitant flooding of the lens core with O_2. The rapid rise in lens Po_2 at lower temperatures may be of clinical relevance. During vitrectomy, cool, O_2-rich solutions are infused into the eye. We hypothesise that rising lens core O_2 levels during vitrectomy are the cause of the strikingly high incidence of post-vitrectomy nuclear cataract. We have initiated a clinical study to examine whether the use of warmed solutions during surgery can decrease the incidence of post-vitrectomy cataract.

Abbreviations

Abbreviation	Name
±	plus or minus
3D	three-dimensional
α	Bunsen or solubility coefficient (gas volume at STP absorbed per unit volume of liquid)
AAH	artificial aqueous humour
ADP	adenosine diphosphate
ATP	adenosine triphosphate
AREDS	age-related eye disease study
ARNC	age-related nuclear cataract
BSA	bovine serum albumin
CCCP	carbonyl cyanide m-chlorophenylhydrazone
CCD	charge-coupled device
COX	cytochrome *c*-oxidase
$\Delta\Psi_m$	inner mitochondrial membrane potential
DAB	diaminobenzidine
DF	differentiating fibres
D	dioptre
DETAPAC	diethylenetriaminepentaacetic acid
Do_2	diffusion coefficient of O_2
DTPA	diethylenetriaminepentaacetic acid

E	embryonic day
EDTA	ethylenediaminetetraacetic acid
EPR	electron paramagnetic resonance
fMRI	functional magnetic resonance imaging
λ	length constant for O_2 consumption (mm)
G	gauge
GSH	glutathione, reduced
GLUT	glucose transporter
GSSG	glutathione, oxidised
Hb	haemoglobin
hif	hypoxia inducible factor
IgG_{2a}	immunoglobulin G_{2a}
K_m	Michaelis constant
λ	length constant
Mb	myoglobin
MF	mature fibres
mmHg	millimeters of mercury (a unit of gas tension or partial pressure)
MPA	metaphosphoric acid
mRNA	messenger ribonucleic acid
mtDNA	mitochondrial deoxyribonucleic acid
n	number of samples
NAD(P)H	nicotinamide adenine dinucleotide (phosphate), reduced

NMR	nuclear magnetic resonance
NMWL	nominal molecular weight limit
NPA	3-nitropropionic acid
OFZ	organelle-free zone
Pa	Pascal (SI unit of gas tension or partial pressure)
PC	personal computer
Po_2	partial pressure of oxygen or oxygen tension
PBS	phosphate-buffered saline
PET	positron-emission tomography
PMOR	plasma-membrane oxido-reductase system
PMRS	plasma-membrane redox system
ppm	ppm
QO_2	oxygen consumption rate
ROS	reactive oxygen species
RT	real time
SD	standard deviation
STP	standard temperature and pressure (273.15 K or 0°C and 101.325 kPa, 760 mmHg or 1 atmosphere)
SVCT	sodium-dependent vitamin C-transporter
τ	time constant for O_2 consumption (s)
TRIS	tris(hydroxymethyl)aminomethane
UV	ultra-violet

VEGF	vascular endothelial derived growth factor
w/v	weight/volume

Chapter 1:

General Introduction

1.1 Inspiration for the thesis

The inspiration for this thesis was to contribute to a better understanding of the most common cause of blindness in the world: cataract (Brian & Taylor, 2001). In age-related nuclear cataract (ARNC), cytosolic and membrane components are oxidised extensively (A Spector, 1984). The identity of the oxidant(s) responsible for ARNC has not been established unequivocally. Molecular oxygen (O_2) could be the source of the reactive oxygen species (ROS) involved in ARNC (Truscott, 2000). This thesis will investigate the regulation of tissue O_2 levels in the ocular lens. This chapter presents an account of O_2, the ocular lens and cataract and serves as the basis for the later chapters. We will end the chapter with an outline of the thesis based on issues arising from the present discussion.

1.2 Physical and chemical properties of oxygen

Oxygen is a chemical element, symbol O, with atomic number 8 and atomic weight 15.9994. It is a colourless, tasteless and odourless gas weighing 1.429 g/l at standard temperature and pressure (STP = 273.15° Kelvin or 0°C and 1 atmosphere, 101.325 kPa or 760 mmHg). O has three structural forms; O_2, O_3 (ozone), and O_4. O_2 is common molecular oxygen. O_3 is produced from the action of UV-light on O_2, and forms a layer approximately 50 km thick (3 mm thick at STP) in the atmosphere, protecting the earth's surface from harmful UV-rays. O_4 is rapidly decomposed into $2O_2$. There are nine isotopes of O. Naturally occurring O_2 consists of three isotopes; ^{16}O, ^{17}O and ^{18}O. Most O (99.75%) is ^{16}O with only 1:500 atoms being ^{17}O and 1:2000 being ^{18}O. O_2 is 5-10 times more soluble in oil and lipid than in water (Linke, 1965). However, the solubility decreases with increases in temperature, protein concentration or salinity (Lide, 1993). Values for the concentration of

O_2 in solution that are used for calculations in this thesis are presented in Chapter 2, Table 2.1.

O_2 is important because of to its ability to act as an oxidant and the reactivity of the excited and reduced forms of the molecule. Although O_2 gave its name to the process of oxidation, it is not necessarily involved in this type of reaction. Oxidation and reduction refer specifically to the process of transferring electrons between molecules. Oxidation is defined as the loss of electrons (also commonly linked to the gain of O or loss of H) and reduction as the gain of electrons (also commonly the loss of O or gain of H). O_2 can be reduced one, two or four electrons at a time (uni-, bi- or tetra-valently).

The univalent reduction of O_2 gives rise to an important group of molecules called the reactive oxygen species (ROS), also known as reactive oxygen intermediates. They include free radical species such as the superoxide anion ($O_2^{\bullet -}$) and the hydroxyl radical (HO•), as well as non-free radical molecules like hydrogen peroxide (H_2O_2) and singlet O_2 ($^1O_2$). The ROS are important in understanding the oxidative damage caused by O_2. The ROS can be created by various types of chemical reaction, including enzymatic, autoxidation and photosensitisation (Davies & Truscott, 2001; Droge, 2002). The univalent reduction of O_2 catalysed by metals produces $O_2^{\bullet -}$, H_2O_2 and HO• in sequential order (Droge, 2002). However, the bi- or tetra-valent reduction of O_2 can bypass these ROS. In the mitochondrial electron transport chain, for example, O_2 receives four electrons simultaneously at complex IV and is reduced to water (see §1.5).

The common stable form of O_2 is called ground state or triplet O_2 ($^3O_2$)[1]. O_2 has a unique arrangement of electrons which explains some of its unusual properties. O_2 is paramagnetic because of the existence of unpaired (or differing spin) electrons in the outer orbitals. In terms of quantum theory, the Pauli Exclusion Principle dictates that unpaired electrons decrease the probability of O_2 engaging in reactions. However, singlet O_2 ($^1O_2$), an important excited form of O_2, contains outer electrons that are paired in a higher orbital, thus increasing its reactivity. This is the principle behind photosensitisation reactions and fluorescence quenching (detailed in §1.6.2) and is used as the basis for photodynamic therapy. $^1O_2$ can be created by exposing ground state O_2 to either UV-light or to visible light and a photosensitiser. $^1O_2$ has a lifetime in the range of μs before reverting to the ground state form (Vanderkooi *et al.*, 1987; Lide, 1993). It is extremely reactive and can autoxidise without a catalytic metal. Examples of damage caused by ROS are found below in §1.5 and §1.8.

1.3 The origins of O_2

It is traditionally held that the atmosphere of the early earth was composed of hydrogen, methane and ammonia[2]. This notion is based on a comparison with the atmosphere of Jupiter, the composition of which has been deduced from its spectral properties. Since the earth and Jupiter were both created from condensations of dust and gas, it is generally assumed that Jupiter's current atmosphere must be similar to the

[1]In this thesis, "O_2" refers only to ground state O_2.
[2]The reader is referred to an excellent synopsis of this area by Nick Lane "Oxygen: the molecule that made the world" (Lane, 2002). This section is a summary of the classic and novel theories found there.

conditions prevailing on the early earth. An implication of this classic theory is that life began on earth in the absence of O_2. Cyanobacteria (previously known as blue-green algae), were probably the first life-forms to use the sun's energy in photosynthetic processes to create O_2. Therefore O_2 originated as a by-product of cyanobacterial metabolism. Initially, O_2 did not accumulate in the atmosphere because of the combined buffering capacity of the earth's oceans, which held it in solution, and the earth's crust, which reacted with the O_2. Only when the buffering capacity was saturated, did atmospheric levels of O_2 begin to rise to the current levels (Po_2 of ~150 mmHg or 21% O_2). This provided the necessary conditions for the development of aerobic life-forms.

However, evidence gleaned over the past few decades supports a different interpretation. The analysis of rock samples from the moon showed that the earth, which formed 4.5 billion years ago, was bombarded with a meteorite shower for the first 500 million years of its existence. It is possible that any Jupiter-like atmosphere was cleared away in this process. Analysis of the earth's oldest rocks in Greenland revealed that the atmosphere nearly 4 billion years ago contained mostly N_2, with some CO_2 and trace amounts of O_2; an atmosphere one would expect from the volcanic activity known to have been a feature of those early ages.

O_2 most likely came originally from UV-light splitting water into H_2 and O_2. The H_2 floated away into space and the O_2 stayed in the atmosphere where it reacted with rocks and the oceans. The early presence of trace amounts of O_2 means that life may have begun in warm mid-ocean trenches using O_2 for energy. The next key development occurred 4 billion years ago: the advent of photosynthesis. This raised atmospheric O_2 levels due to the

fast rate of O_2 formation, overwhelming the capacity of the ocean and crust buffers to accept O_2. Therefore, early forms of life created the atmosphere necessary for complex aerobic life to blossom.

Rather than the steady rise proposed by the classic theory, the current geological and biological evidence suggests that atmospheric O_2 levels rose in a step-like fashion due to changes in glaciation and plate tectonic activity. Each rise in O_2 was linked with a significant biological development. Evidence from the Hamersly Ranges in Western Australia of biomarkers from cyanobacteria indicates that a burst of eukaryotic activity 2.7 billion years ago coincides with a rise in atmospheric Po_2 levels to 1.5 mmHg (i.e., 1% of the current value). Also, fossil soils and continental red-beds from 2.2 billion years ago indicate a larger rise in atmospheric Po_2 to 7-37 mmHg which is linked to the development of mitochondria. After probably 1 billion years at this level, another rise in O_2 occurred after a series of ice-ages from 750-550 million years ago. This brought the atmospheric Po_2 up to the current level of ~150 mmHg (21% O_2), allowing the Cambrian explosion of multi-cellular life approximately 500 million years ago.

1.4 The history of O_2

Many “eureka” moments in the history of science are accompanied by controversies amongst the scientists involved over the struggle for recognition. The discovery of O_2 is a dramatic example. Set against the backdrop of the French revolution, the characters include Carl Wilhelm Scheele, a meek Swedish apothecary, Joseph Priestley, an English inventor

cum religious dissident, and Antoine Lavoisier, the founding father of modern chemistry (Figure 1.1). Who of these was the first to discover O_2? Most anglophones would say that Joseph Priestley was the first to isolate the gas in 1774. However, this is anathema to Scandinavians who are taught that credit belongs to Wilhelm Scheele who made the discovery two years earlier (Severinghaus, 2002). In addition, one must also acknowledge the role of Antoine Lavoisier who was the first to develop the discovery and realise its significance. In the process he revolutionised our thoughts on combustion and chemistry.

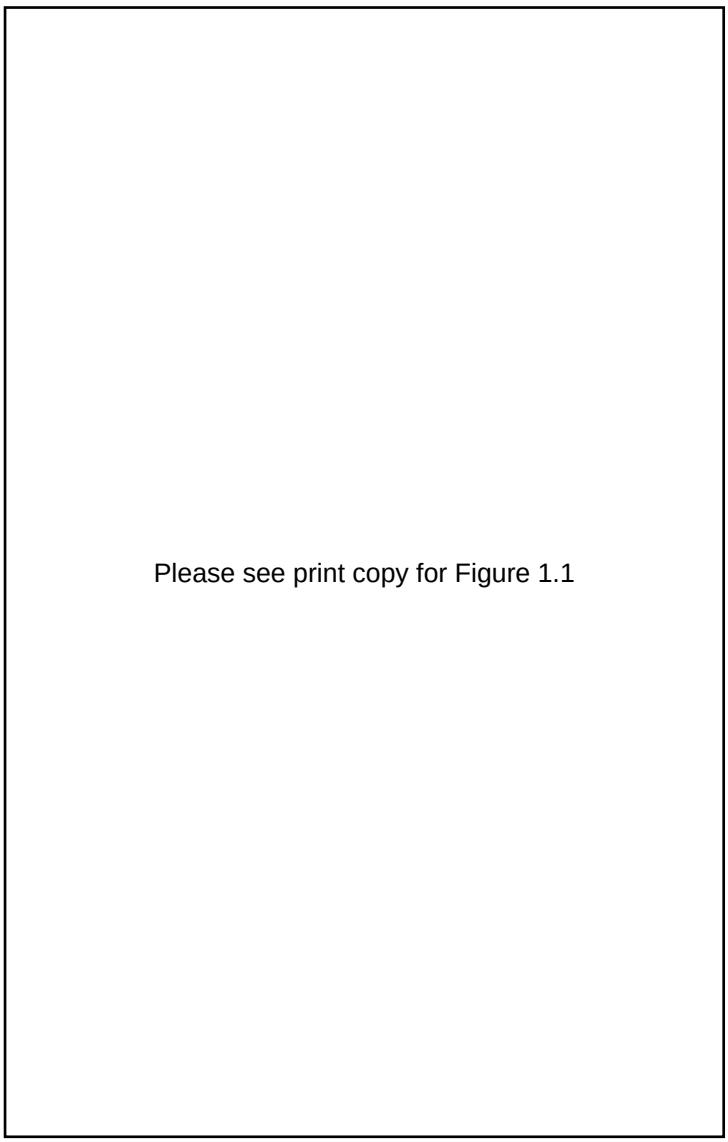

Figure 1.1 *Key thinkers in the discovery of O_2.* ***A.*** *John Mayow. Linked respiration and combustion to parts of air, but did not isolate the gas.* ***B.*** *Joseph Priestley. He is seen stomping on a Bible, a reference to his religious heterodoxy. The flaming papers in his hand could be a symbol of his work on O_2 or to the fact that his laboratory was razed to the ground by zealots.* ***C.*** *Carl Wilhelm Scheele looking forlorn as he awaits a reply from Antoine Lavoisier.* ***D.*** *Lavoisier investigating the nature of O_2, instead of writing to Scheele (Figures from nov.lkg-bp.sulinet.hu, www.chemheritage.org, portrait by Falander and www.fundooz.com respectively).*

To understand the history we must go back to Aristotle (384-322 BC). His theory of the four elements (earth, air, fire and water) from *Physics* dominated intellectual life until the seventeenth century when significant experiments were made by several individuals. John Mayow (1640-1679) showed parts of air were removed by respiration and fire. He placed a mouse or a burning candle in a jar over water and showed that the water level rose over time. The flame was extinguished before all the air was consumed, showing that combustion was dependent on only a part of air. Bayern and Borch, amongst others, prepared O_2 but neither collected nor studied it. However, progress in combustion theory was hindered by the interpretation of results under the prevailing phlogiston theory, initially proposed by JJ Becher and George Ernst Stahl (1660-1734). The theory stated that all things combustible contained the non-material substance *phlogiston* (Greek for "flammable"). An interesting ramification of this theory is that phlogiston must have a negative weight because combustion made most materials lighter. It was not until the eighteenth century that Scottish and English scientists rekindled an interest in experiments involving air. Prior to the discovery of O_2, other gases had already been isolated. Joseph Black, for example, discovered "fixed air" (CO_2) in 1754 by studying the decomposition of chalk. Robert Boyle and Henry Cavendish discovered "inflammable air" (H_2) in 1766 by adding metals to acid. And in 1772, Daniel Rutherford isolated phlogisticated air (N_2).

It is at this time that we encounter the figure most commonly referred to as the discoverer of O_2: Joseph Priestley (1733-1804). Some of his many significant achievements include inventing soda water and India gum, observing photosynthesis, and creating dew from air and H_2. His interest in gases seems to have been sparked from his experience of living next to a brewery. He realised that the gas (CO_2) produced there was heavier than air

and showed that it extinguished lighted wood chips and made water bubble. His first experiments with O_2 were similar to those of Mayow. He placed a plant in water and showed that the gas produced would keep a flame alight and a mouse alive. He isolated O_2 in 1774 by heating mercury oxide. However, he interpreted his results in terms of the prevailing phlogiston theory and called it "dephlogisticated" air. Ironically, even after the work of Lavoisier, he remained a devotee of the phlogiston theory until he died.

However, the accolades for actively producing and isolating O_2 should be given to Carl Wilhelm Scheele (1742-1786). In Uppsala in 1772, two years before Priestley, he isolated O_2 by heating metals. Also, like Priestley, he was unaware of the real significance of the finding and decided to write of the discovery to the already famous chemist Antoine Lavoisier (1743-1794) in Paris. Unfortunately for Scheele, Lavoisier denied ever seeing the letter. Meanwhile, Priestley himself went to Paris to inform Lavoisier of his independent discovery. In an early example of the principle of "publish or perish," Scheele did not release "On air and fire" until 1777, after Priestley and Lavoisier had published their results. Thus Scheele would be denied credit for the discovery for another two centuries until the rediscovery of the letter to Lavoisier. This letter was alluded to by a cataloguer of Lavoisier's work in 1800, but its absence caused later historians to question its existence. Finally, in 1993, the letter was found amongst some artefacts belonging to Madame Lavoisier which were being donated to a museum. This raises the interesting question of whether Lavoisier ever saw the letter. In a recent play about this issue called "Oxygen," Madame Lavoisier hid the letter from her husband to increase his fame (Djerassi & Hoffman, 2001). She repents as Lavoisier is being led to the guillotine and apologises for keeping it secret. Poetic licence aside, we will never know if Lasvoisier saw the letter. One

thing is clear, however: it was Lavoisier who was foremost in elucidating the nature of O_2. He included O_2 as one of his fundamental substances or elements. He created and decomposed water into its elements, showing that, according to his calculations, air was one fourth O_2. He also showed heated metal is heavier because it takes up O_2, and linked combustion with respiration by showing animals consume O_2 and produce CO_2. Initially naming it "eminently respirable air," in 1777 he coined the term "oxygene" ("acid former" from the Greek *oxys*: sharp or acid and *genes*: forming) because he thought that O_2 was necessary for the formation of all acids.

Further characterisations of the properties of O_2 were made by several other scientists. In 1811, Amedeo Avogadro discovered O_2 is a diatomic molecule. In the 1840's Michael Faraday discovered O_2 is magnetic. Nearly 100 years later, with the development of quantum physics, the paramagnetic nature of O_2 was explained by Robert Mulliken who found that it had two unpaired electrons (electrons of differing spins) in its highest orbitals. The transfer of energy due to electrons changing orbitals proved to be the basis of several phenomena. Hans Kautsky in 1931, showed this was the explanation of fluorescence quenching. Herzberg in 1934 explained the formation of $^1O_2$, and Foote and Wexler in 1964 showed it played a role in photo-oxidation by $^1O_2$.

1.5 The roles of O_2

O_2 is the focus of much attention in the geological, ocean and solar sciences. It is the third most abundant element in the sun and may play a role in the creation of solar energy. It comprises 47% of the earth's crust, 89% of the oceans by weight and 20.9% of

the earth's atmosphere by volume. Excited forms of the molecule give rise to the reds, yellows and greens of the aurora borealis (Lide, 1993). In biology, it is regarded as one of the main elements making life possible, along with carbon, hydrogen and nitrogen (Lide, 1993; Banasiak *et al.*, 2000). From a purely anthropocentric viewpoint, O_2 is the *sine qua non* for complex aerobic life-forms like ourselves. Some key cellular processes necessary for aerobic life cease in the absence of O_2 due to a lack of energy. O_2 is also involved in cell death or apoptosis (Banasiak *et al.*, 2000), cell signalling (Droge, 2002), and the control of gene transcription through factors such as hypoxia inducible factor (hif) (Bruick, 2003). There are nearly 60 biological reactions catalogued thus far which use O_2 as a substrate (Vanderkooi *et al.*, 1991). While O_2 and oxidation are clearly essential for aerobic life-forms, they are also the cause of some diseases (possibly including ARNC) and are implicated in the process of ageing (Beckman & Ames, 1998; Lane, 2002). Below we will discuss mitochondrial and non-mitochondrial O_2 consumption, whose possible role in lens O_2 consumption will be the subject of later chapters.

1.5.1 Mitochondria and oxidative phosphorylation

Mitochondria are membrane-bound intracellular organelles found in nearly all eukaryotes. Fossil evidence indicates the existence of mitochondria in two-billion-year-old eukaryotic cells (Lane, 2002). Mitochondria are generally accepted to have originated from prokaryotes that developed a symbiotic relationship with eukaryotes. The main role of mitochondria is to provide the bulk of cellular energy in the form of ATP and, as such, they are commonly referred to as the powerhouses of the cell. The proportion of cellular O_2 consumption attributed to mitochondria ranges from 50-90% (Kessler, 1973; Sastre *et al.*, 2000). Since mitochondrial oxidative phosphorylation and O_2 consumption may decrease

with age (Beckman & Ames, 1998; Hagen *et al.*, 1998), we will examine the effect of age on lens QO_2 and tissue O_2 levels in this thesis.

The production of ATP via oxidative phosphorylation occurs on the inner membrane of the mitochondria (Figure 1.2). A series of enzyme complexes in the membrane acts as an electron transport chain (Figure 1.3). As each electron is passed along the chain, a proton is pumped out across the inner mitochondrial membrane, forming a proton gradient. The electrons are ultimately donated to O_2, forming water. Each of these complexes can be inhibited pharmacologically, allowing for an examination of the role of mitochondria in regulating lens O_2 levels.

An ATP synthase uses the proton gradient to phosphorylate ADP and create ATP. Oxidative phosphorylation is an efficient way of making cellular energy from glucose. Anaerobic glycolysis produces only 2 ATP net from each molecule of glucose whereas aerobic oxidative phosphorylation produces 36 ATP net.

Recently, other significant roles have been attributed to mitochondria. Cytochrome *c*-release from mitochondria is an important trigger of apoptosis, and complex II has been implicated in tumour suppression and cellular O_2-sensing (Duchen, 1999). More importantly, mitochondria are the main producers of ROS in cells (Brand, 2000). Perhaps 0.1-2% of O_2 is utilised inefficiently by the electron transport chain, resulting in $O_2^{\bullet-}$ production (Boveris & Chance, 1973; Chance *et al.*, 1979; Fridovich, 2004). All cells produce $O_2^{\bullet-}$ in the range of 4-7 nmol/min/mg protein, which may be the most important source of $O_2^{\bullet-}$ in cells (Droge, 2002).

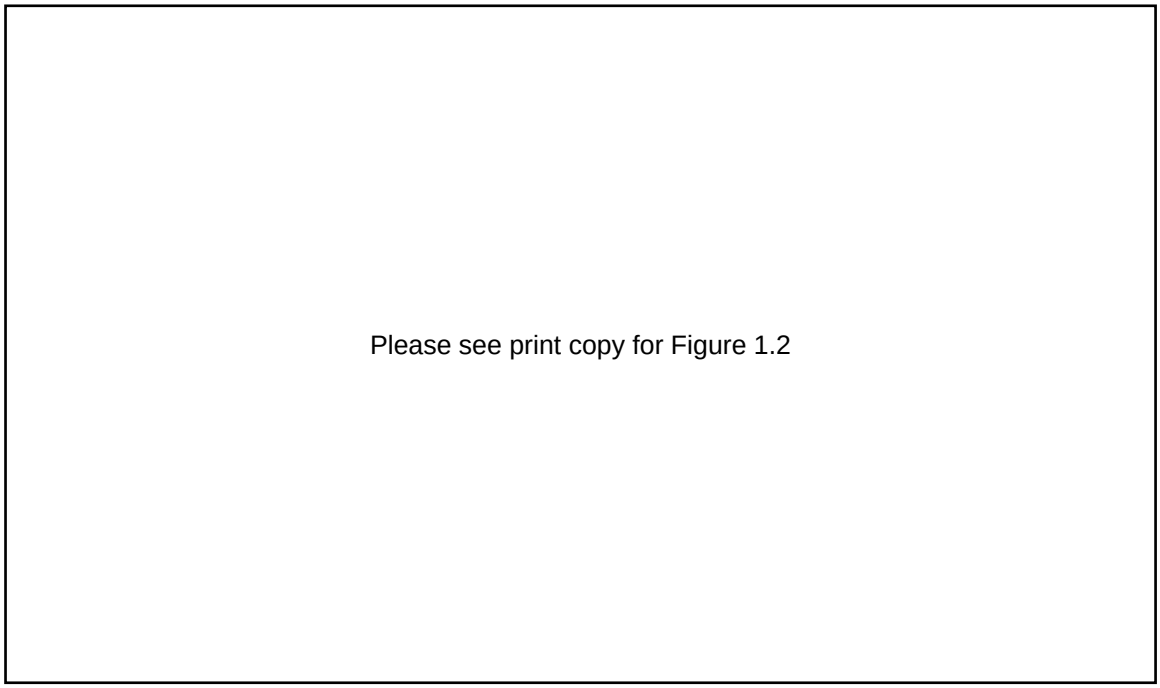

Figure 1.2 *Mitochondrial morphology.* ***A.*** *The well known cross-sectional shape of a mitochondrion visualised by electron micrography, showing highly convoluted inner membrane folded into christae (arrowheads). However, these cross-sectional images do not reveal the overall shape of mitochondria.* ***B.*** *A high-voltage electron micrograph of snail epithelial cells reveals mitochondria as branching, elongated structures (arrows) (Figures modified from Alberts et al, 1994).*

Figure 1.3 *Mitochondrial oxidative phosphorylation enzymes. The system consists of an electron transport chain (complexes I-IV) and an ATP-synthase (complex V) located in the inner membrane of the mitochondrion. As electrons pass from one complex to the next, a proton is pumped into the lumen between the inner and outer mitochondrial membranes, forming a gradient.* O_2 *is the terminal electron acceptor at complex IV, resulting in the formation of water. The proton gradient is used by complex V (ATP-synthase) to create ATP. In this way,* O_2 *consumption is linked to creation of cellular energy (modified from Shoubridge, 2001).*

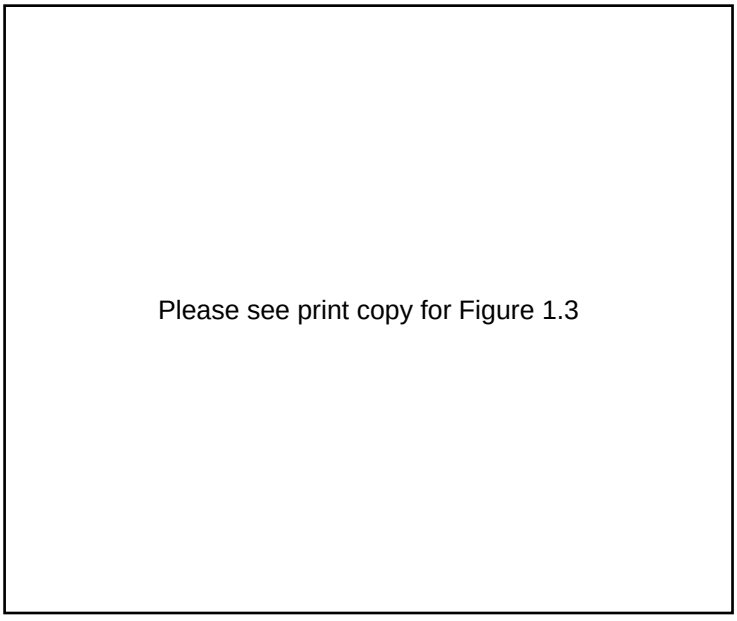

There is some evidence that oxidant production increases with age (Sohal *et al.*, 1994), possibly due to cytochrome *c*-oxidase (COX or complex IV) of the respiratory chain becoming increasingly inefficient (Droge, 2002). With age, COX utilisation of O_2 decreases, which is paralleled by lower electron consumption by the electron transport chain, resulting in more electrons available for $O_2^{\bullet -}$ production (Droge, 2002). Mitochondrial dysfunction can lead to increased $O_2^{\bullet -}$ production, as is the case in Complex I deficiency (Pitkanen *et al.*, 1996). It is worth noting that mitochondrial dysfunction is also linked with cataract formation (§1.8). The role of mitochondria in regulating O_2 levels in the lens will be addressed in this thesis.

1.5.2 Non-mitochondrial O_2 consumption

In some cells, non-mitochondrial O_2 consumption can account for a significant fraction (10-20%) of total O_2 consumption (Rolfe & Brown, 1997). Therefore, as well as oxidative phosphorylation, non-mitochondrial O_2 consumption in the lens will be examined in this thesis. Candidate O_2 consumers in the lens include ascorbic acid (vitamin C), photo-oxidation and trans-plasma membrane oxido-reductase (PMOR) systems. An introduction to these O_2 consumers follows.

i. Ascorbic acid (ascorbate) is a water soluble, colourless molecule abundant in fruits and vegetables such as cabbage, broccoli, capsicum and tomatoes. Ascorbic acid exists in two physiological forms: ascorbate, the reduced form, and dehydroascorbate, the oxidised form (Carr & Frei, 1999) (Figure 1.4).

Figure 1.4 *Structure of ascorbic acid. The reduced form, ascorbate, is shown on the left (A) and the oxidised form, dehydroascorbate, on the right (B).*

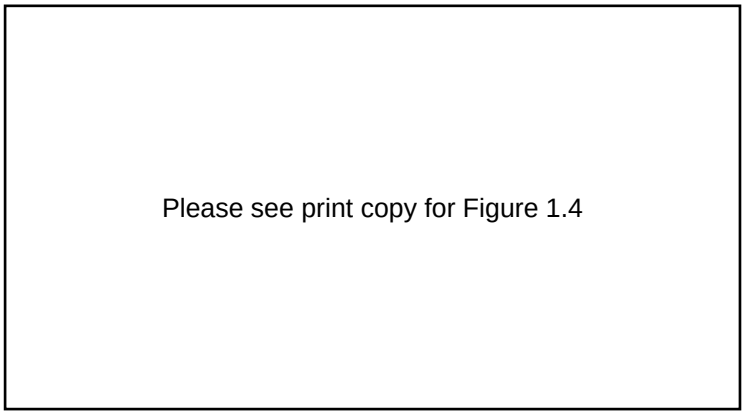

The accumulation of ascorbic acid into cells is mediated by two distinct families of transporters. The sodium dependent vitamin C transporters (SVCT1 and 2) utilise the sodium gradient to move ascorbate into cells. Dehydroascorbate, however, is transported by the facilitated diffusion glucose transporters (GLUT 1, 2 and 4) (Liang *et al.*, 2001). The mRNA of SVCT2 was found in human foetal lenses and in cultured human lens epithelial cells, suggesting a role for SVCT2 in the human lens (Kannan *et al.*, 2001).

Since ascorbate was first isolated by Szent-Gyorgzi in 1928 (Szent-Gyorgi, 1928), a number of physiological functions have been identified. The reduced form is a cofactor keeping transition metals reduced in enzymatic reactions (Smirnoff, 2000). Other metabolic roles include regulation of iron uptake, stabilisation of collagen, biosynthesis of neurotransmitters, and transcriptional regulation (Toth *et al.*, 1995; Halliwell, 2001). Ascorbate is also the most important water soluble anti-oxidant in plasma (Frei *et al.*, 1989). The importance of ascorbate in the eye is suggested by the high concentrations found there. In diurnal species like humans, ascorbate is actively concentrated in the lens and aqueous humours. Concentrations in the eye are higher than in the plasma, reaching millimolar levels in the human lens (Garland, 1991). Of particular relevance to lens physiology and cataract is the ability of ascorbate to act as a free radical scavenger

(Garland, 1991). This finding leads to the hypothesis that high levels of ascorbate in diurnal species serve to protect tissues from the effects of solar irradiation (Reiss *et al.*, 1986; Koskela *et al.*, 1989).

Whether ascorbate helps prevent cataract has been a topic of debate for many years. Early monographs on scurvy claimed there was a link between scurvy and cataract (Hood & Hodges, 1969). Scurvy is the clinical condition of acute ascorbate deficiency famously seen in sailors on long sea voyages in previous centuries. The disease usually manifests as connective tissue anomalies such as bleeding gums and joints (haemarthrosis), and swollen tissues (oedema). Contrary to the initial reports, later scientific studies noted comparatively few ophthalmic manifestations of scurvy and the link to cataract was not confirmed (Hood & Hodges, 1969). However, the relevance of ascorbate to the prevention of cataract may be over the long term, rather than the short term. The evidence comes from retrospective surveys of dietary habits. It was found that people who had a high ascorbate intake, especially those taking supplements for more than 10 years, had a decreased risk of nuclear cataract formation (Taylor & Hobbs, 2001). Unfortunately, the ability of ascorbate supplements to prevent cataract was not confirmed in more recent prospective placebo controlled trials (see §1.8).

In this study, the possible role of ascorbate as an O_2 consumer in the lens will be investigated. Ascorbate, in the presence of redox active metals (e.g., iron or copper) or light and a photosensitiser (e.g., riboflavin), rapidly oxidises to dehydroascorbate and consumes O_2 in the process (Figure 1.5). Dehydroascorbate may be converted back to ascorbate through the glutathione redox cycle (Wolff & Spector, 1987; Eaton, 1991). In turn,

reduced glutathione is regenerated in the surface layers of the lens via the action of glutathione reductase or NADPH (the ultimate source of the latter being hexose monophosphate shunt activity) (Eaton, 1991). This linked series of reactions provides a plausible pathway by which metabolic activity near the surface of the lens could facilitate non-mitochondrial O_2 consumption in the centre of the tissue. In light of its ability to consume O_2, it has been hypothesised that ascorbate oxidation in the aqueous and vitreous humours lowers Po_2, which helps prevent oxidative damage to the lens (Eaton, 1991). In Chapter 2, this idea is extended to encompass the possibility that ascorbate may consume O_2 in the lens itself.

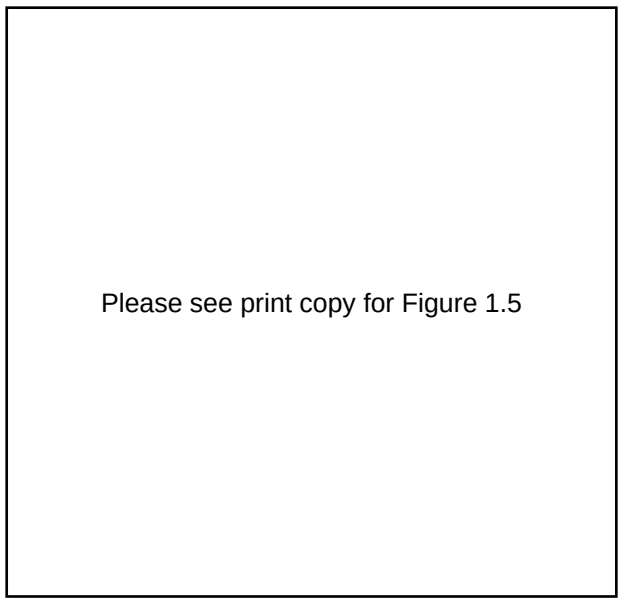

Figure 1.5 *The glutathione (GSH) redox cycle and ascorbic acid. The cycle provides a plausible mechanism by which ascorbic acid may consume O_2 in the lens. Ascorbic acid can be oxidised to dehydroascorbate (DHA) in the presence of redox active metals or light and a photosensitiser. O_2 is consumed in this process. The reducing power of GSH could be used to convert ascorbic acid back to its reduced state, producing oxidised GSH (GSSG). The enzyme GSH-reductase regenerates the reduced form of GSH. (modified from Eaton,1991).*

To test the role of ascorbate as an O_2 consumer, we will utilise a guinea pig model. The guinea pig is a well established animal model for studying the effects of ascorbate deficiency. Most vertebrates can synthesise ascorbate from hexose sugars (Burns, 1959). However, for primates, fruit bats and guinea pigs, ascorbate is an essential dietary requirement. This has been the case in humans for perhaps 150,000 years, when the ability to synthesize ascorbic acid was lost due to the accumulation of mutations in the gene for L-

gulono-γ-lactone oxidase, an enzyme in the pathway from glucose to ascorbate (Nishikimi & Yagi, 1991).

ii. Trans-plasma membrane oxido-reductase (PMOR) system. PMOR is a member of an expanding family of trans-plasma membrane electron transporters, also known as plasma membrane redox systems (PMRS). PMRS are membrane redox systems which have many and diverse cellular functions (Ly & Lawen, 2003). For example, constitutive NADH-oxidase plays a role in cell growth and enlargement. NADH-diferric transferrinreductase (DCT1) is involved in iron uptake. NADPH oxidase of sperm is needed for fertility. NADH:ascorbate free radical oxidoreductase and NADH:ubiquinone oxidoreductase protect against ROS. PMOR is a complex containing at least two enzyme functions: namely, NADH-oxidase and ferricyanide-reductase activities (Ly & Lawen, 2003). PMOR transfers electrons from cytoplasmic NADH to extracellular electron acceptors such as O_2, ferricyanide, transferrin and ascorbate (Ly & Lawen, 2003). Although its main role may be in cell redox homeostasis (Ly & Lawen, 2003), PMOR has been shown to consume O_2 in some cell types. In cells lacking oxidative phosphorylation due to an absence of mtDNA (called ρ^0 cells), O_2 consumption due to PMOR accounted for 13% of the value of control cells (Shen *et al.*, 2003). The presence of PMOR in the ocular lens has not been established to date. In this thesis, we will treat lenses with NADH (Berridge *et al.*, 2002) and PMOR-inhibiting drugs such as capsaicin (Hail, Jr. & Lotan, 2002) to assess the potential contribution of the PMOR system to lens O_2 consumption.

iii. Photo-oxidation. Since the lens is frequently exposed to light, it is conceivable that O_2 could be consumed in photo-oxidative reactions. Light can interact with protein-

bound or other chromophores, converting them to excited forms. O_2 receives the energy from the excited forms, converting it to the highly active singlet oxygen ($^1O_2$). $^1O_2$ can engage in chemical reactions with proteins (called Type 2 reactions) resulting in indirect oxidation of the protein and consumption of O_2 (Davies & Truscott, 2001). Furthermore, as discussed in §1.5i, O_2 is consumed in the process of ascorbate oxidation in the presence of light and photosensitisers like riboflavin (Eaton, 1991). In the next chapter, the effect of light on lens QO_2 and Po_2 will be investigated.

1.6 Oximetry

The amount of dissolved O_2 present in a sample can be expressed in various forms. For instance, the amount of O_2 in the atmosphere can be articulated in relative terms such as 20.9% or 209 000 parts per million (ppm). O_2 levels can also be expressed as a unit of pressure. Po_2, the partial pressure of O_2, refers to the amount of pressure due to O_2 alone. The SI unit of pressure is the Pascal (Pa), which is 1 Newton/m^2. One Pa of pressure "is the same push that butter exerts on sliced bread" (Simpson, 1989). However, Po_2 is more commonly expressed in mmHg, referring to the height of a column of Hg in a vacuum that can be supported by the gas. To illustrate this, again using the atmosphere as an example, the atmospheric pressure at sea level is 760 mmHg, of which about 40 mmHg is due to H_2O vapour pressure, leaving 720 mmHg for gases, therefore atmospheric Po_2 is 0.209 x 720 ≈ 150 mmHg.

Although O_2 is soluble, it is the Po_2 rather than the concentration of O_2 that is the parameter most often measured in oximetry of solutions or tissues. However, Po_2 does not

directly indicate the absolute amount of O_2 present in the sample. The Po_2 and $[O_2]$ are related by the solubility co-efficient α:

$$[O_2] = \alpha \cdot Po_2$$

In practice, it is difficult to determine α, hence the preferred use of Po_2.

The techniques used to measure O_2 vary in the specific parameter detected such as Po_2, the concentration of O_2, saturations of haemoglobin (Hb) or myoglobin (Mb), or the oxidation-reduction (redox) state of molecules (Swartz & Dunn, 2003). Some techniques that could theoretically be applied to the lens, such as functional magnetic resonance imaging (fMRI) or positron-emission tomography (PET) scanning, currently lack the necessary sensitivity or spatial resolution for lens oximetry. Other modalities, including infrared monitoring of Hb saturation, proton-NMR spectroscopy of Mb and NMR "BOLD" effect, depend on the presence of a blood supply, and are therefore unsuitable for lens oximetry (Swartz & Dunn, 2003). In the following section, practicable approaches for measuring Po_2 within the lens will be considered in detail.

1.6.1 Polarography

The most common way to measure Po_2 is the polarographic technique using Clark-style electrodes (Figure 1.6) (Swartz & Dunn, 2003). Polarography is so named because of the constant voltage held across two electrodes. Redox reactions occur at the electrode tips giving rise to a current. The reactions occur at a rate proportional to the Po_2 at the electrode tip.

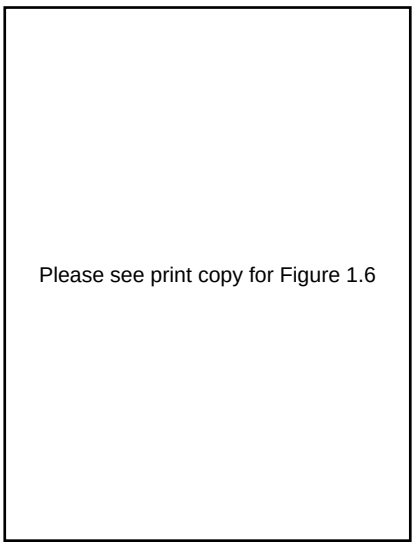

Figure 1.6 *Diagram of a Clark style micro-electrode tip. O_2 diffuses to the tip and engages in redox reactions, creating a current that can be correlated to Po_2 (model 723, Diamond General Corp., Ann Arbor, MI, USA).*

The electrodes consist of a Pt cathode and an Ag anode, surrounded by an electrolyte solution encased in glass. In Clark-style electrodes, the two electrodes are combined into one instrument. The Pt cathode supplies electrons for the reduction of O_2:

$$4H^+ + 4\bullet^- + O_2 \rightarrow 2H_2O$$

O_2 is converted to water and thus consumed in the process. The reaction at the anode is oxidative:

$$4Ag + 4Cl^- \rightarrow 4AgCl + 4\bullet^-$$

When approximately –1.0 V is held across the electrodes, the current produced is proportional to the rate of diffusion of O_2 to the cathode. The standard curve shows the linear relationship between current and Po_2 (Figure 1.7). A meter converts the current detected in the sample to a voltage and amplifies this to a recording device, usually a strip-chart recorder, to monitor Po_2 over time.

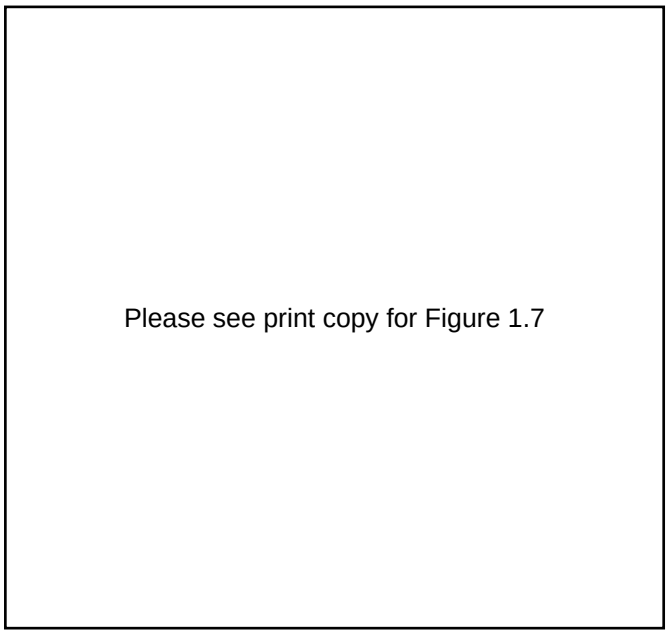

Figure 1.7 *Polarographic standard curve. A Clark electrode was placed in solutions of known Po_2. The current generated shows a linear correlation with Po_2 (modified from chemical microsensor 1201 operating manual, Diamond General Development Corp., Ann Arbor, MI, USA).*

Limitations of the technique include a decrease in sensitivity by protein deposition, H_2S, and sulphydryl poisoning (Silver, 1973; O'Riordan *et al.*, 2000) and silver ion migration causing signal drift (Zhao *et al.*, 1999).

More importantly, the consumption of O_2 in the measurement process necessitates that the solution be well stirred to constantly replenish O_2 at the electrode tip. This can affect readings, especially in the presence of protein, which may attach to the electrode and change the surface area of the tip (operating manual, model 723 micro-electrode, Diamond General Corp., Ann Arbor, MI, USA). The human lens contains 30-38% protein by weight (Fagerholm *et al.*, 1981), and is therefore not an ideal, well stirred solution.

The effect of protein on electrode measurements calls into question the suitability of using electrodes for Po_2 measurements in the lens. To address this issue, we tested a Clark-style micro-electrode (model 723, Diamond General Development Corp., Ann Arbor, MI, USA) in solutions containing various concentrations of BSA (Figure 1.8). A voltage of -0.76 V was applied to the electrode. Calibration was performed in a solution of PBS

gassed with air (Po_2 of 150 mmHg or 21% O_2). Protein solutions of 0-50% w/v were prepared and equilibrated with air. Although the solutions presumably had the same Po_2, the electrode current decreased with increasing protein concentrations up to 20% and was stable thereafter. The results suggest that Clark-style electrodes may be unreliable in tissues with a high concentration of protein, like the lens. A further impediment to calibration of electrodes in the lens is that the concentration of protein varies with lens depth (Fagerholm *et al.*, 1981). For these reasons, we will utilise the novel technique of a fluorescent optode for measuring lens Po_2 in this thesis.

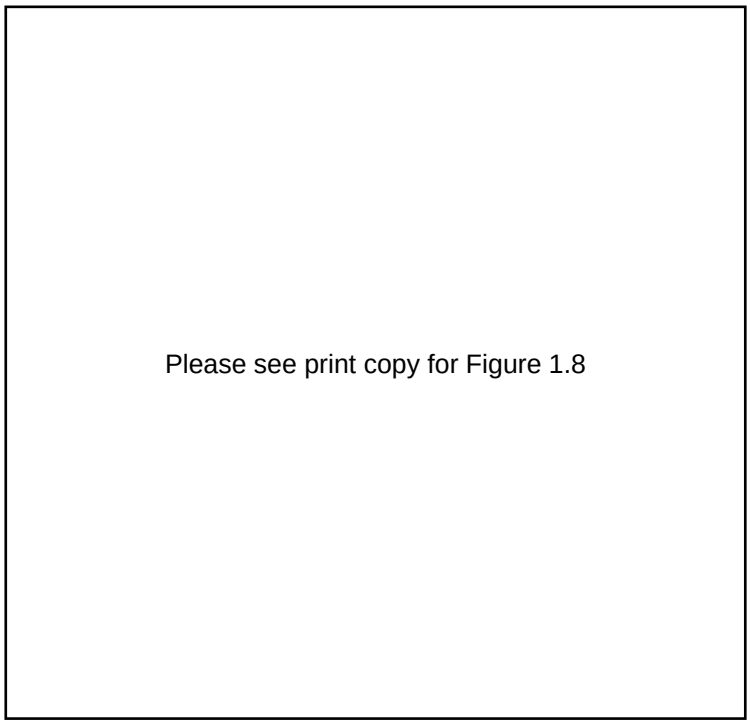

Figure 1.8 *The effect of protein concentration on electrode readings. A Clark-style micro-electrode (model 723, Diamond General Development Corp., Ann Arbor, MI, USA) was placed in solutions of normal saline containing 0-50% w/v BSA equilibrated with atmospheric levels of O_2 (Po_2 of 150 mmHg or 21% O_2). The current produced at the electrode tip (used to indicate the Po_2) decreased sharply with increased protein concentration up to ~20% and then stabilised thereafter. This shows current may not be calibrated to Po_2 at high protein concentrations.*

Electrodes are not only utilised to make spot measurements in tissues and solutions, but can also be incorporated into respirometers to measure Po_2 over time. In respirometry, a sample is immersed in solution with a known level of O_2 in a closed chamber. An electrode placed into the chamber reports the Po_2 of the solution over time and the $\Delta Po_2/\Delta t$ is used to calculate the O_2 consumption rate (QO_2) of the sample. Respirometry will be used to determine lens QO_2 in later chapters.

1.6.2 Fluorescence and phosphorescence quenching

Luminescence, of which fluorescence and phosphorescence are types, is the ability of a molecule to be excited by one wavelength of light (excitation wavelength) and release this energy as light of a different wavelength (emission wavelength) when returning to its stable state. The laws of quantum mechanics dictate that the emission wavelength is always longer than the excitation wavelength. Fluorescence does not stop immediately when excitation ceases, but rather decays over μs as shown in Figure 1.9. Phosphorescence, however, commences after a longer post-excitation period and has a longer lifetime decay (up to ms).

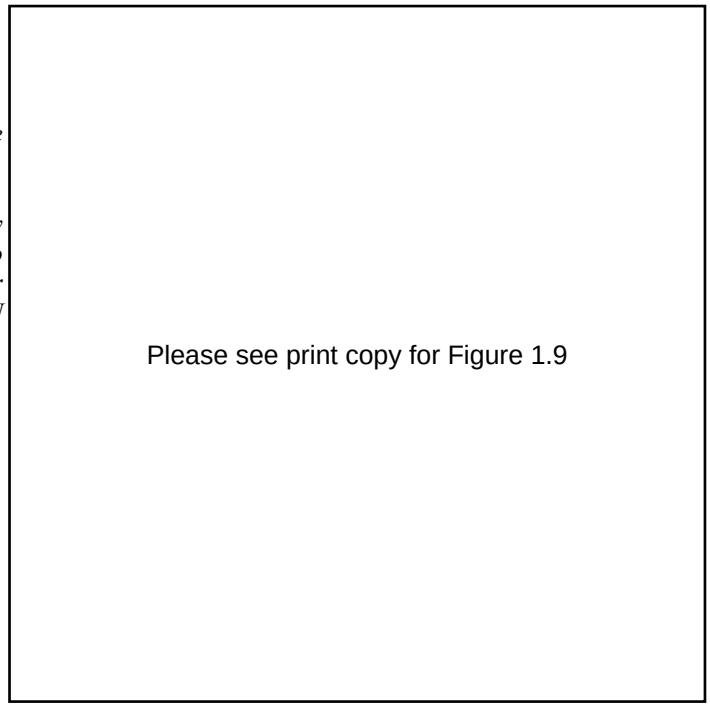

Figure 1.9 *Graph of fluorescence lifetime decay. After excitation ceases (time=0), fluorescence intensity decays over μs. Measurement of fluorescence intensity decay over time (Δt) can be used to calculate* Po_2 *via the Stern-Volmer equation (see text). Modified from (U Wang, Coleman, Minang, 1991).*

O_2 "quenches" the fluorescence of an excited molecule by receiving its energy, thereby sending O_2 into an active state and diminishing the fluorescence of the original molecule. Thus, the intensity and the lifetime decay of a molecule's fluorescence is at its maximum in the absence of O_2, decreases in the presence of O_2 and is at its minimum in 100% O_2.

The fluorescence intensity and lifetime is related to the concentration of O_2 via the Stern-Volmer equation:

$$T_o /T = I_o /I = 1 + k.[O_2]$$

Where:

- T_o is the fluorescence lifetime in the absence of O_2.
- T is the fluorescence lifetime at the given $[O_2]$.
- I_o is the fluorescence intensity in the absence of O_2.
- I is the fluorescence intensity at the given $[O_2]$ and
- k is the Stern-Volmer quenching constant.

The ability of O_2 to influence fluorescence in a well defined manner has lead to the development of techniques which use fluorescent molecules as O_2-sensors. Both fluorescence intensity and lifetime decay have been used in oximetry. However, the interpretation of intensity measurements has been shown to be problematic. Fluorescence intensity is dependent on O_2-sensor concentration and absorption of emitted light by the tissue. Furthermore, washout or leakage of the O_2-sensor and photobleaching affect calibration and sensitivity. On the other hand, fluorescence lifetime is considered to be independent of O_2-sensor concentration (Lakowicz *et al.*, 1992). Importantly, fluorescence oximetry does not significantly change the concentration of O_2 in the tissue (Vanderkooi *et al.*, 1987).

Both endogenous and exogenous molecules have been used as O_2 sensors. Utilising the fluorescence of intracellular molecules such as pyridine nucleotides and flavoproteins avoids the introduction of an exogenous sensor into tissues. However, calibration of endogenous fluorescence is difficult and often reflects the redox state of the cell rather than

the absolute Po_2 (Chance *et al.*, 1962). Therefore, it is usually necessary to use exogenous fluorophores to report Po_2. The structure of both fluorescent and phosphorescent O_2-sensors is a transition metal-organic ligand complex. Fluorescent sensors are typically Ru-based compounds and phosphorescent sensors are Pd-based derivatives of porphines, porphyrin and fluorescein. Phosphorescence sensing is mainly achieved by injecting the sensor into the tissue of interest. Signal is detected by an optic fibre positioned a few millimeters away from the site (Wilson, 1993). Time resolved measurements of the lifetime decay (as exemplified in Figure 1.9) are used to calculate the Po_2. Phosphorescence quenching has been used in ophthalmology to measure Po_2 of the corneal tear film (Bonanno *et al.*, 2002), aqueous humour (McLaren *et al.*, 1998), optic disc (Chamot *et al.*, 2003) and retina (Shonat & Kight, 2003).

In this thesis, Po_2 in the lens will be measured with a fluorescent optode system (OxyLab, Oxford-Optronix, Oxford, UK). The optode consists of an O_2-sensor embedded in a polymer located at the end of a 320-μm wide optic fibre (model BF/OT/2.0) (Figure 1.10B). The O_2-sensor is a fluorophore whose structure is a Ru atom surrounded by an organic ligand (Figure 1.10A). The optic fibre is connected to a monitor that houses an oscillating blue light which illuminates the sensor. The optic fibre also transmits the emitted fluorescence to the monitor. In contrast to the above mentioned technique of time-resolved measurements, this instrument uses phase-modulation (Bambot *et al.*, 1995) to measure the fluorescence lifetime. Both the excitation and the emission light are phase-modulated and the phase-angle is used to calculate the lifetime.

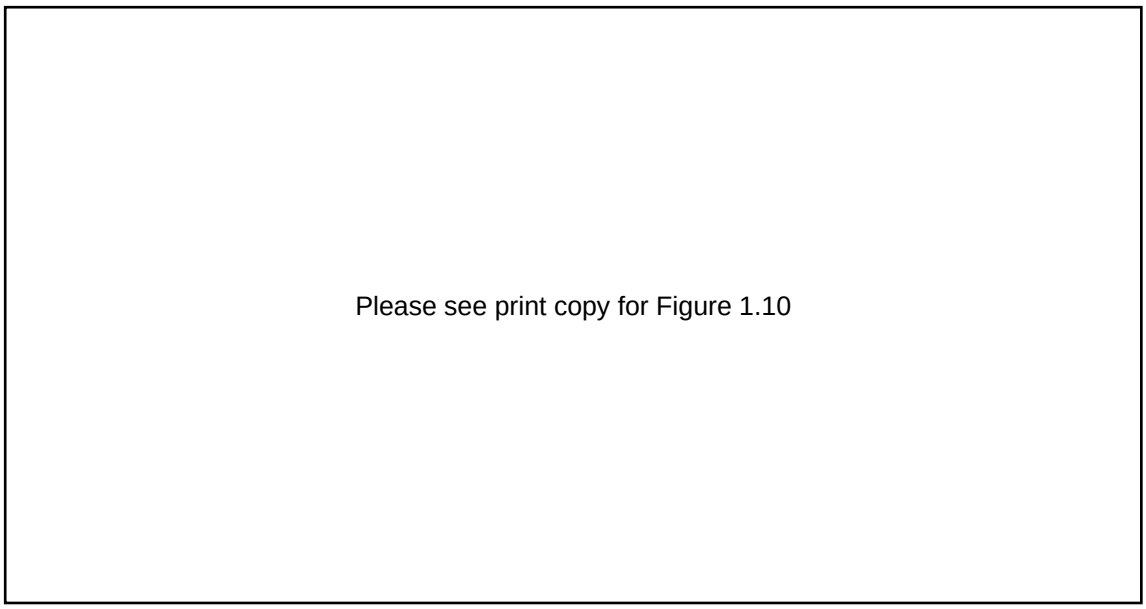

Figure 1.10 *The OxyLab fluorescent optode.* ***A.*** *The O_2 sensor is a fluorophore compound consisting of a ruthenium atom surrounded by an organic ligand.* ***B.*** *The optode is a 320 µm-wide optic fibre with the O_2 sensor in (A) embedded in a polymer at the tip. A thermocouple is also incorporated into the optode to enable temperature monitoring at the same site as Po_2 (Figure modified from Oxford-Optronix literature).*

Optodes were obtained pre-calibrated by the manufacturer. The measurement range of the optode system was 0 - 100 mmHg with P_{O2} resolution of 0.1 mmHg and accuracy of 0.7 mmHg (as reported by the manufacturer). Each optode was viable for 12 hours of continuous measurements. A thermocouple was incorporated into the tip of the optode (Figure 1.10B). This not only allowed for temperature measurements at the same site as Po_2, but was important for the calculation of the correct Po_2 by the monitor. The monitor was connected to a PC via a PowerLab 2/20 analogue to digital converter (ADInstruments, Sydney, NSW). Data were recorded digitally using Chart v4.1.2 for windows software (ADInstruments, Sydney, NSW).

Optodes provide an accurate measure of Po_2 within the physiological range (Seddon *et al.*, 2001). The application of optodes to measure Po_2 in vivo has been almost

exclusively in animal models in the fields of oncology and cerebral vascular physiology (Dewhirst *et al.*, 2000; Brurberg *et al.*, 2003). In ophthalmology, optodes have been used to measure aqueous and vitreous Po_2 in dogs (Stefansson *et al.*, 1989). In the following chapters, optodes will be used to measure Po_2 in isolated lenses and also in the vitreous of the developing chicken eye.

1.6.3 Hypoxia markers

The 2-nitroimidazoles, part of the nitroheterocycle family, were initially developed for the use of radiation oncologists to sensitise tumours to the effects of radiation. It was subsequently discovered in 1976 that the metabolic products of these molecules were retained inside cells only at very low Po_2 (Varghese *et al.*, 1976), making them suitable markers for hypoxia. The key to this property is the selective metabolism of the compound. 2-nitroimidazole metabolism begins with enzymatic nitro-reduction in the cytoplasm (Franko, 1986). Further metabolism depends on the presence or absence of O_2. In the presence of O_2, the compound is oxidised, resulting in a stable molecule that can diffuse out of the cell. However, in hypoxic conditions, further reductions occur resulting in the product becoming covalently bound to intracellular molecules. Covalent binding occurs via thiol groups in proteins, peptides, and amino acids (Figure 1.11) (Raleigh *et al.*, 2001). Binding occurs at O_2 concentrations of 2000-4000 ppm (Franko, 1986) or 14 μM (Mueller-Klieser *et al.*, 1991) corresponding to a Po_2 <10 mmHg (Varghese *et al.*, 1976). The binding is specific to hypoxic areas and not dependent on areas of increased nitro-reductase activity or the redox state of the cell (Van Os-Corby & Chapman, 1986; Van Os-Corby *et al.*, 1987; Parliament *et al.*, 1992; Arteel *et al.*, 1995). Hypoxia marker binding increases with time (Chapman *et al.*, 1983). Therefore, intensity of staining cannot be calibrated

precisely to Po_2, and a positively stained sample is best interpreted as being below the hypoxic threshold Po_2 of ~10 mmHg.

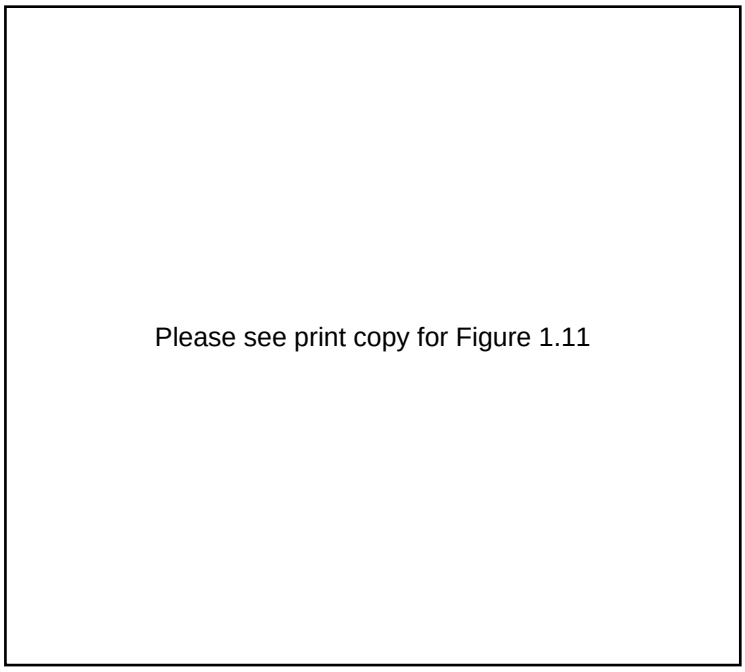

Figure 1.11 *The metabolism of the hypoxia marker pimonidazole. In hypoxic conditions, pimonidazole (left) is reduced and forms adducts with peptides and proteins (right). The Km for this reaction is ~4 μM. The adducts can then be visualized using immunohistochemistry.*

In 1981 it was proposed that 2-nitroimidazole binding could be used as a method of visualising hypoxic cells by immunohistochemistry. This approach has been used to visualize tissue hypoxia in the thymus (Hale *et al.*, 2002), liver (Corpechot *et al.*, 2002), and various types of tumours (Bennewith *et al.*, 2002; Kaanders *et al.*, 2002). An example of hypoxia staining in a uterine carcinoma is shown in Figure 1.12.

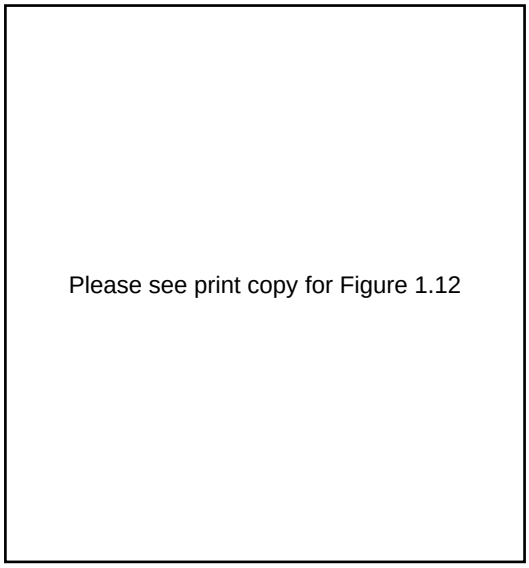

Figure 1.12 *Pimonidazole staining in a squamous cell carcinoma of the human cervix. After administration of pimonidazole to the patient, a biopsy of the uterine cervix was taken. The sample was fixed, sliced and treated with a pimonidazole antibody and then a horseradish-peroxidase conjugated secondary antibody. Following incubation in with the DAB chromogen, hypoxic cells stained brown and are situated between an arteriole (a) and an area of necrosis (n) (modified from www.radonc.un.edu/pimo).*

Applications of hypoxia markers are almost exclusively in the field of oncology. Tumour Po_2 is a variable in the prognosis and treatment of cancer. Hypoxia creates resistance to radiotherapy and some chemo-therapeutic agents (Nordsmark *et al.*, 2001) and has been correlated with metastatic disease (Brizel *et al.*, 1996). Hypoxia markers have been used in animal tumour models and for gauging response to treatments (Bussink *et al.*, 2003).

Hypoxia markers have also been applied to animal models of alcoholic liver damage to explore the link between exposure to ethanol and liver hypoxia (Bardag-Gorce *et al.*, 2002). To date they have not been used in ophthalmology. Hypoxia markers are an attractive option for lens oximetry as it is strongly suspected that the lens core is hypoxic (see §1.7). The technique is minimally invasive prior to sacrifice of the animal, making it suitable for in vivo use. Hypoxia markers will be used in the embryonic chick eye in Chapter 4.

1.6.4 Electron Paramagnetic Resonance (EPR)

EPR spectroscopy dates back to the 1940's (Zweier & Kuppusamy, 1988). The principle behind EPR is that paramagnetic substances, which have two-unpaired electrons in their outer orbitals, interact to produce a distinctive signal (the spectral line) in a resonator. Samples containing a probe or label are placed in a magnetic field in a resonator and electromagnetic radiation (usually microwaves) is passed across the field. EPR can be used in oximetry because O_2 interacts with paramagnetic materials to produce a change in the EPR spectra. The presence of O_2 usually results in a broadening of the spectral line

width. The judicious selection of paramagnetic probes that exhibit a linear change to their signal in the presence of O_2 allows calibration of the signal to Po_2.

In vivo EPR has been mostly confined to animal models. Nitroxide probes have been used in mice to monitor Po_2 changes after administration of anaesthetic gases (Subczynski *et al.*, 1986; Glockner *et al.*, 1991). India ink (famous for its use in tattoos), has been employed to monitor Po_2 in organs such as liver in rodents (Jiang *et al.*, 1996). Another probe, lithium phthalocyanine, a metallic-organic paramagnetic crystallite, has been successfully inserted into kidney (Liu *et al.*, 1993). There has been limited use of EPR in humans. In 1994, India ink in a tattoo provided the first ever EPR measurement in a human (Goda *et al.*, 1995). Although in vivo EPR is progressing with the development of non-toxic materials, there are some features of the technique that make it problematic for use in ophthalmology. An important factor is the limited depth to which measurements are possible. Large band microwave frequencies, such as 8-10 GHz (X-band) or 35-40 GHz (Q-band), can measure signals in tissue only to a depth of 0.2-1 mm. Newer techniques utilise 1-2 GHz (L-band) enabling deeper readings to approximately 10 mm (Swartz, 2002). In addition, most probes are insensitive to low Po_2 values (Chen *et al.*, 1994; Swartz & Clarkson, 1998), making them unsuitable for lens oximetry. India ink, one of the few probes sensitive to low Po_2, requires direct insertion into the tissue which would compromise the integrity of the lens. These issues clearly limit the use of EPR in its current form in lens oximetry.

1.7 Oxygen and the eye

1.7.1 Ocular anatomy

The eye consists of a tough outer layer called the globe which houses the delicate transparent structures for the transmission and focusing of light on the retina (Figure 1.13). The globe consists of the cornea and sclera surrounding the highly pigmented and vascularised uvea (choroid, ciliary body and iris) and the neurosensory retina. The transparent tissues of the eye, moving along the light path towards the retina, are the cornea, aqueous humour, the crystalline or ocular lens and the vitreous humour.

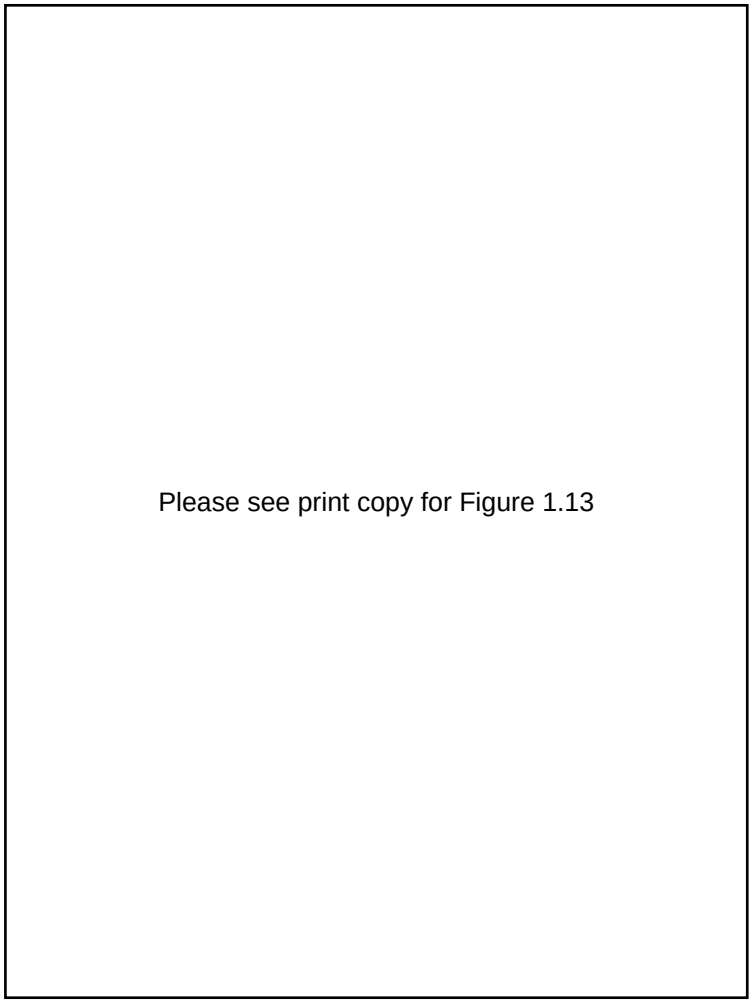

Figure 1.13 *Diagram of the human eye. The right eye has been sectioned horizontally and viewed from above. The ocular lens lies behind the iris and pupil and in front of the vitreous humour. Situated in the light path (dotted line), the lens helps focus images onto the retina (large arrow). The zonules from the ciliary body keep the lens in position and also allow the lens to change shape during accommodation. Note the asymmetry of the lens with the posterior surface having a smaller radius of curvature than the anterior surface (modified from cti.itc.virginia.edu/~psych220/eye).*

The ocular lens, which serves along with the cornea to focus light on the retina, is suspended behind the iris by the ciliary zonules (zonules of Zinn). The lens is circular when viewed from in front or behind. From the side the lens is asymmetrically biconvex, having a larger radius of curvature at the anterior surface. The adult human lens is approximately 9 mm across the equatorial diameter and 4 mm thick (Bron, *et al,* 1997).

The lens consists of a mass of closely packed fibre cells bounded anteriorly by an epithelial monolayer and enveloped by a thick basement membrane, the lens capsule (Figure 1.14A). Fibre cells are produced continuously by the differentiation of epithelial cells in the germinative zone near the lens equator. Due to the steady addition of newly formed fibres, the lens grows throughout life in layers somewhat like an onion. All cells since inception are retained within the tissue. The oldest fibre cells are located in the centre of the lens and those that differentiated most recently are located near the surface. During terminal differentiation, all organelles are eliminated from the fibre cell cytoplasm, presumably to avoid light scatter (Bassnett, 2002). As a result, the adult lens contains two populations of fibre cells: an outer layer of differentiating fibres (DF), which contain organelles, and a core of mature fibres (MF), which do not (Figure 1.14A). As fibres reach cells from the opposite hemisphere, they form lines of contact called sutures. Humans have a complex Y-shaped pattern of sutures at both the anterior and posterior poles (Bron, *et al*, 1997). In summary, there are several structural features of the lens that aid in transparency. The lack of blood supply, tightly packed cells and a predominance of cells lacking intracellular organelles may be features that had a selective advantage in the course of evolution due to minimizing light scatter.

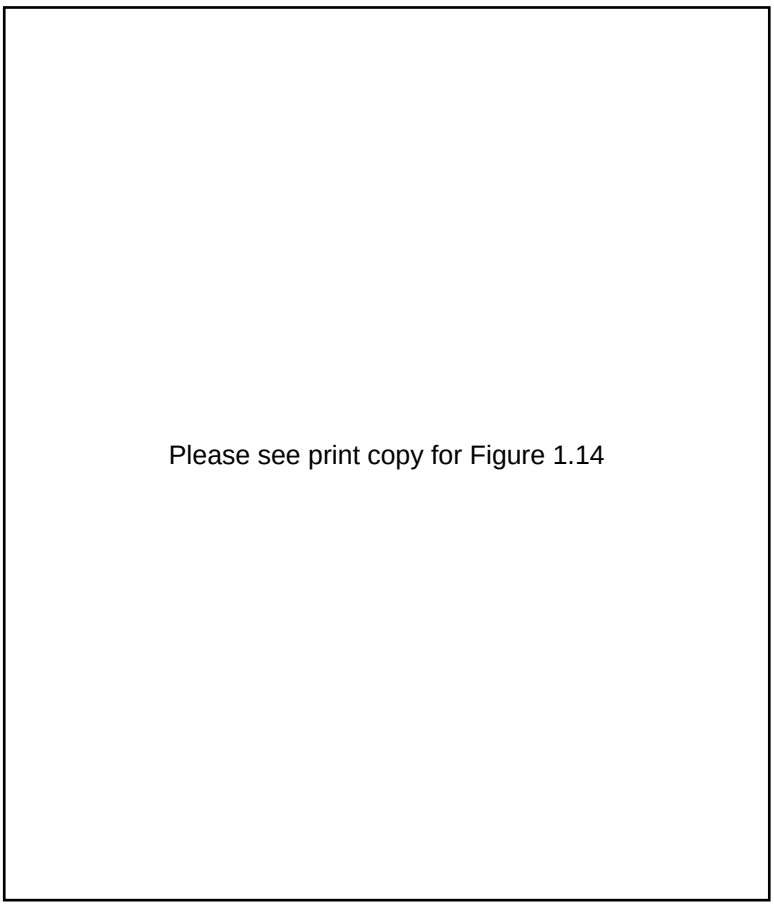

Figure 1.14 *The structure of the ocular lens.* ***A****. Diagram of a lens, sliced horizontally to reveal the internal structure. All lens cells are contained within the capsule. The suspensory zonules attach near the equator. The anterior lens is bounded by a single layer of epithelial cells which differentiate at the germinative zone to become elongated fibre cells. These differentiating fibre cells (DF) reach other fibre cells at the sutures. At a specific depth in the outer cortex, the DF lose all organelles to become mature fibre cells (MF).* ***B****. Scanning electron micrograph showing hexagonal cross-sections (arrows) of tightly packed fibre cells. A and B modified from (A Kaufman, 2003).*

Vessels in the eye are located peripherally, contained in and under the layers of the globe (Figure 1.15). In primates, there are two separate blood supplies to the eye. The first, the central retinal artery and its branches, is devoted to the sensory retina. The second, the uveal supply via the ciliary and conjunctival arteries, supplies the outer retina, the uvea and the rest of the globe (Bron, *et al,* 1997).

The ciliary body, containing the ciliary muscle and a vascular plexus, lies adjacent to the lens equator (Figure 1.15). The vessels are significant to the lens as a possible source

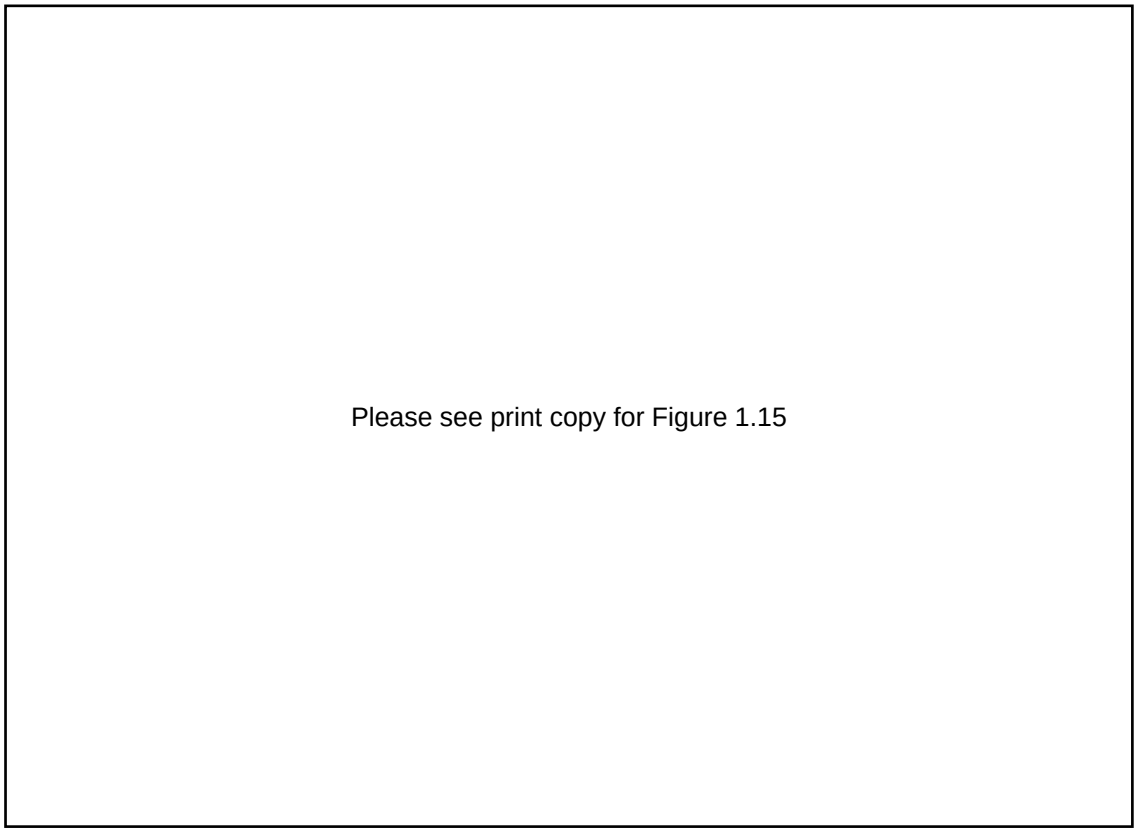

Figure 1.15 *The ocular vascular supply.* ***A.*** *The blood vessels in the eye are situated in the periphery in the globe. The eye is supplied by vessels of the ophthalmic artery. Most branches enter the eye posteriorly (the retinal artery and the long and short posterior ciliary arteries). The anterior structures also have a contribution from anterior arteries (anterior ciliary and conjunctival arteries).* ***B.*** *Blood supply near the lens (enlarged view of similar area boxed in A). In the adult, structures in the visual axis (cornea, lens, aqueous and vitreous humours) do not have a blood supply. Consequently, the nearest vessels to the lens are in the iris anteriorly and the ciliary body at the lens equator (vv: vessels). Aqueous humour is secreted into the posterior chamber (p) and later flows into the anterior chamber (a) (A and B modified from Bron et al, 1997).*

of O_2 and the muscle is important in the process of accommodation (see below). The zonules, bands of inelastic microfibrils composed primarily of fibrillin (Los *et al.*, 2004), connect the ciliary body to the lens equator and act as the physical support for the lens in the eye. Behind the lens lies the vitreous humour which comprises the bulk of the intraocular substance. Although macroscopically an amorphous gel-like substance, the vitreous micro-structure consists mainly of the glycosaminoglycan hyaluronic acid and collagen in a hygroscopic meshwork (Bishop *et al.*, 2002).

The anterior half of the lens is bathed in aqueous humour. The aqueous humour is a serum-like solution containing few large molecular weight proteins. It is secreted by the ciliary body into the narrow channel between the lens, ciliary body and iris called the posterior chamber (Figure 1.15B). The aqueous humour flows past the lens epithelium and through the pupil. Having entered the anterior chamber (the space bordered by the cornea and iris), the aqueous outflow is mainly via the trabecular meshwork and the Canal of Schlemm. The turnover time of the 250 µl of aqueous humour is approximately 100 minutes (Kaufman, 2003).

1.7.2 Lens physiology

The most important function of the lens is to focus visible light onto the retina. Refractory power is measured in dioptres (D), which is defined as the inverse of the focal length in meters. In human adults, the lens normally contributes 12 D out of a total of 60 D (Rubin, 1993). The refractory power of the lens is achieved by the high refractive index of the tissue and its bi-convex structure. The high refractive index is due to the high concentration of proteins called crystallins in the fibre cells (Kaufman, 2003). The lens has the highest concentration of protein of any tissue, comprising 30-40% of human lens wet weight (Fagerholm *et al.*, 1981). To focus on near objects during accommodation, the ciliary muscle contracts and loosens the zonules, allowing the lens to become more spherical. Under these circumstances, the lens can contribute even more refractive power, from an extra 18 D in children, decreasing to 2 D in the middle aged (Rubin, 1993). At about the age of 50, however, insufficient accommodation leads to the need for reading glasses (presbyopia or “old eyes”).

Although the main task of the lens is the transmission of light, some absorption also occurs. No light of wavelength <295 nm passes through the cornea to the lens (Dillon, 1991). A significant portion of UV-light in the range 295-400 nm is absorbed by the UV-filters of the lens (Ellozy *et al.*, 1994). As ageing progresses, the lens becomes increasingly yellow. This is accompanied by the absorption of visible light of short wavelength (~400-420 nm), resulting in a decrease in our ability to perceive colours at the blue end of the spectrum (Truscott, 2003). The UV-filters, along with advanced glycation end products (AGE's) from glucose and ascorbate, may be the cause of this colouration and may also be subject to further oxidation and contribute to cataract formation (Truscott, 2003).

Although many interesting points could be made about the physiology involved in maintaining lens transparency, the remainder of this section will address aspects of lens physiology directly relevant to O_2 metabolism, oxidation and cataract formation.

Perhaps as an adaptive response to a lack of blood supply and a low O_2 environment, the lens is less dependent on O_2 metabolism for energy production than most other tissues. The lens derives 80% of its ATP from anaerobic glycolysis and the remaining 20% from oxidative phosphorylation (Chylack, Jr., 1971; Hockwin, 1971; van Heyningen & Linklater, 1975).

Short term in vitro studies on bovine and rabbit lenses analysed various physiological parameters and found them to be relatively stable in the absence of O_2. The concentration of Na^+ in the calf lens, for example, remained unchanged at 16 mM after incubation in 100% N_2 and glucose. In the same study, an absence of O_2 had little effect on

concentrations of ATP and lactate, and protein synthesis (Kinoshita *et al.*, 1961). Other parameters that were maintained by anaerobic glycolysis alone include recovery of cation levels after cold exposure (Kinoshita *et al.*, 1961), amino acid uptake (Kinoshita *et al.*, 1961; Kern, 1962; van Heyningen & Linklater, 1975), rubidium uptake (Becker & Cotlier, 1962) and inositol uptake (Varma *et al.*, 1970). However, in the absence of O_2 *and* glucose, ATP levels decreased, tyrosine incorporation into protein decreased and sodium concentration increased (van Heyningen & Linklater, 1975), suggesting that lens homeostasis can be maintained in an absence of O_2 as long as an energy source is present.

There may be advantages for the lens in having limited access to O_2 in the form of protection against oxidation. Lens protein and membrane constituents last until the death of the organism and are, therefore, under the threat of accumulated damage from post-translational modifications including oxidation. Presumably as an adaptive mechanism to minimize oxidative stress, the lens contains high concentrations of anti-oxidant compounds such as glutathione (GSH) and ascorbate (Vitamin C) as well as protective enzymes such as superoxide-dismutase, GSH peroxidase and catalase (Harding, 1991). The tri-peptide GSH exists in millimolar amounts in the lens and is the most important anti-oxidant (Giblin, 2000). Although biosynthesis of GSH in the lens cortex does not decrease dramatically with age (Giblin, 2000), it may not be able to easily diffuse into the lens nucleus from middle-age onwards (Sweeney & Truscott, 1998). This may have ramifications for cataract formation because low levels of GSH in the human lens nucleus are linked to ARNC (see §1.8). Ascorbate, discussed in §1.5, is known for its ability to scavenge free radicals, is actively accumulated in the lens to millimolar concentrations in diurnal animals (Garland,

1991). Whether this compound may also act as an O_2-consumer in the lens will be addressed in Chapter 2.

1.7.3 Ocular Po_2

The most commonly used unit for Po_2 in the literature is mmHg, despite the fact that the SI unit for pressure is the pascal (Pa). Therefore, to avoid confusion, the more common unit will be utilized in this thesis. Table 1.1 shows conversions between mmHg and Pa for commonly cited Po_2 values used in this thesis. Since custom made gases used in experiments were ordered according to % O_2 content, this unit is also included in the table.

Table 1.1 Po_2 unit conversions

mmHg	% O_2	kPa
7.2	1	0.96
10	1.389	1.333
14.4	2	1.92
36	5	4.8
72	10	9.599
150	20.9	19.998
360	50	47.996
720	100	95.992

The lens is situated in a relatively low O_2 environment. Arterial P_{O_2} is approximately 100 mmHg (Braunwald, 2001), already below the atmospheric value of 150 mmHg. Po_2 in the aqueous and vitreous humours is lower still. In this section are presented the Po_2 values from the literature for the lens, aqueous and vitreous humours and an account of the sources of O_2 to these structures.

Aqueous humour Po_2

The average Po_2 in the aqueous humour of several vertebrate species is 38 mmHg (Fitch *et al.*, 2000). However, there is a wide range in values both within and across species. A summary of the published values is presented in Table 1.2.

Table 1.2 Aqueous humour Po_2

Please see print copy for Table 1.2

Please see print copy for Table 1.2

All measurements are with the polarographic technique except: (a) Krog's microtonometry, (b) N_2 in the anterior chamber, (c) sample withdrawn, (d) fluorescent optode, (e) phosphorimetry. Po_2 stated as mean ± SD (range). Number: number of eyes. [#]corrected to 40-45. (Table modified from Fitch et al, 2000, with additions).

A number of studies, including some in humans, showed Po_2 gradients in the anterior chamber. In the rabbit, monkey and human, values over the pupil were approximately 10-15 mmHg, lower than in the periphery of the anterior chamber where values of 45-55 mmHg were encountered (Hoper *et al.*, 1989; Helbig *et al.*, 1993). However, gradients may only exist under experimental conditions which involve immobilisation of the eye. Under normal conditions, the high frequency of eye movements (voluntary in the day and rapid eye movement (REM) sleep at night), may serve to stir the aqueous humour in the anterior chamber and dissipate any gradients (Maurice, 1998).

A range of values have been reported even within a single species (Table 1.2). This may reflect artefacts associated with each of the measurement techniques. Incisions into the anterior chamber might allow O_2 into the aqueous humour, resulting in falsely high values. The use of anaesthetics in animals can result in falsely low Po_2 values due to the constriction of blood vessels in the uvea. Aqueous Po_2 near the anterior surface of the lens can be underestimated by 30-50% for this reason (Barr & Silver, 1973).

The major source of O_2 in the aqueous humour is probably the vasculature of the iris and ciliary body. The large gradient between the arterial and aqueous Po_2 should result in diffusion of O_2 from the iris and ciliary body to the aqueous humour. There are a number of direct experimental observations to support this conclusion. The aqueous humour Po_2 is higher over the iris arteries (33-35 mmHg) than at the pupil in front of the lens (~13 mmHg) (Helbig *et al.*, 1993; Helbig *et al.*, 1994). In addition, increasing or decreasing the arterial Po_2 causes parallel changes in aqueous P_{O_2} (Hoper *et al.*, 1989; Fitch *et al.*, 2000). Diminishing the contribution of the vasculature, either through iridectomy or the addition of vasoconstrictor agents such as adrenaline or phenylephrine, results in a decrease in aqueous Po_2 (Stefansson *et al.*, 1983; Pakalnis *et al.*, 1988; Hoper *et al.*, 1989). Also, rabbit and monkey studies reveal that aqueous Po_2 values correlate with vascular density of the iris (Hoper *et al.*, 1989). Finally, some studies report that the aqueous Po_2 is higher than that found in the posterior layers of the cornea (corneal endothelium and posterior stroma), suggesting that the cornea does not relay O_2 to the aqueous (Kwan *et al.*, 1972).

An alternative view, suggested by some authors, is that the atmosphere is the source of aqueous O_2. This is largely based on two experimental observations. First, placing a contact lens on the cornea causes the aqueous Po_2 to drop (Barr & Silver, 1973). Secondly, there is evidence of a Po_2 gradient from the corneal endothelium to the lens (Kwan *et al.*, 1972). This is consistent with O_2 diffusing across the cornea from the atmosphere. However, another interpretation of these results is as follows. The cornea, which is supplied with O_2 from the atmosphere, will consume O_2 from the aqueous humour if the atmospheric supply is interrupted, as is the case with a contact lens in situ.

A further consideration is the presence of the lens and vitreous which act as a diffusional barrier to the passage of O_2 to the posterior segment of the eye. Thus, the removal of the lens and vitreous in ophthalmic procedures results in a decrease in aqueous humour Po_2 (Stefansson *et al.*, 1982; de Juan, Jr. *et al.*, 1986). Therefore, the origin of the O_2 in the aqueous humour is most likely the surrounding vasculature.

Vitreous humour Po_2

Vitreous humour Po_2 is consistently reported to be lower than aqueous humour Po_2. Published values for many species are presented in Table 1.3.

Table 1.3 Vitreous humour Po_2

Species	Po_2 (mmHg)	Position	Number	Reference
cat	53 (47-72)		20	(SB Goren & AC Krause, 1956)
rabbit	(2-30)	anterior to posterior		(KW Jacobi, 1965)
cat	18.9±1.5	pre-retinal	33	(A Alm & A Bill, 1972)
cat	<5-35	anterior to posterior	5	(R Briggs, 1973)
cat	11±4.4 (6.4-18.8)	10 μm from optic disc	5	(JT Ernest, 1973)
cat	30	10 μm from optic disc	31 cats	(JT Ernest, 1974)
	35	pre-retinal		(M Tsacopoulos *et al.*, 1976)
monkey	8±3	anterior to posterior		(KR Diddie & JT Ernest, 1977)
monkey	(1-20)	10 μm from optic disc	3	(KR Diddie & JT Ernest, 1977)
monkey	18.8 (13-34)	pre-retinal	6	(JT Ernest & DB Archer, 1979)
cat	22	200 μm pre-retina	10	(C Enroth-Cugell *et al.*, 1980)
cat	(15-20)	pre-retinal	5	(RA Linsenmeier *et al.*, 1981)
rabbit	21.5±3.2	posterior vitreous		(Miyazawa, 1981)
monkey	8.6±4.5	100 μm pre-retinal	8	(MB Landers, 3rd *et al.*, 1982)
cat	20.2±2.3	pre-retinal	5	(VA Alder *et al.*, 1983)
dog	21.8 (13-32)	pre-retinal	4	(JT Ernest *et al.*, 1983)
cat	35.6±5.4		6	(VA Alder & SJ Cringle, 1985)
pig	(13-49)	pre-retinal	11 pigs	(I Molnar *et al.*, 1985)
cat	19±5	pre-retinal	3	(E Stefansson *et al.*, 1986)
rabbit	(2-20)	anterior to posterior	6	(LD Ormerod *et al.*, 1987)
cat	20±7	pre-retinal	10	(E Stefansson, 1988)
cat	(20-40)	adjacent to retinal vein	4	(VA Alder & SJ Cringle, 1989)

	(30-80)	adjacent to retinal artery	1	
cat	26.1±5 (21-34)	150-300 μm pre-retinal	5	(RA Linsenmeier & CM Yancey, 1989)
mini pig	(32-41)	125 μm pre-retinal	5	(CJ Pournaras *et al.*, 1989)
rabbit	(14-23)	central to pre-retinal	8	(H Sakaue *et al.*, 1989a)
human*	(16-20)	central to pre-retinal	9	(H Sakaue *et al.*, 1989b)
dog	26±5 #	pre-retinal	5	(E Stefansson *et al.*, 1989)
cat	20±7	pre-retinal	10	(E Stefansson *et al.*, 1990)
rat	24	pre-retinal	1	(C Yu, Alder, 1990)
human*	(6-9)^	pre-retinal	1	(CA Wilson *et al.*, 1992)
human*	16.2	mid-vitreous	30	(N Maeda & Y Tano, 1996)
rabbit	>40 ~20 12.4 ± 3.1	Pre-retinal Mid-vitreous Behind lens	26 rabbits	(IA Barbazetto *et al.*, 2004)

Po_2 is expressed as mean±SD (range) using polarography unless otherwise indicated. Number: number of eyes. *diabetics. ^^{19}F- magnetic resonance spectroscopy. # fluorescent optode.

In humans, Po_2 in the centre of the vitreous is 16 mmHg (Sakaue *et al.*, 1989a; Maeda & Tano, 1996). An important feature of vitreous Po_2 is the gradient from the retina to the lens, indicating that the lens acts as a sink. The steepest part of the gradient is in the outer vitreous within 1.5 mm of the retina, most notably in front of the retinal arteries, indicating that they are the main source of O_2 for the vitreous (Linsenmeier *et al.*, 1981; Molnar *et al.*, 1985). Values decrease more gradually moving across the bulk of the vitreous towards the lens. Po_2 in the anterior vitreous immediately behind the lens is <5 mmHg as measured in cat, rabbit, and embryonic chicken eyes (Jacobi & Driest, 1966; Briggs, 1973; Ormerod *et al.*, 1987; Bassnett & McNulty, 2003). Unlike the gradients

found in the aqueous humour, those found in the gel-like vitreous are probably present under normal circumstances.

Conclusions on peri-lenticular Po_2

The lens is situated in a low Po_2 environment (Figure 1.16). There is a Po_2 asymmetry around the lens with lower values posteriorly in the vitreous humour. O_2 consumption by the lens is expected to further decrease Po_2 within the lens. An interesting ramification of this situation is that hypoxia may be part of the normal physiology of the lens. For our QO_2 and in vitro Po_2 studies, surrounding the lens with solutions of Po_2 <38 mmHg should yield physiological results.

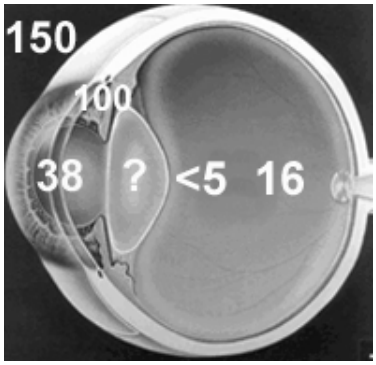

Figure 1.16 *Po_2 environment of the lens. Average or representative values (in mmHg) are presented for the atmosphere, ciliary body, aqueous humour, mid-vitreous and anterior vitreous in descending order.*

1.8 Cataract

Cataract is the major cause of world blindness. There are 20 million people bilaterally blind and hundreds of millions more visually impaired from this condition (Thylefors, *et al*, 1995). Despite our best efforts and modern developments in cataract surgery, these figures are expected to double by the year 2020 (WHO/PBL/97.61, 1997). In India alone, 4 million people become blind each year (Minassian & Mehra, 1990). Cataract also imposes a heavy burden on the health budget (Javitt *et al.*, 1996). It is estimated that if the development of cataract were delayed by even 10 years, the prevalence of cataracts would be halved (Brian & Taylor, 2001).

The vast majority of cataracts seen in clinical practice are of the nuclear, cortical or posterior subcapsular type (McCarty, 1999). Age-related nuclear cataract (ARNC) is found in the majority of cases, either alone or in conjunction with another type of cataract (Marcantonio *et al.*, 1980; Harding, 1991). Examples of nuclear and cortical cataracts are shown in Figure 1.17.

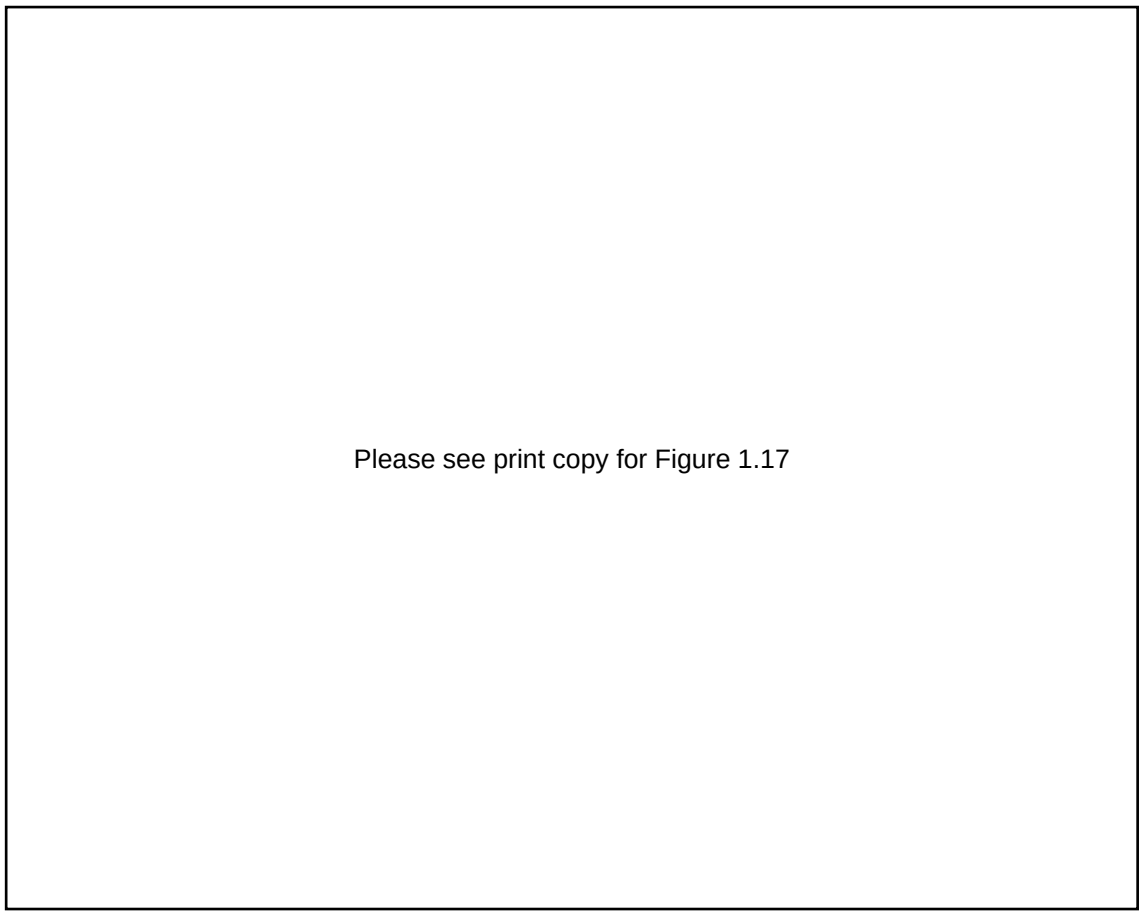

Figure 1.17 *Cataracts in the ocular lens. A. Age-related nuclear cataract appears as a cloudiness and colouration in the center of the lens. The cataract blocks light in the visual pathway causing the patient to see the world as if through a frosted window, simulated in (D). B. Cortical cataract occupies the outer part of the lens, often in triangular portions (arrow). C. Woman with bilateral cataracts. The pupil appears white instead of black, especially in the right eye (arrow) (figures from www.eyeshealth.com, ophthalmology.auckland.ac.nz, www.aim-uganda.org, www.lasersurgeryforeyes.com).*

The risk factors for nuclear and cortical cataracts and the limited amount known about their respective pathophysiology suggest that they are distinct diseases. Although many risk factors for nuclear cataract have been suggested, only age and smoking are

widely accepted (West & Valmadrid, 1995; Brian & Taylor, 2001). Cortical cataract, on the other hand, is linked to UVB-light exposure, diabetes and the use of glucocorticoid medication (West & Valmadrid, 1995; Brian & Taylor, 2001). Cortical cataract is associated with water and electrolyte changes, possibly leading to cell rupture by osmotic stress (Harding, 1991). A link has also been found to the loss of Ca^{2+} homeostasis and the presence of abnormally high Ca^{2+} levels in the cytoplasm (Duncan & Jacob, 1984). Other imbalances reported in cataract formation include elevated Na^{+}, decreased lens membrane potential and decreased levels of reduced glutathione (GSH) (Harding, 1991). Posterior subcapsular cataract is also associated with diabetes and glucocorticoid use (Harding, 1991; West & Valmadrid, 1995). Below we will concentrate on the pathophysiology of ARNC.

Clear lenses have little to no oxidation. The pathophysiological hallmark of ARNC is the development of progressive oxidative changes to crystallins and membranes (Truscott & Augusteyn, 1977a; Spector, 1984). The damage is cumulative because in cells of the nuclear region *de novo* protein synthesis probably does not occur (Faulkner-Jones *et al.*, 2003) and, consequently, oxidised components cannot be replaced. Loss of protein sulphydryls starts early and levels decrease to 5% in advanced (type IV) cataract (Truscott & Augusteyn, 1977b). There is also selective oxidation of crystallin amino acids. Cysteine and methionine groups are oxidized to cystine and methionine sulfoxide, respectively.

The presence of oxidation implies an imbalance between toxic oxidants and protective antioxidants. The levels of the tri-peptide glutathione (GSH), the most important antioxidant in the lens, are low in ARNC (Giblin, 2000). Unfortunately, little is known about the possible oxidant(s) involved. Furthermore, the precise reactions responsible for the changes seen in ARNC are not well understood. The ROS H_2O_2 and HO• have been

implicated (Truscott & Augusteyn, 1977a; Spector & Garner, 1981; Spector, 1984; Fu *et al.*, 1998). For example, lens crystallins treated with H_2O_2 show loss of reduced cysteine and methionine in the same proportions found in ARNC (McNamara & Augusteyn, 1984). In addition, evidence of HO• damage was seen in cataractous lenses in the form of the hydroxylation of protein-bound amino acids which increases with the severity of cataract (Fu *et al.*, 1998). These latter changes can be produced in vitro by incubating crystallins with iron (Fu *et al.*, 1998). There have been extensive studies on the potential role of H_2O_2 derived from the surrounding aqueous humour in causing oxidative damage to the lens (Spector & Garner, 1981; Spector, 1984). Another alternative, advocated by others, is the site-specific production of ROS. This could be achieved by the production of ROS via Fenton-style or photosensitisation reactions, the components of which have been identified in the lens (Garland, 1990). At this stage, however, we do not know whether the ROS diffuse in from the exterior, or are produced inside the lens. In summary, the oxidative changes found in ARNC suggest reactions with ROS, the ultimate source of which could be O_2.

Apart from the above biochemical suggestions that O_2 is linked to nuclear cataract, there is also some clinical evidence to support this notion. Cataracts developed in human patients who were exposed to hyperbaric O_2 therapy (Palmquist *et al.*, 1984). The cataracts were nuclear and had an accompanying myopic shift, similar to that seen in ARNC patients (Harding, 1991). This has inspired the use of hyperbaric O_2 treatment of guinea pigs as an animal model for nuclear cataract formation. Analysis of these lenses has revealed features that are also found in human ARNC. These include cross-linking of proteins, loss of sulphydryls and an increase in the insoluble protein fraction (Giblin *et al.*, 1995;

Padgaonkar *et al.*, 1999; Borchman *et al.*, 2000). Although the time frame for cataract development with hyperbaric O_2 (<2 years) is much shorter than in the development of ARNC, the key finding is that exposure to O_2 can result in a similar clinical picture and produce similar biochemical changes. In light of the possible link between ARNC and O_2, some authors have speculated that the effective exclusion of O_2 from the centre of the lens could be one mechanism by which cells in this region preserve their transparency over a prolonged period (Eaton, 1991).

Also of relevance to a study of O_2 in the lens and its relation to cataract, are recent findings concerning transport of small molecular weight molecules in aged human lenses. It has been found that, starting from middle age, the human lens has a decreased ability to transport the anti-oxidant glutathione (Sweeney & Truscott, 1998), and water (Moffat *et al.*, 1999) into the lens core. Whether O_2 is able to penetrate into the lens core will be addressed in this thesis. If O_2 is freely diffusible in the elderly human lens yet glutathione is not, then the lens core may be subject to oxidative stress.

When considering the connection between ARNC and oxidation, it is noteworthy that other diseases associated with ROS production are also linked to cataract formation. The mitochondrial encephalomyopathies, for example, are a group of diseases with the common feature of oxidative phosphorylation deficiency. Although they have a wide range of clinical presentations, ranging from muscle weakness to early death, they are also linked to the early development of cataract, some of which are of the nuclear type (Table 1.4). These diseases are usually caused by mitochondrial DNA (mtDNA) mutations with over 100 mutations catalogued thus far (Shoubridge, 2001). Since diseases of mitochondrial

dysfunction can lead to nuclear cataract, it is interesting to speculate that ARNC may be the result of age-related mitochondrial dysfunction. It may be that mitochondria, which produce increasing amounts of ROS with ageing and mitochondrial dysfunction (Droge, 2002), are the source of the ROS that cause ARNC. From this viewpoint, it will be interesting to investigate the role of the mitochondria in controlling lens O_2 levels in subsequent chapters.

Table 1.4 Cataract and the mitochondrial encephalomyopathies

CLINICAL PRESENTATION	DEFICIENCY/ DEFECT	*n*	REFERENCE
I. Congenital cataract			
myopathy/LA		2	(RC Sengers *et al.*, 1975; RC Sengers *et al.*, 1985)
HOCM/LA		6	(J Valsson *et al.*, 1988)
HOCM		12	(JR Cruysberg *et al.*, 1986; GJ van Ekeren *et al.*, 1987; GJ van Ekeren *et al.*, 1993)
PEO		3	(SA Barron *et al.*, 1979)
HOCM/LA	complex I deficiency	4	(S Pitkanen *et al.*, 1996)
II. Early onset cataract			
bilateral cataract		1	(K North *et al.*, 1996)
LA	complex I deficiency	1	(TA Ciulla *et al.*, 1995)
KSS	5kb mtDNA deletion	1	(Y Isashiki *et al.*, 1998)
Pearson Syndrome, zonular cataract		1	(C Cursiefen *et al.*, 1998)
myopathy, posterior cataract		1	(B Pepin *et al.*, 1980)
myopathy,hypoparathyroidism, bilateral cataract		1	(M Toppet *et al.*, 1977)

III. Adult onset cataract			
neuropsychiatric disorder, bilateral cataracts	A3274G in mt tRNA Leu (UUR) gene	1	(M Jaksch *et al.*, 2001)
myopathy, bilateral cataract	multiple mtDNA transitions	1	(J Finsterer *et al.*, 2000)
MELAS	GtoA mtDNA point mutation	1	(Y Isashiki *et al.*, 1998)
MELAS	A3243G in mt tRNA Leu (UUR) gene	1	(V Rummelt *et al.*, 1993)
MELAS, bilateral cataracts	A3243G in mt tRNA Leu (UUR) gene	1	(RK Mosewich *et al.*, 1993)
myopathy, PEO, bilateral cataracts	multiple mtDNA deletions	5	(S Servidei *et al.*, 1991)
MELAS, nuclear cataract		1	(M Kuchle *et al.*, 1990)
myopathy		1	(T Fritz *et al.*, 1988)
myopathy		2	(B Pepin *et al.*, 1980)
PEO, cortical cataract		1	(R Zintz & W Villiger, 1967)

n: number of patients. HOCM: hypertrophic obstructive cardiomyopathy, LA: lactic acidosis, mt: mitochondrial, MELAS: mitochondrial encephalomyopathy, lactic acidosis and stroke-like episodes, PEO: progressive external ophthalmoplegia.

In light of the connection between cataract and oxidation, a cataract prevention strategy was developed which aimed to stave off oxidation by administering dietary supplements of antioxidant vitamins and minerals to patients. Some preliminary data supported this approach (Sperduto *et al.*, 1993). However, in the Age Related Eye Disease Study (AREDS), people who took ascorbate supplementation of 250 mg daily for over 6 years did not show a decrease in the incidence of nuclear cataract compared to those who took a placebo (AREDSresearchgroup., 2001). Another study examining vitamin E reported that the rate of cataract progression was not decreased in a group of patients given 500 IU of vitamin E for 4 years (McNeil *et al.*, 2004). Therefore, it may be that normal

dietary levels of vitamins are necessary to avoid an increased risk of cataract, but supplements taken in addition to a well-balanced diet will not further reduce the risk. Clearly, additional research is needed into the mechanisms of cataract formation that may lead to new possibilities for preventing this disease.

1.9 Outline of the thesis

The main aim of the thesis is to examine the mechanisms that regulate the levels of O_2 within the lens. Bovine, rabbit and guinea pig lenses will be used as models in Chapter 2, and in Chapter 3 we will examine human donor lenses. Lens Po_2 will be measured in vitro with a fluorescent optode. The contribution of mitochondrial O_2 consumption in regulating O_2 levels will be determined. The distribution of mitochondria in the lens will be mapped and compared to Po_2 profiles. We will investigate the effect of mitochondria-inhibiting drugs on lens O_2 consumption rate (QO_2) and Po_2. The role of non-mitochondrial O_2 consumers such as ascorbate, PMOR, and photo-oxidation will also be examined. We will also test our hypothesis that old lenses may consume less O_2 and consequently have higher O_2 levels. From these data, a mathematical model of O_2 regulation in the mammalian lens will be formulated allowing for the calculation of time and length constants for O_2 consumption (τ (s) and λ (mm), respectively), as well as an effective diffusion coefficient for O_2 (D_{O_2}) in the lens.

In Chapter 4, we examine the possibility that lens O_2 gradients provide positional cues to coordinate a key event in fibre cell differentiation, namely, the degradation of intracellular organelles. In Chapter 5 we will conclude by outlining the main findings of the

thesis and assessing the significance of the data for our hypotheses on ageing, mitochondria and cataract.

Chapter 2:

Regulation of O_2 levels

in

the mammalian lens

2.1 Introduction

The aim of this chapter is to measure the level of O_2 in the mammalian lens in vitro and define the processes that influence its concentration and distribution.

Lacking a blood supply, O_2 enters the lens via diffusion from the aqueous humour anteriorly and the vitreous humour posteriorly. This limits the flux of O_2 to the lens, both because diffusion is a relatively slow process, and because the Po_2 in the humours is already comparatively low (see §1.7.3). The diffusion coefficient of O_2 (D_{O_2}) in water is about $3x10^{-5}$ cm^2/s (Himmelblau, 1964), compared to $1x10^{-5}$ cm^2/s in plasma membrane from erythrocytes (Fischkoff & Vanderkooi, 1975), indicating that O_2 readily crosses cell membranes.

However, it is expected that lens O_2 consumption will significantly influence tissue O_2 levels. It has been known since 1937 that the lens consumes O_2 (Field, 1937), but at a fraction of the rate of most other tissues. For example, QO_2 of intact mammalian lenses, measured using modern polarography-based respirometers, ranged from 4-49 µl/g/h (Griffiths, 1966;Talaat, et al., 1974). In comparison, QO_2 of the brain is 1.8 ml/g/h (Van Lieshout, et al., 2003) and resting myocardium is 3 ml/g/h (Tune, et al., 2002).

The lack of blood supply and the consumption of O_2 by the lens lead us to suspect that O_2 levels in the lens core will be significantly lower than at the surface. In fact, Eaton (1991) and Harding (1991) have suggested that the lens core could be anoxic. The little data published concerning Po_2 within the lens is cited in Table 2.1.

Table 2.1. Lens Po_2

Species	Po_2 (mmHg)	Comment	Reference	Technique
rabbit	<20	germinative zone	(Howard-Flanders & Pirie, 1957) (estimate)	
cat	1	posterior cortex and nucleus	Rodenhauser cited in (Uyama, 1973)	electrode
rabbit	(21-28)	anterior cortex (n=3)	(Kwan, et al., 1972)	electrode
cow	$<3 \times 10^{-5}$ M		(Roberts, 1992)#	phosphorescent
human	2.5±0.6 (0.8-4)	anterior cortex (n=7)	(Helbig, et al., 1993)	electrode
cow	2.5	5 h post-mortem	(Huang, 2001)#	optode
rabbit	~10	core	(Dillon, 2003)	optode
rabbit	10-22	asymmetrical profile	(Barbazetto, et al., 2004)	optode

Abstract only. n=number of eyes.

To our knowledge, there is only one report of lens Po_2 profiles, which were measured in rabbit lenses in vivo (Barbazetto, et al., 2004). The Po_2 profile was asymmetrical with a longer gradient posteriorly. Po_2 values ranged from 22 mmHg in the cortex to 10 mmHg in the lens centre. In other mammalian species, values ranged from 1 mmHg in the posterior cortex and nucleus of the cat (Uyama, 1973) to 21 mmHg measured 400 μm into the anterior cortex of the rabbit lens (Kwan, et al., 1972). In humans, values of 0.8–4.0 mmHg were measured in the anterior cortex during cataract surgery (Helbig, et al., 1993). Yet, as discussed in §1.6.1, the high viscosity of the lens raises problems for the interpretation of electrode results in the lens. In light of this, we will employ a fluorescent optode in this thesis.

2.2 Materials and Methods

Chemicals. All chemicals used in this thesis were obtained from Sigma Chemical Co. (St. Louis, MO, USA) unless otherwise stated.

Gases. All custom-made gas mixtures used in this thesis were obtained from Airgas Inc. (St. Louis, MO, USA). Gases contained defined amounts of O_2 with 5% CO_2 and the remainder N_2.

Artificial Aqueous Humour (AAH) solution. Lenses were equilibrated and measurements were made in artificial aqueous humour (AAH) solution. This solution resembles the aqueous humour in composition and has been used previously for physiological studies of the lens (Bassnett, 1990). The AAH had the following composition (mM): NaCl, 113; KCl, 4.5; $MgCl_2$, 1; $CaCl_2$, 1.5; D-glucose, 6; *N*-(2-hydroxyethyl) piperazine-*N'*-(2-ethanesulphonic acid) (HEPES), 10; $NaHCO_3$, 20; and 1:1000 penicillin/streptomycin. The pH of the AAH was adjusted to 7.3.

Data processing. Data was collected on Excel 2002 spreadsheets (Microsoft Corporation, USA). All graphs in this thesis were made using Sigmaplot 2001 for Windows version 7.101 (SPSS Inc., Chicago, IL, USA). All images in this thesis were prepared using Photoshop 6.0 (Adobe Systems Inc., San Jose, CA, USA).

Statistical analysis. Statistical significance was assessed by Student's *t*-test. *P*-values <0.05 were regarded as significant.

Animals. Animal care was in accordance with the guidelines set forth by Washington University in St Louis. This study was approved by the Washington University Animal Studies Committee.

Eyes from cattle aged approximately 1.5 years old were obtained on the day of slaughter from local abattoirs (Schubert's Packing Co., Milstadt, IL; Trenton Processing Center, Inc., Trenton, IL and Zerna Meat Co., St Louis, MO, USA). Whole eyes were transported to the laboratory on ice. A limbal incision was made to remove the cornea and the lens was released from the eye by carefully cutting the zonules. The average lens weight of dissected lenses was 2.09 ± 0.18 g (mean ± SD; n=20). The equatorial diameter of the same lenses was 16.65 ± 0.81 mm (n=20) and the thickness along the optic axis was 11.05 ± 0.89 mm (n=20). To allow lenses to equilibrate under test conditions, they were placed in artificial aqueous humour (AAH, detailed above) containing antibiotics for at least four hours at a specified temperature and Po_2. In some experiments, dried bovine lenses were needed. These were prepared by removing the lens capsule from a fresh lens, recording the weight and then placing the lens in an incubator containing desiccant at 50°C for several days. The weight was recorded daily until a constant value was reached, denoting the removal of all water. Measured in this fashion, the water content of bovine lenses was 65 ± 1% (n=3).

Guinea pigs, which have an absolute requirement for dietary ascorbate, were used to examine the effect of ascorbic acid depletion on lens QO_2. Young adult (approximately 3-

months-old) pigmented NIH strain guinea pigs weighing 677-913 g were randomly divided into two groups. After a week of stabilisation on a diet of normal guinea pig chow (Diet 5025, Purina, Richmond, IN, USA), the experimental group was given ascorbic acid-free chow (Diet 5710-6 Purina, Richmond, IN, USA) *ad libitum* for four weeks while the control group continued on a normal diet. Both groups were given water *ad libitum*. Animals were weighed twice a week. At the end of the four week period, animals were sacrificed by CO_2 inhalation and their lenses were removed, photographed and weighed. Lens QO_2 was measured as described above. Following QO_2 measurements, lenses were frozen at -70°C pending high performance liquid chromatography (HPLC) determination of ascorbic acid levels. The effect of age on lens QO_2 was ascertained using 2-year-old Albino Hartley guinea pigs (Charles River Laboratories, Wilmington, MA, USA), which were the kind gift of Dr. Frank J. Giblin, Oakland University, MI, USA.

Rabbits were obtained from the laboratory of Prof. David C. Beebe, Department of Ophthalmology, Washington University in St Louis. Rabbits were sacrificed via an injection of 35 mg/ml ketamine and 5 mg/ml xylazine and then CO_2 inhalation. Eyes were dissected from the animal and the lens removed from a posterior approach. Lenses were equilibrated as described for bovine lenses.

Ascorbate assay. Lens ascorbate was measured using an HPLC assay in collaboration with the laboratory of Dr. Beryl J Ortwerth (Mason Eye Institute, Columbia, University of Missouri, Columbia, USA).

An ascorbic acid standard curve was made from a 1 mM solution of ascorbic acid dissolved in 0.1% metaphosphoric acid (MPA)/ 0.1 mM diethylenetriaminepentaacetic acid (DTPA). Solutions containing 40, 30, 20, 10, and 5 nmoles/100 µl were processed and a trend line plotted. A recovery test was performed by homogenizing two lenses in 800 µl of 50 mM K_2HPO_4, 0.1 mM DTPA in water. The sample was divided into two tubes and 30 µl of 1mM ascorbic acid was added to one of them. After centrifuging both tubes for 40 minutes at 15,000 rpm, the supernatant was removed to a new tube, 200 µl of 10% MPA/ 0.1 mM DTPA was added to each tube and centrifuging repeated for 20 minutes. The supernatant was transferred to a 5,000 nominal molecular weight limit (NMWL) filter (Millipore, Billerica, MA, USA) and centrifuged for 60 minutes at 6,000 rpm. Percentage recovery was calculated from 100 µl filtered samples. Test samples were prepared by homogenizing each lens in 400 µl of 50 mM K_2HPO_4, 0.1 mM DTPA, and water. After centrifuging at 15,000 rpm for 40 minutes, the supernatant was transferred to new tube, 100 µl of 10% MPA/ 0.1 mM DTPA was added and the sample centrifuged again at 15,000 rpm for 20 minutes. Samples were then microcentrifuge filtered using a 5,000 NMWL filter at 6,000 rpm for 60 minutes. HPLC was performed on 100 µl samples using 7.8 X 300 mm Resex RNM carbohydrate column in the sodium form (Phenomenex, Torrance, CA, USA) with 1% MPA and 0.1 mM DTPA solvent. The flow rate was 0.3 ml/min for 50 minutes.

O_2 measurement. Lens Po_2 was measured using a fibre optic fluorescent optode system (OxyLab, Oxford-Optronix, Oxford, UK) as described in §1.6.2. The OxyLab monitor was connected to a PC via a PowerLab 2/20 analogue to digital converter (ADInstruments, Sydney, NSW). Data were recorded digitally using Chart v4.1.2 for windows software

(ADInstruments, Sydney, NSW). After the 4 hour period of equilibration in AAH, lens P_{O_2} in vitro was measured in a custom built chamber. Lenses were placed on a fenestrated plastic stand within a Plexiglas chamber (Figure 2.1). This 200 ml chamber of 9 mm thick plexiglass consisted of four walls and a base with dimensions of 9 x 10 x 5 cm. Lenses were bathed continuously by well-mixed AAH warmed and circulated from a water-bath (type B water-bath, Lauda and Co., Konigshofen, Germany; variable flow pumps, Cat # 138762 and Tygon plastic tubing, Fischer Scientific Co., Pittsburgh, PA, USA). A gas dispersion tube (Top Fin, Pacific Coast Distributing Inc., Phoenix, AZ, USA) in the chamber next to the lens allowed the Po_2 of the AAH to be regulated to the same value used during the equilibration period. The optode was mounted on a micromanipulator (model M3301R, World Precision Instruments Inc., Sarasota, FL, USA) vertically above the lens. A nick was made in the lens capsule with a 25G needle. The tip of the optode was then aligned with this small hole and incrementally advanced into the lens. At each location, the optode was allowed to record a steady value (this typically took <30 s) before being advanced. The optode was driven through the lens along either the optic or equatorial axis and Po_2 profiles were recorded.

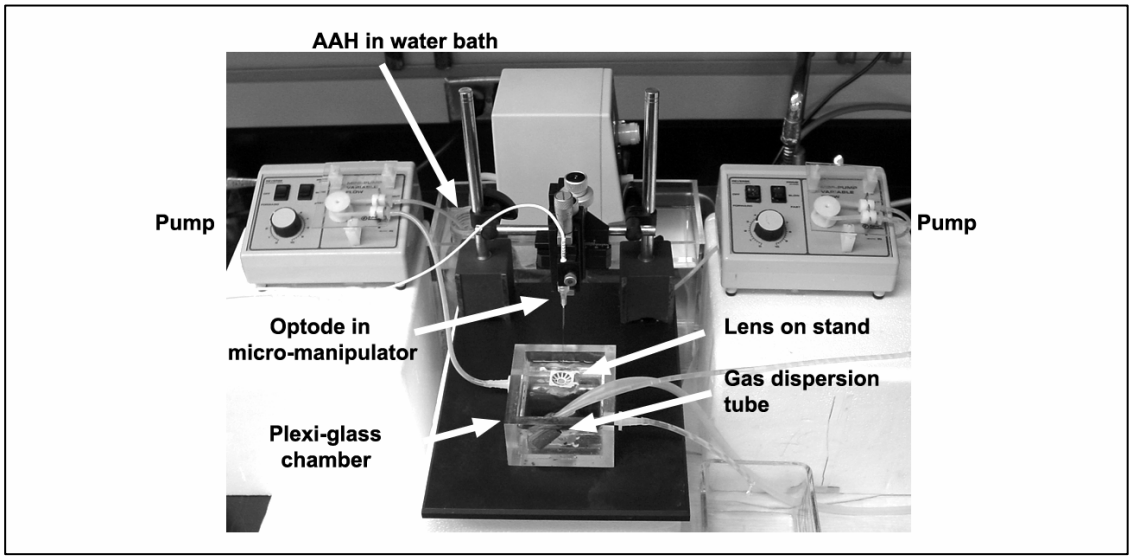

Figure 2.1 *Experimental apparatus for in vitro Po_2 measurements. The lens was placed on a plastic stand surrounded by warmed AAH in a custom-made plexiglass chamber. AAH was heated in a water bath and circulated to and from the chamber by pumps. The Po_2 of the AAH was determined by gases delivered through the dispersion tube. The optode was mounted in an overhead micro-manipulator allowing it to be moved through the lens (thanks to Cheryl Shomo for assistance with photography).*

Respirometry. Lens QO_2 was measured using a respirometer consisting of a 5300A biological O_2 monitor, a 5301B standard bath, a 5304 micro-adaptor kit and a 5331A electrode (YSI Inc., Yellow Springs, OH, USA). After equilibration, lenses (or parts thereof) were placed in the measurement chamber in 3 ml of AAH. The Po_2 and temperature of the AAH during respirometry were the same as during equilibration. Respirometry was performed at 37°C unless otherwise stated. The Po_2 of the AAH bathing the lens was monitored by an electrode built into a plunger designed to seal the chamber. The same experiment, but without a lens in the chamber, served as a control for each measurement. At the end of the measurement period (usually 20 minutes), lenses were removed from the chamber and weighed. QO_2 (µl/g/h) was calculated from the slope of a regression line fitted to the (usually decreasing) Po_2 data set and control values were subtracted. For this calculation, it was assumed that 1 ml of AAH at 1 atmosphere and 37^{o}C

contained 5.02 µl of O_2 (Operations Manual for 5300A system, YSI Inc, Yellow Springs, OH, USA). Values used for the concentration of O_2 at lower temperatures are shown in Table 2.2.

Table 2.2 Concentration of O_2 in solutions

Please see print copy for Table 2.2

*[O_2] in µl/ml solution at 101.325 kPa (1 atmosphere) which have been equilibrated with stated Po_2. # AAH approximates Ringer's solution (Table modified from 5300 series respirometer handbook, YSI Inc., Yellow Springs, OH, USA).

While it was possible to obtain a reliable measure of QO_2 on individual bovine lenses, it was necessary to pool two to four guinea pig lenses in 2 ml of AAH for each QO_2 determination. The error of the respirometer was measured by performing blank experiments where AAH, but no lens, was placed in the respirometer. The error with AAH equilibrated with Po_2 of 150 mmHg (21% O_2) or 36 mmHg (5% O_2) was 0.1 ± 0.2 µl/h (n=6 each, data not shown). Respirometry was also performed on bovine lens core homogenates. These were prepared by dissecting fresh lenses to remove the capsule and outer few mm of cortex leaving the central 1g of core tissue. The core was homogenised with a pestle in an Eppendorf tube with 3 ml of PBS solution equilibrated with atmospheric levels of O_2.

Mitochondrial mapping. Although mitochondria are not present in abundance throughout the lens (Bassnett & Beebe, 1992), they are expected to play a major role in shaping lens Po_2 profiles. Therefore, it was important to establish the precise distribution of mitochondria within the tissue. Two methods, rhodamine 123 staining and cytochrome *c*-oxidase (complex IV or COX) immunofluorescence, were used to visualise the distribution of mitochondria.

Rhodamine 123 is a mitochondria-specific dye that is taken up due to the membrane potential ($\Delta\Psi_m$) across the inner mitochondrial membrane (Emaus, et al., 1986). Fresh bovine lenses were incubated for 30 minutes at 37°C in AAH containing 100 µg/ml of rhodamine 123 (Molecular Probes, Eugene, OR, USA). After a brief wash, lenses were transferred to glass-bottomed Petri dishes and viewed on either a confocal (LSM 410, Carl Zeiss Inc., Thornwood, NY) or 2-photon (Bio-Rad Laboratories, Hercules, CA) microscope. Lenses treated with 100 µM carbonyl cyanide m-chlorophenylhydrazone (CCCP), served as negative controls. CCCP is a protonophore which inserts into the inner mitochondrial membrane and hence collapses $\Delta\Psi_m$ (Duchen, 1999). For three dimensional reconstructions, stacks of optical sections were collected at 4 µm intervals along the z axis using the 2-photon microscope. The anterior polar region, the posterior polar region or the equatorial region of the lens were imaged using a 20 X water immersion objective lens. Image stacks were reconstructed using volume rendering software (Voxblast 3.0; VayTek Inc., Fairfield, IA, USA) and the distribution of mitochondria was visualised by adjusting the alpha (transparency) value in the rendering algorithm.

Immunoflourescence was performed on fixed tissue using a mouse anti-bovine IgG_{2a} antibody to cytochrome *c*-oxidase of the mitochondrial respiratory chain (A-6431, Molecular Probes, Eugene, OR, USA). Lenses were fixed overnight in 4% paraformaldehyde/PBS. After rinsing in PBS, the lenses were boiled for 15-30 minutes in 50 mM TRIS, pH 8 (BP152-1, Fisher Scientific, Fairlawn, NJ, USA) for antigen retrieval. Lenses slices (200 μm thick) were prepared on a tissue sectioner (Vibratome 1000 Plus, The Vibratome Company, St Louis, MO, USA). Samples were permeablised in 0.1% Triton X (BP151 100, Fisher Scientific, Fairlawn, NJ, USA) in PBS for 15-30 minutes. Slices were then treated with a blocking solution (1% BSA/10% normal goat serum in PBS) for 1 hour. Then primary antibody to complex IV was added at a concentration of 1:200 to slices in fresh blocking solution. Samples were incubated overnight at 4°C in a moist environment. The next day, after rinsing for 30 minutes, slices were treated with a goat anti-mouse IgG secondary antibody conjugated to an Alexa 488 fluorescence (Alexa Fluor A-11001, Molecular Probes, Eugene, OR, USA) at 1:500 in blocking solution for two hours. After rinsing for 30 minutes, slices were mounted on slides, coverslipped and viewed on a confocal microscope (LSM 410, Carl Zeiss Inc., Thornwood, NY, USA).

Mitochondrial inhibition studies. The contribution of oxidative phosphorylation to lens QO_2 and its role in the establishment and maintenance of intralenticular P_{O2} gradients was examined by treatment with inhibitors of respiratory chain enzymes. Lenses were incubated in AAH containing inhibitors for four hours prior to QO_2 determination to ensure full equilibration. The effects of four different inhibitors: myxothiazol, 3-nitropropionic acid (3-NPA), and sodium cyanide and sodium azide were examined. Myxothiazol is an

irreversible blocker of cytochrome b-c_1 (Thierbach & Reichenbach, 1981), 3-NPA irreversibly blocks succinate dehydrogenase (complex II) (Coles, et al., 1979), and sodium cyanide and sodium azide both block cytochrome *c*-oxidase (complex IV or COX) (Leary, et al., 1998).

2.3 Results

Preliminary and control experiments

Optode performance

Optodes do not consume sufficient O_2 during the measurement process to alter the Po_2 of the solution or tissue (Vanderkooi, et al., 1991). To verify that this was indeed the case, we performed preliminary Po_2 measurements in water containing various concentrations of BSA (Figure 2.2). The Po_2 measurements were insensitive to protein concentration at least up to 30% (w/v) BSA, which is approximately equivalent to the protein concentration in the centre of the human lens (Fagerholm, et al., 1981).

Figure 2.2 *Effect of protein on optode Po_2 readings. Solutions containing various concentrations of bovine serum albumin were equilibrated overnight with gas containing Po_2 of 38 mmHg (horizontal line). The apparent Po_2 measured with the optode was insensitive to the protein concentration. Results shown are from one optode only.*

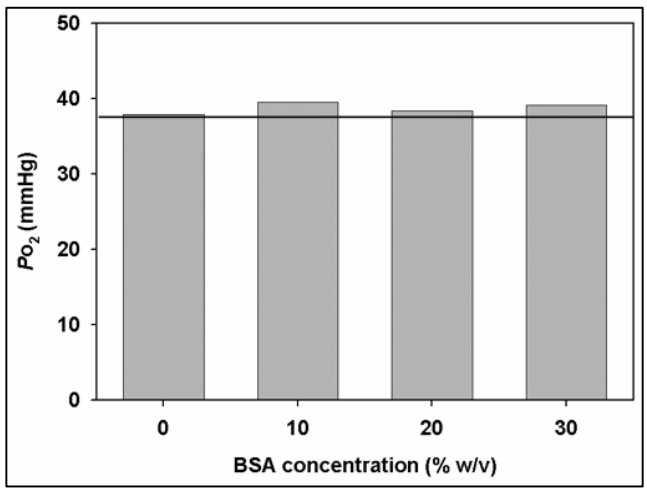

As lens Po_2 is expected to be low (§1.7.3), it was important to examine optode performance under hypoxic conditions. The manufacturer reports an error of ± 0.7 mmHg at low Po_2 values. To test this, the optode was placed in solutions where the Po_2 was known to be 0 mmHg: namely, in H_2O gassed with 100% N_2 and a chemical zero solution of sodium sulphite/sodium tetraborate (S4150, Radiometer Copenhagen, Willich, Germany). In addition, the Po_2 was measured in an isolated bovine lens incubated in AAH gased with 100% N_2. In all of these situations, the optode reading was within 0.7 mmHg of zero (n=3 for each condition). Optode measurements in the isolated bovine lens equilibrated with 100% N_2 are presented in Figure 2.3. These experiments established that there was no systematic instrumental offset and that the optode gave reproducible readings with an acceptable level of accuracy in hypoxic conditions.

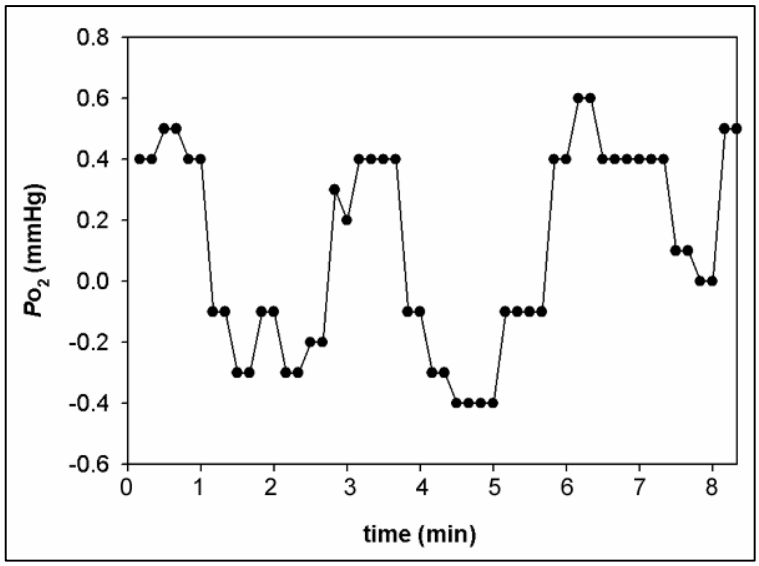

Figure 2.3 *Optode accuracy in anoxic conditions. The graph shows the optode reading from the centre of a bovine lens equilibrated with 100% N_2. A measurement was taken every 10 s over several minutes. The error was within ± 0.6 mmHg in this example.*

The lens is surrounded by a thick basement membrane, the lens capsule, which is thickest over the epithelium and thinnest posteriorly (Bron, 1997). Experiments in rabbit

lenses were undertaken to examine whether the capsule acted as a physical barrier to the introduction of the optode. When inserted into a lens with an intact capsule, the optode indented but remained tethered to the capsule and was unable to pierce it until at a point 2-3 mm into the lens (Figure 2.4C).

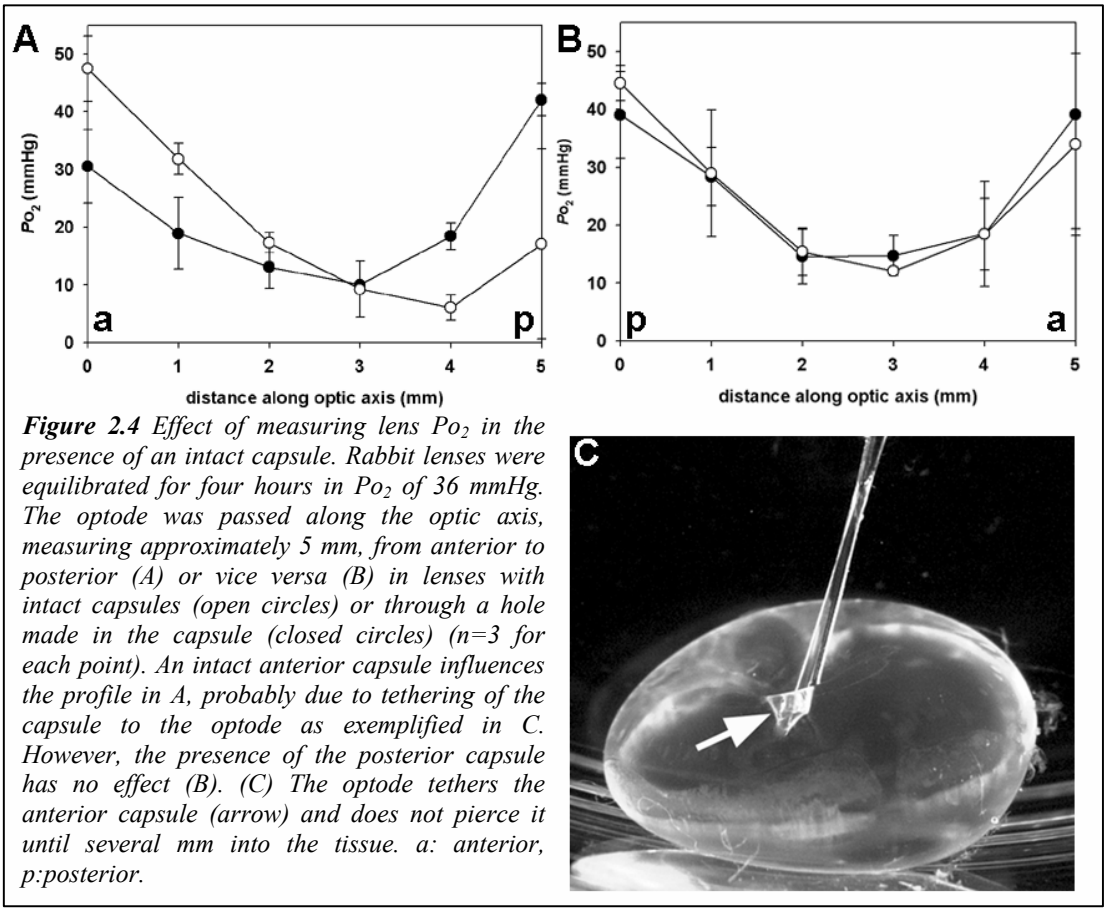

Figure 2.4 *Effect of measuring lens Po_2 in the presence of an intact capsule. Rabbit lenses were equilibrated for four hours in Po_2 of 36 mmHg. The optode was passed along the optic axis, measuring approximately 5 mm, from anterior to posterior (A) or vice versa (B) in lenses with intact capsules (open circles) or through a hole made in the capsule (closed circles) (n=3 for each point). An intact anterior capsule influences the profile in A, probably due to tethering of the capsule to the optode as exemplified in C. However, the presence of the posterior capsule has no effect (B). (C) The optode tethers the anterior capsule (arrow) and does not pierce it until several mm into the tissue. a: anterior, p:posterior.*

To examine whether the inability of the optode to readily penetrate the capsule had an effect on Po_2 profiles, we compared profiles in rabbit lenses with intact capsules to lenses in which a small hole was made in the capsule with a 25G needle (Figure 2.4, A and B). Lenses were equilibrated for four hours in a Po_2 of 36 mmHg (5% O_2) at 37°C and the

optode was driven through the lens along the optic axis from anterior to posterior or vice versa. The presence of an intact posterior capsule had no effect on lens profiles recorded from posterior to anterior (Figure 2.4B). However, the intact anterior capsule had a distorting effect on profiles recorded from anterior to posterior (Figure 2.4A), probably due to the greater thickness of the capsule over the epithelium. Therefore, all lens Po_2 profiles were recorded by inserting the optode through a small hole made in the capsule.

We also wanted to assess the signal:noise for the optode Po_2 measurements in the lens. The optode was passed in millimetre increments through bovine lenses equilibrated in AAH containing Po_2 of 36 mmHg (5% O_2). Figure 2.5 shows an example of an optode trace along the optic axis from anterior to posterior. Optode readings were stable within approximately 2 minutes and had a good signal:noise ratio.

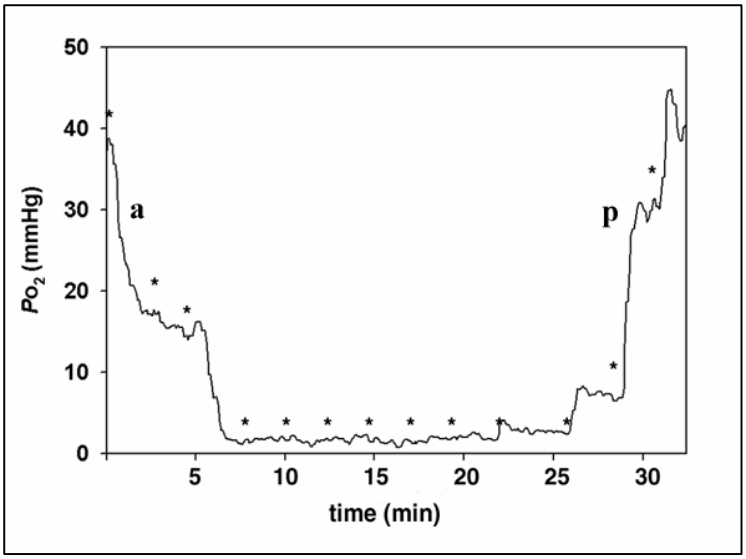

Figure 2.5 *Optode trace through an isolated bovine lens. A lens was equilibrated in a Po_2 environment of 36 mmHg (5% O_2). The optode was passed along the optic axis from anterior (a) to posterior (p) and the Po_2 monitored over time. The optode was advanced via the micromanipulator in mm steps (asterisks) every 2-3 minutes. At time zero, the optode was at the anterior surface. The readings at each position were stable prior to the next advancement. The trace also shows a high signal: noise ratio.*

Lens equilibration

Ideally, in vitro Po_2 and QO_2 measurements on isolated lenses should accurately reflect a system at steady state. To ensure this, we investigated lens equilibration time by inserting the optode into the geometric centre of isolated bovine lenses in AAH. Po_2 was monitored over time in response to a change in Po_2 of the AAH. In an AAH solution Po_2 of 7 mmHg (1% O_2), the core Po_2 stabilised at <2 mmHg after a few hours. An increase in the AAH Po_2 to 150 mmHg (21% O_2) caused a rise in core Po_2. A new stable Po_2 value was reached within four hours (n=4, one example shown in Figure 2.6). This value was stable for at least 12 hours (the longest time assessed), indicating that a new steady state had been reached. In light of this, all bovine lenses were equilibrated for four hours in the test environment before Po_2 or QO_2 measurements were made.

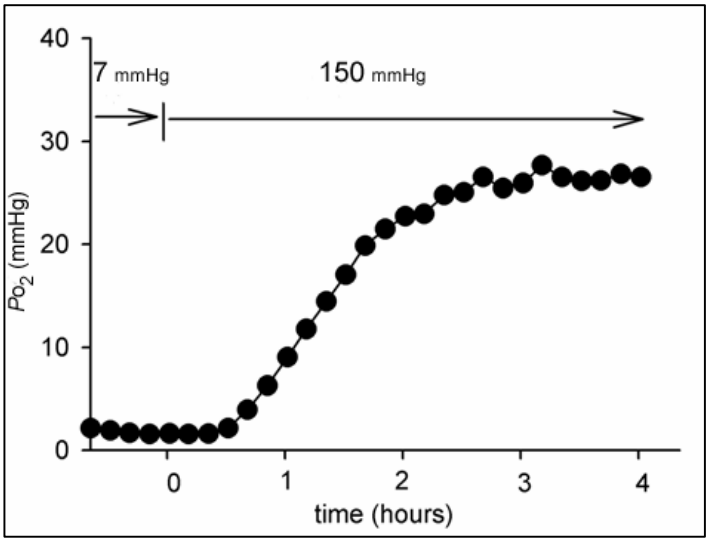

Figure 2.6 *Bovine lens equilibration time. The optode tip was inserted into the lens core and the response of core P_{O_2} to a change in the Po_2 of the bathing medium (from 7 to 150 mmHg or from 1% to 21% O_2) was monitored. Note that a new steady state value is established within three hours in this example.*

The change to lens tissue O_2 levels that occurs after varying the lens environment raises the issue of whether lens O_2 measurements made immediately after arrival in the laboratory are reflections of the lens in a steady state. It may be that changes in eye Po_2

after death of the animal have caused significant changes to lens Po_2 in the 4-5 hours during transport on ice to the lab. Therefore, we compared Po_2 profiles in bovine lenses straight after dissection from the eye (unequilibrated lenses) to lenses that were equilibrated in a Po_2 environment of 36 mmHg (5% O_2) for 4 hours (Figure 2.7). Measurements on both groups of lenses were made in a Po_2 environment of 36 mmHg.

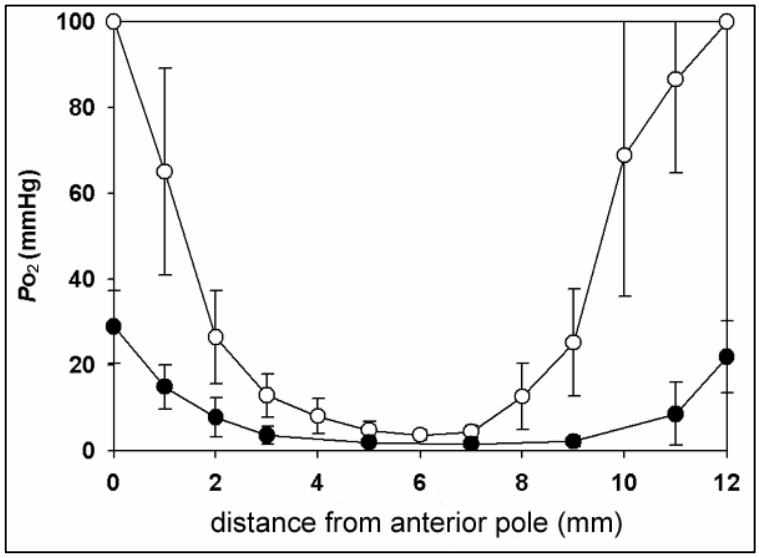

Figure 2.7 *Comparison of Po_2 profiles in equilibrated and unequilibrated bovine lenses. Isolated bovine lenses were placed in an environment of 36 mmHg (5% O_2) and the optode was passed along the optic axis from anterior to posterior. The unequilibrated bovine lenses (which were examined immediately after dissection, open circles) consistently showed higher values and longer gradients than the equilibrated lenses (which had been incubated in AAH with a Po_2 of 36 mmHg for 4 hours, closed circles) (n=6 each).*

Po_2 in the lens centre was not dramatically different between the two groups, being 1.6 ± 0.5 mmHg and 3.7 ± 1.3 mmHg (n=6 each) for the equilibrated and unequilibrated groups respectively. However, unequilibrated lenses had a consistently different Po_2 profile to that of the equilibrated lenses. The Po_2 in the outer 3 mm of cortex in unequilibrated lenses decreased from ≥100 mmHg to ≤20 mmHg. The gradient in equilibrated lenses, on the other hand, decreased from approximately 30 mmHg to ≤5 mmHg over the same distance. The explanation for the higher Po_2 in unequilibrated lenses may lie in the effect of low temperature on the eye during transportation. As demonstrated later in this chapter, sub-physiological temperature reduces lens QO_2 and hence raises lens Po_2.

From the above studies, we conclude that bovine lenses require approximately 3-4 hours equilibration time to provide measurements that reflect a lens in a steady state.

Po_2 profiles and QO_2 in the mammalian lens in vitro

Po_2 profiles

The distribution of O_2 was mapped in detail in isolated bovine lenses. Lenses equilibrated in a solution Po_2 of 36 mmHg (5% O_2) were examined along the equatorial and optic axes (Figure 2.8). Profiles were symmetrical across both axes. A steep Po_2 gradient was present in the superficial cortex across both axes resulting in a low Po_2 (1-2 mmHg) throughout most of the lens interior.

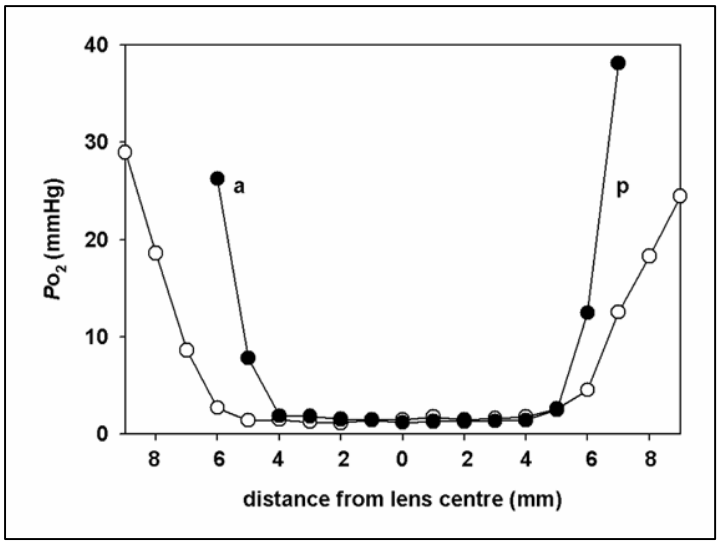

Figure 2.8 *Po_2 profiles along perpendicular axes in the bovine lens. A lens was equilibrated in physiological conditions (Po_2 of 36 mmHg or 5% O_2) and the optode passed along the optic (filled circles. a: anterior, p: posterior) and equatorial (open circles) axes. The profiles have been aligned with reference to the centre of the lens for comparison. Note the steep gradients in the cortex resulting in a low Po_2 (<2 mmHg) throughout most of the lens core. The profiles are symmetrical along both axes.*

We examined the effect of varying the external Po_2 on the internal Po_2 profile of the lens (Figure 2.9). The optode was passed along the optic axis from anterior to posterior (or vice versa) in lenses after equilibration in AAH containing various levels of O_2.

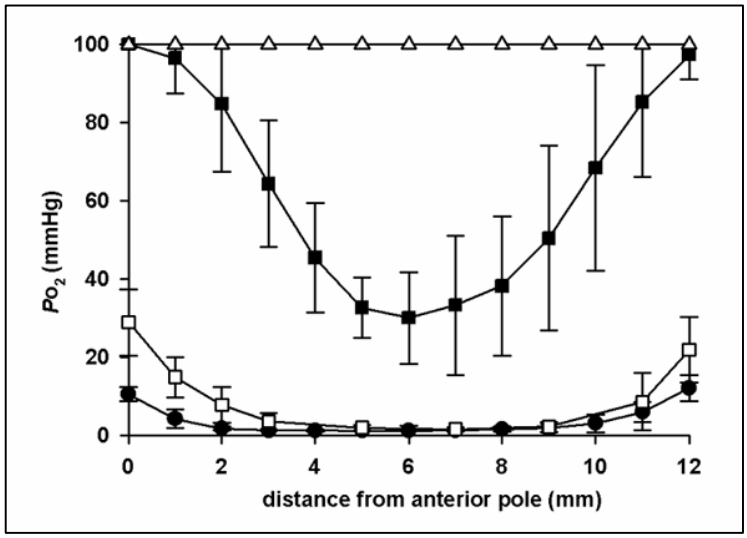

Figure 2.9 *The effect of external Po_2 on bovine lens Po_2 profiles. Bovine lenses were equilibrated with a Po_2 of 7 mmHg (1% O_2, filled circles), 36 mmHg (5% O_2, open squares), 150 mmHg (21% O_2, filled squares) or 720 mmHg (100% O_2, open triangles) and profiles measured along the optic axis from anterior to posterior or vice versa. In each case, data represent the mean ± SD of at least six independent measurements. In all cases the profiles were symmetrical. Under physiological conditions (≤ 36mmHg or 5% O_2), the P_{O2} throughout most of the lens is <2 mmHg. Note that the upper range of the O_2 sensor is 100 mmHg and is exceeded following treatment with 100% O_2.*

Under physiological conditions (external Po_2 of 7-36 mmHg, or 1-5% O_2), the internal Po_2 profiles were symmetrical, with gradients across the outer 2-3 mm of cortex (n=6 each). Po_2 was low and relatively constant throughout most of the lens core, being approximately 1.5 mmHg in the lens centre. The direction in which the lens was traversed (anterior to posterior or vice versa) did not significantly influence the profile (data not shown). Lenses in atmospheric levels of O_2 (Po_2 of 150 mmHg or 21% O_2) also displayed symmetrical gradients. However, the gradients extended from the surface to the lens centre. The central Po_2 was 30.1 ± 11.7 mmHg (n=6), significantly higher than under physiological conditions. Lenses equilibrated with 100% O_2 saturated the optode readings (n=6). For all conditions examined, profiles were symmetrical, suggesting that the anterior epithelial layer does not disproportionately influence tissue O_2 levels compared to the same volume of fibre cells in the cortex.

The relationship between external Po_2 and Po_2 measured in the geometric centre of the lens is shown in Figure 2.10. In a low Po_2 environment of 7, 14 or 36 mmHg (1, 2 or 5% O_2), the core Po_2 is below approximately 1.5 mmHg (n=6, each), suggesting the bovine lens has a capacity to buffer O_2 levels in the lens centre. However, this resistance to change diminishes when the external Po_2 is raised to the supra-physiological level of 72 mmHg (10% O_2) or above. Interestingly, the core Po_2 is always substantially lower than that of the bathing solution, even when the bathing solution Po_2 is above physiological levels.

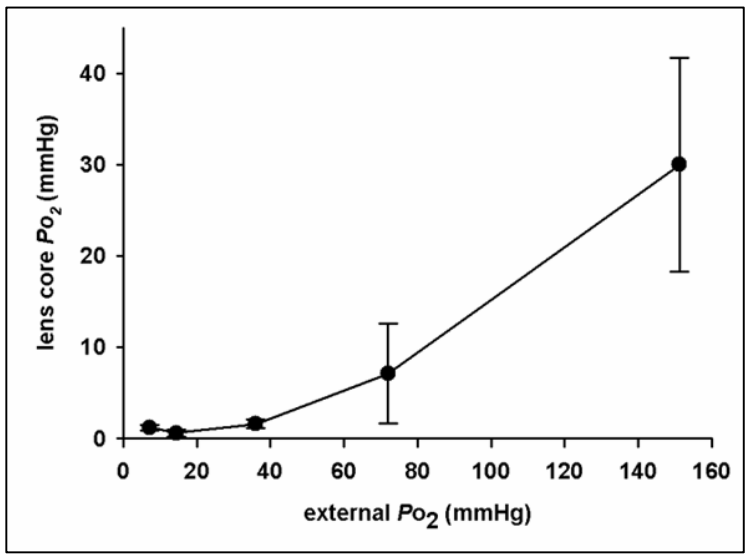

Figure 2.10 *Bovine lens core Po_2 as a function of external Po_2. Data represent at least six independent measurements in each Po_2 environment. Lens core P_{O_2} is relatively constant at ~1.5 mmHg under physiological conditions (≤36 mmHg). Core Po_2 does not increase until external Po_2 is raised to supra-physiological values (≥ 70 mmHg or 10% O_2).*

Bovine lens core Po_2measured immediately after death

The mean Po_2 in the centre of the bovine lens in a Po_2 environment of 36 mmHg (5% O_2) was 1.6 ± 0.5 mmHg (n = 6). Because this environment approximates the concentration of O_2 surrounding the lens *in vivo*, we suspected that core Po_2 measured under these conditions might be close to the *in vivo* value. To obtain a better estimate of the *in vivo* core Po_2, we took the optode system to a local abattoir to record lens core Po_2 values as soon as

possible after animals were killed. It was usually possible to complete the measurements within 15 minutes of death. Measurements made in this fashion gave a core Po_2 value of 1.3 ± 0.5 mmHg (n=6). This value did not differ significantly from that recorded in vitro in a Po_2 environment of 36 mmHg.

Calculation of tissue O_2 concentration

Values for O_2 solubility range from 1.52 μM/mmHg in serum (Groebe & Vaupel, 1988) to 1.35 μM/mmHg in pure water (Hitchman, 1978) and 0.93 μM/mmHg in tumour tissue (Grote, et al., 1977). If we assume a comparable solubility of O_2 in the bovine lens of 1 μM/mmHg, then the concentration of O_2 in the centre of a lens equilibrated in a Po_2 environment of 36 mmHg is 1-2 μM.

Po_2 profiles in the rabbit lens

To establish whether Po_2 gradients are a feature of other mammalian lenses, we measured profiles along the optic axis of rabbit lenses equilibrated in a Po_2 of 36 mmHg (Figure 2.11). Similar to the bovine lens, gradients were found in the outer ~2mm of cortex of rabbit lenses. However, due to the smaller size of the rabbit lens (9 x 5 mm), the gradient covered a larger proportion of the lens radius. A further difference between the two species was that the rabbit core Po_2 was higher at ~12 mmHg, a value similar to a recent report of 10.3 mmHg in the centre of a rabbit lens measured in vivo (Barbazetto, et al., 2004).

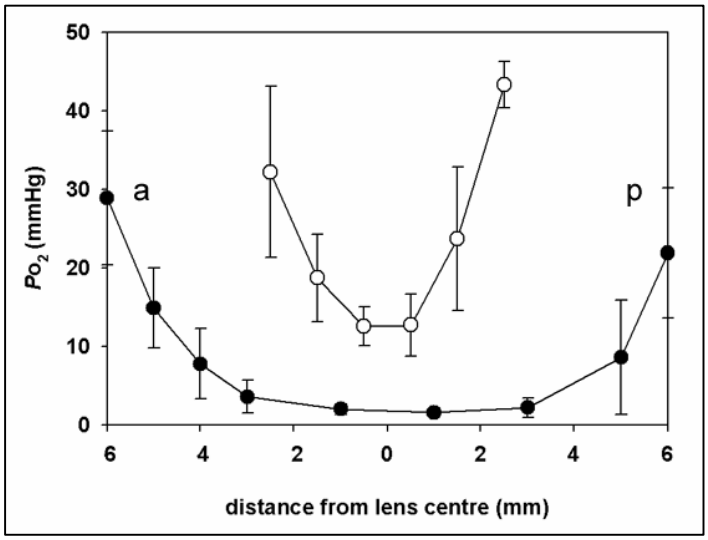

Figure 2.11 *Po_2 gradients in bovine and rabbit lenses. Lenses were equilibrated in Po_2 of 36 mmHg and the optode passed along the optic axis from anterior (a) to posterior (p). Bovine profiles from Figure 2.9 are included for comparison with the rabbit lens. Gradients were found in the cortex of both the rabbit (open circles, n=6) and the bovine lens (closed circles, n=6) leading to core hypoxia. The smaller rabbit lens, however, has a significantly higher core Po_2.*

In summary, the in vitro Po_2 measurements in bovine and rabbit lenses show Po_2 gradients in the lens cortex which lead to a low Po_2 in the lens core. O_2, however, is usually a permeant molecule (see §2.1), and would be expected to be evenly distributed throughout the lens in the absence of O_2 consumption. Therefore, the presence of Po_2 gradients implies O_2 consumption in the cortex. We will now examine lens O_2 consumption and in a later section analyse the contribution of the various regions of the lens to the O_2 consumption rate (QO_2).

Lens QO_2

To establish the relationship between Po_2 and QO_2, respirometric measurements were undertaken. The consumption of O_2 by the bovine lens in atmospheric amounts of O_2 (Po_2 of 150 mmHg or 21% O_2) is shown in the respirometry trace presented in Figure 2.12. Control experiments, where AAH, but no lens, was placed in the chamber, established that the AAH was not responsible for the O_2 consumption.

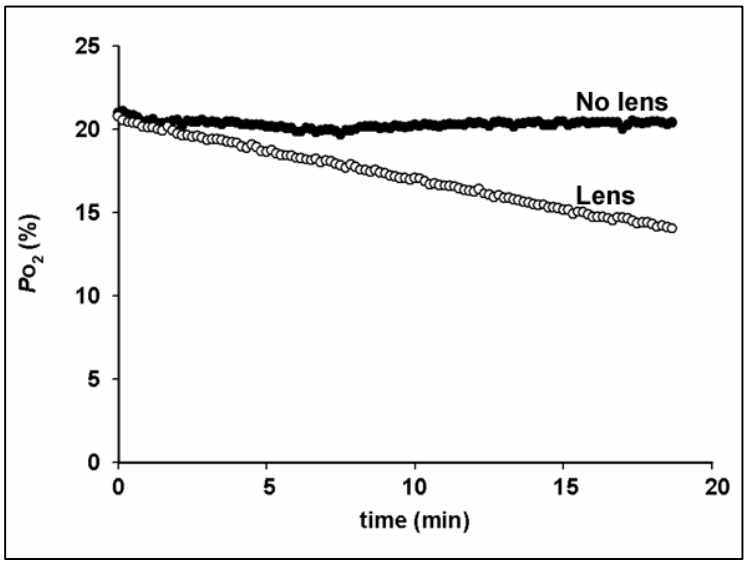

Figure 2.12 *Respirometry trace produced by a bovine lens in atmospheric levels of O_2 (150 mmHg or 21% O_2) at 37°C. An equilibrated lens was placed in 3 ml of AAH in the sealed respirometry chamber. Po_2 of the AAH surrounding the lens was monitored over time via an electrode incorporated into the sealed chamber. O_2 consumption by the lens reduced the Po_2 of the AAH (open circles). The slope of the line produced is used to calculate QO_2. The control experiment where AAH was placed in the chamber without a lens (filled circles), showed that O_2 was consumed by the lens.*

Previous reports of lens QO_2 values were obtained usually from unequilibrated lenses placed in solutions containing atmospheric levels of O_2 (Po_2 of 150 mmHg or 21% O_2) at a variety of temperatures (see §2.4). Therefore, we compared bovine lens QO_2 at 37°C after a 4 hour equilibration in atmospheric levels of O_2 to the QO_2 of lenses equilibrated with a physiological Po_2 environment of 36 mmHg (5% O_2). Bovine lens QO_2 varied with the Po_2 of the bathing solution, being 7.5 ± 1.8 (n=8) and 4.8 ± 0.1 µl/g/h (n=10) in a Po_2 environment of 150 mmHg and 36 mmHg, respectively (Figure 2.13).

Figure 2.13 *Effect of external Po_2 on bovine lens QO_2. Respirometry was performed on lenses at 37°C in AAH containing known amounts of O_2. QO_2 was approximately 50% higher under atmospheric conditions (150 mmHg or 21% O_2) compared to physiologic levels (36 mmHg or 5% O_2) (n)= number of lenses.*

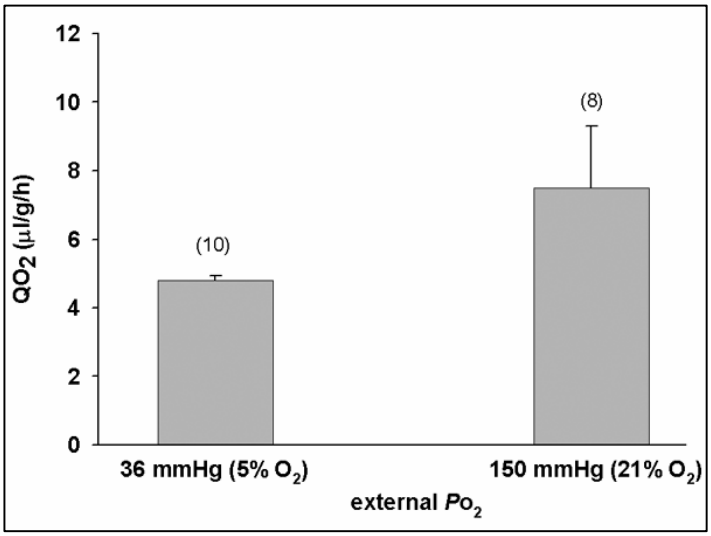

We also measured QO_2 in rabbit lenses in a Po_2 environment of 36 mmHg (5% O_2). Rabbit lenses consumed O_2 at the rate of 6.8 ± 1.3 µl/g/h (or 1.8 ± 0.3 µl/lens/h) (n=10).

The effect of temperature on lens QO_2, Po_2 and the diffusibility of O_2

The shape of Po_2 profiles in the lens is determined by both lens QO_2 and the effective diffusion coefficient of O_2 (D_{O2}). For example, if the D_{O2} was high, then this would lead to high Po_2 values in the lens core and relatively flat Po_2 gradients. To study the diffusion of O_2 in the lens, we will need to curtail lens O_2 consumption. One possible way of decreasing metabolism is by lowering the temperature of the tissue. In light of this, bovine lens QO_2 and Po_2 was examined at sub-physiological temperatures.

The effect of temperature on lens QO_2 in a Po_2 environment of 36 mmHg is shown in Figure 2.14.

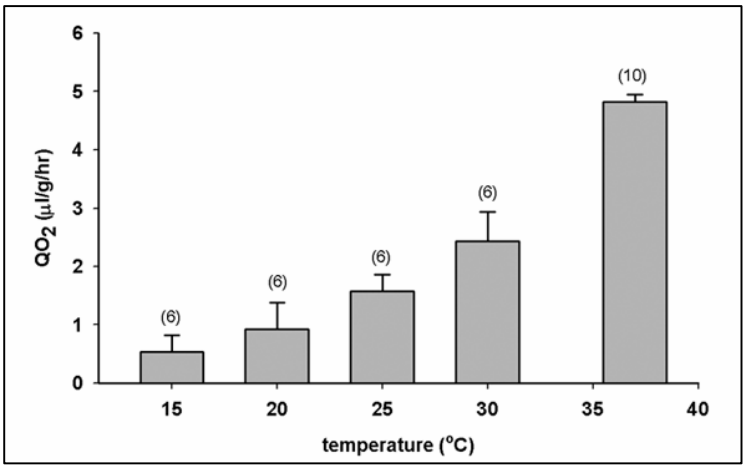

Figure 2.14 *Effect of temperature on bovine lens QO_2. Respirometry was performed with AAH equilibrated with a Po_2 of 36 mmHg (5% O_2) and at various temperatures ≤37°C. QO_2 dropped with a decrease in temperature. At room temperature (20°C) or below, QO_2 was reduced by ≥80%. (n) = number of lenses.*

Incremental decreases in temperature below physiological values resulted in lower QO_2. Lowering the temperature from 37°C to room temperature (20°C) resulted in a fall in QO_2 from 4.8 ± 0.1 to 0.9 ± 0.5 µl/g/h (n=10 and 6, respectively), a decrease of >80%.

To examine the diffusion of O_2 within the lens, we took advantage of the effect of temperature on QO_2 values. Po_2 and temperature in the lens centre were monitored as the external temperature was alternated between 37°C and room temperature (20°C) in a bovine lens surrounded by atmospheric levels of O_2 (150 mmHg or 21% O_2) (Figure 2.15).

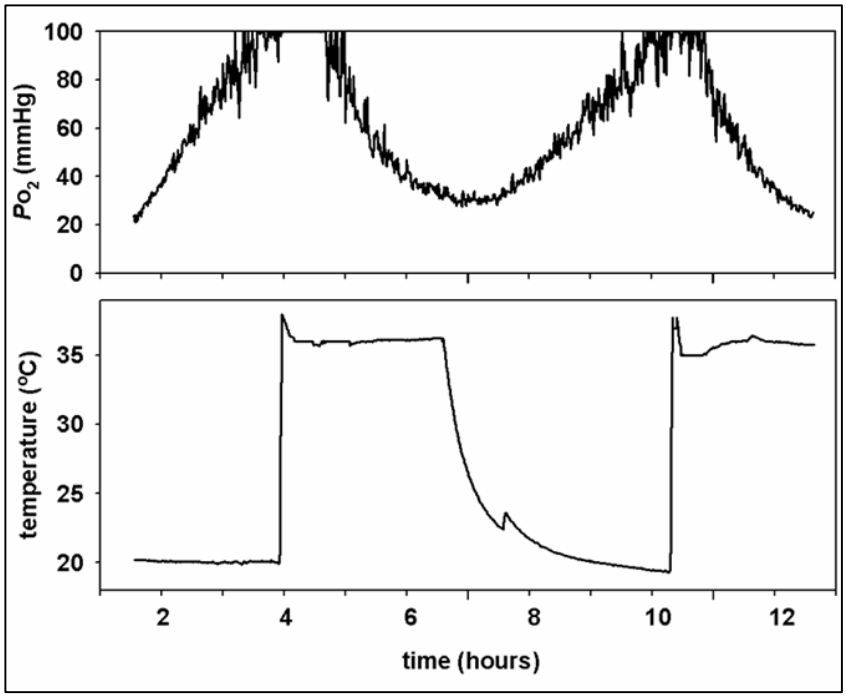

Figure 2.15 *The effect of temperature on bovine lens P_{O2}. Lenses were equilibrated in AAH with atmospheric levels of O_2 (150 mmHg or 21% O_2). The P_{O2} and temperature in the centre of the lens were recorded as the temperature of the AAH was alternated between 37°C and room temperature (20°C). The lower temperature caused a steady rise in core P_{O2} to >100 mmHg over ~3 hours. Warming the lens caused a decrease in P_{O2} back to control values.The phenomenon was repeatable as shown in the latter (right) half of the figure.*

The lower temperature resulted in a rise in Po_2 to >100 mmHg over ~3 hours. Switching to physiological temperature caused a decrease in Po_2 which stabilised at expected control values of ~30 mmHg (see Po_2 in centre of bovine lens equilibrated with 150 mmHg in Figure 2.10). This pattern was repeatable with subsequent alternations in

temperature. Although a decrease in temperature increases the solubility of O_2 in solution (Table 2.2), the change in solubility does not explain the effect on Po_2 measurements. Therefore, from these data, we can conclude that O_2 levels in the lens are very dependent on QO_2 and temperature. Furthermore, there appears to be no barrier to the diffusion of O_2 in the bovine lens.

The role of mitochondria

The distribution of mitochondria in the bovine lens

Mitochondria are suspected to play a role in determining O_2 levels in the lens due to the consumption of O_2 in oxidative phosphorylation. However, mitochondria are not evenly distributed throughout the lens (see §1.7.1). They are present only in the anterior epithelium and outer fibre cells. At a well defined depth below the lens surface, mitochondria are eliminated from the cytoplasm along with all other intracellular organelles. Therefore, the lens contains two populations of fibre cells: differentiating fibres (DF), which contain mitochondria, and mature fibres (MF), which do not. We sought to map the distribution of mitochondria in the bovine lens in order to understand their influence on Po_2 gradients.

Living bovine lenses were treated with the vital mitochondria-specific dye rhodamine 123 (Emaus, et al., 1986) for 30 minutes at 37°C, rinsed and viewed on either a confocal or a 2-photon microscope. The density of mitochondria was higher in the anterior epithelium (Figure 2.16A and E), than in cortical fibre cells (B-F). Consistent with

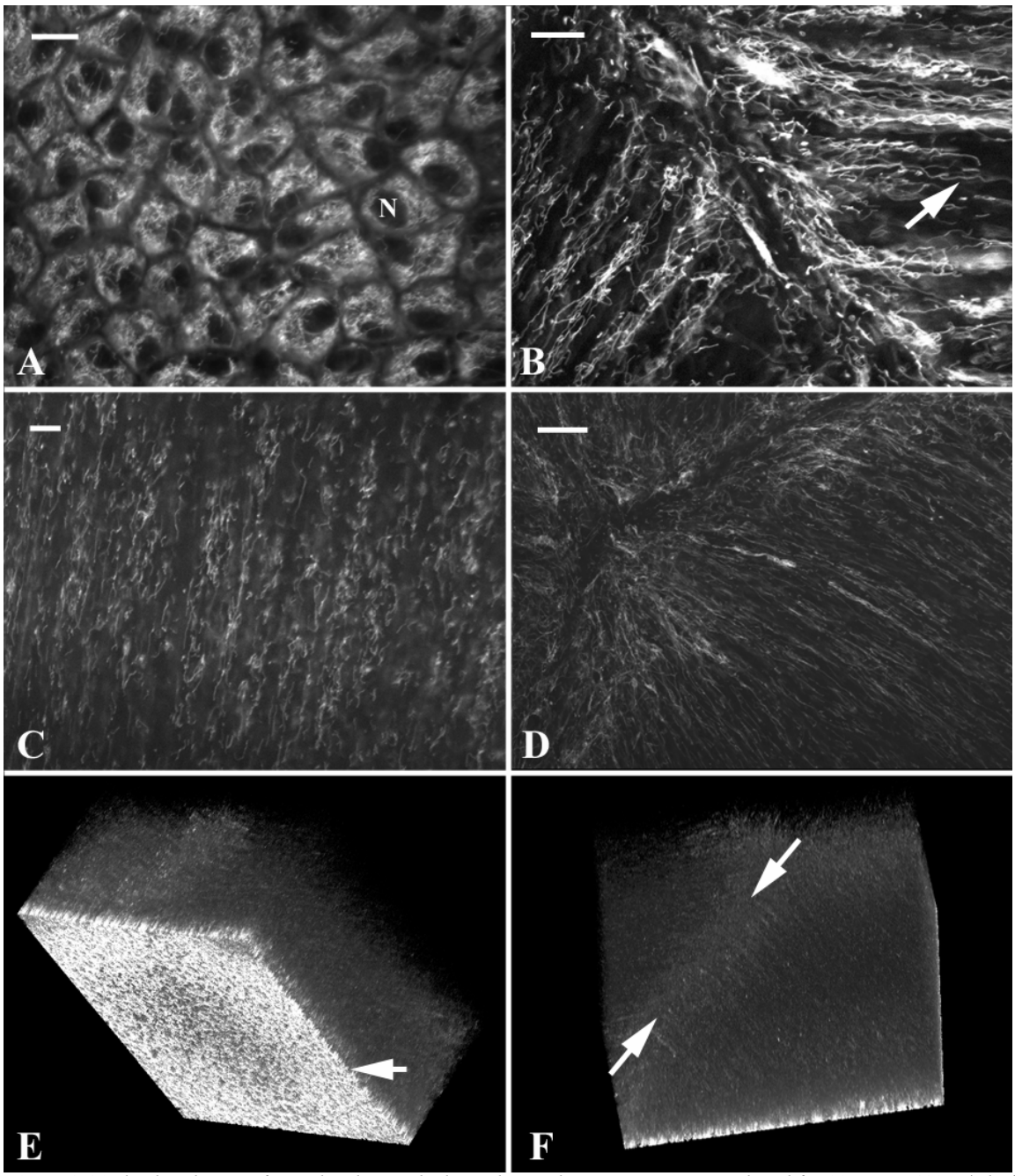

Figure 2.16 *The distribution of mitochondria in the living bovine lens. Lenses were incubated for 30 min in 100µg/ml of rhodamine 123.* ***A****. Confocal image of the lens epithelium viewed en face. Bundles of mitochondria surround the unstained epithelial cell nuclei (N).* ***B.*** *Confocal image of mitochondria in fibre cells immediately beneath the anterior epithelium. Mitochondria were aligned with the long axis of the fibres and relatively abundant in the region where the fibre tips converged at the sutures. Note the elongated morphology of the mitochondria (an example of which is arrowed).* ***C****. 2-photon image of fibre cells at the equator. Mitochondria run vertically, parallel to the long axis of the cell.* ***D.*** *2-photon image of the posterior pole. Mitochondria congregate near the fibre cell tips, similar to B, thus outlining the Y-shaped suture on the left.* ***E.*** *Three dimensional reconstruction of a 845 x 845 x 476 µm region of the anterior lens cortex imaged with a 2-photon microscope. The highly fluorescent lens epithelium (arrowed) overlies a region of less intense fibre cell fluorescence. In this region, mitochondrial staining extends approximately 0.5 mm into the cortex.* ***F.*** *The same data set as E viewed from behind to reveal the enhanced mitochondrial fluorescence adjacent to the anterior suture (indicated by the arrows). Scale bars: A, B, C=10 µm, D=25 µm.*

previous reports on chicken and rat lenses (Bantseev, et al., 1999;Bassnett & Beebe, 1992), mitochondria in the underlying fibre cells were branched, elongated structures aligned with the long axis of the cell. Mitochondria existed in a continuous shell in the outer cortex. The depth of the mitochondria-containing layer in the anterior, equatorial and posterior cortices was 525 ± 75, 725 ± 25, and 500 ± 25 μm, respectively (n=3). This represents approximately 9% of the lens diameter for each axis. In control experiments, where lenses were pre-treated with the $\Delta\Psi_m$ collapsing drug CCCP, no fluorescence is observed (data not shown), showing that rhodamine 123 specifically labelled active mitochondria.

The depth of the mitochondria containing cell layer in rhodamine 123 treated lenses may be an underestimate due to a number of factors. The rhodamine 123 may not have completely penetrated into the lens core. In addition, there may be a limit to the depth to which the microscope lens can detect signal within the intact lens. Therefore, we employed a second technique using lens slices instead of whole lenses in order to avoid these potential difficulties. Fixed bovine lens slices were processed for immunofluorescence using an antibody to cytochrome *c*-oxidase. The distribution of mitochondria revealed using immunofluorescence was similar to that seen with rhodamine 123 staining. Mitochondria were confined to the outer cortex of the lens with a predominance in the epithelium (Figure 2.17A). Mitochondrial depths in the anterior, equatorial and posterior cortices were 380 ± 88 μm, 816 ± 54 μm and 305 ± 2 μm (n=3 lenses each), respectively. The shallower depths across the anterior and posterior cortices are probably reflections of the shrinkage in the tissue that occurs during fixation and antigen retrieval. The larger value for the equatorial cortex reported with the immunofluorescent technique could be a result of slices taken at an

oblique angle. However, the morphology of the mitochondria differed slightly with the two techniques. Using immunofluorescence, the appearance of the mitochondria ranged from

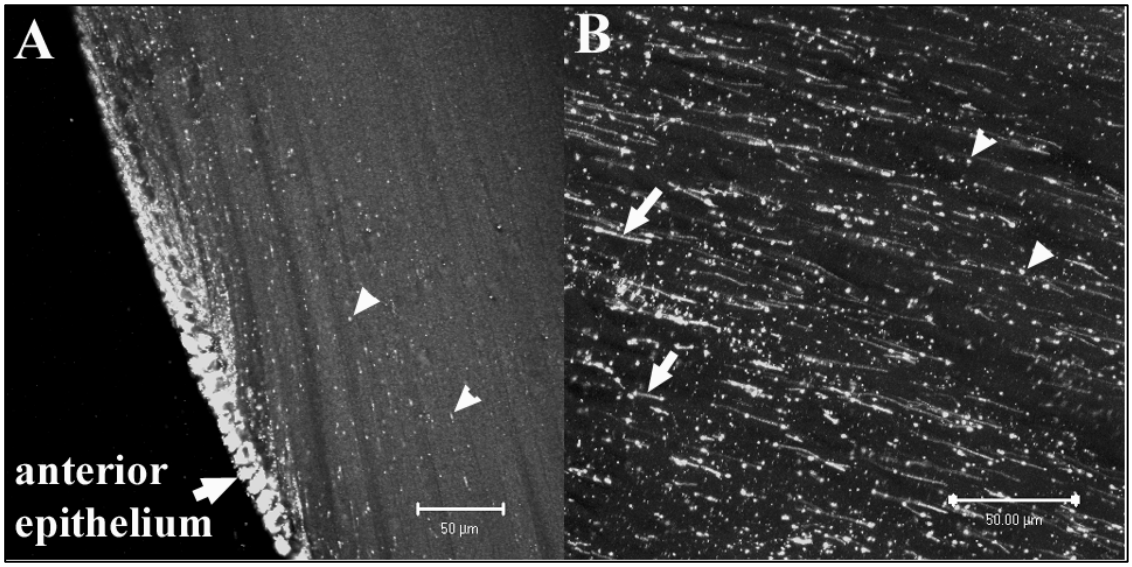

Figure 2.17 *Distribution of mitochondria in the bovine lens using COX-antibody immunofluorescence.* ***A.*** *Low power micrograph of equatorial region showing mitochondria in the outer cortex. The density of mitochondria was highest in the anterior epithelium (arrow). Mitochondria were punctate in appearance (arrowheads). Scale bar=50µm.* ***B.*** *High power view of equatorial region. Although some mitochondria appeared punctate (arrowheads), others were elongated (arrows). Scale bar= 50µm.*

elongated to punctate (Figure 2.17). The punctate appearance of the mitochondria may be an artefact of fixation or antigen retrieval. Alternatively, these truncated mitochondria may have lacked a membrane potential and consequently were not detectable using rhodamine 123.

Mitochondria and their relation to Po_2 gradients

Mitochondria exist to a depth of approximately 500 µm below the surface of the bovine lens according to rhodamine 123 staining (Figure 2.16). However, the bovine lens Po_2 gradients under physiological conditions (external Po_2 of 36 mmHg or 5% O_2) extend from the surface 2-3 mm into the lens (see Figure 2.9). The gradients therefore cross the DF, which contain mitochondria, and also extend into the MF, which do not (Figure 2.18).

This implies that there are at least two O_2-consuming compartments in the lens: the outer DF region, in which mitochondrial O_2-consumption may occur, and an inner MF region in which non-mitochondrial O_2 consumption occurs. The ability of the lens core to consume O_2 will be tested directly in the section on regional analysis.

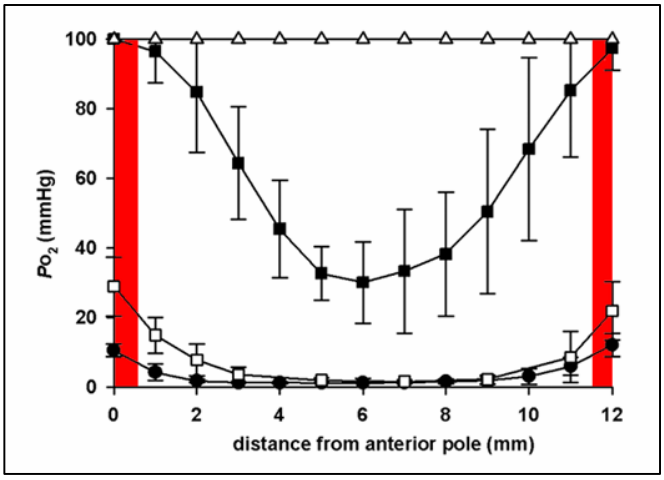

Figure 2.18 *The relationship between mitochondria and Po_2 profiles in the bovine lens. The depth of mitochondria (~500 μm, red columns) is superimposed on the Po_2 profiles from Figure 2.9. The Po_2 gradients extend into the lens beyond the region which contains mitochondria. This implies that there is non-mitochondrial O_2 consumption in the lens core.*

Mitochondrial inhibition studies

The contribution of oxidative phosphorylation in the DF region to bovine lens QO_2 and its effect on Po_2 gradients were assessed by treating lenses with drugs that inhibit mitochondrial respiration. QO_2 and Po_2 were measured following a 4-hour incubation at 37°C in AAH equilibrated with a Po_2 of 36 mmHg (5% O_2) and containing the mitochondria-inhibiting drugs.

The effects of all the drugs used were similar. Myxothiazol inhibited bovine lens QO_2 in a dose-dependent fashion (Figure 2.19). In a Po_2 environment of 36 mmHg, control bovine lens QO_2 was 4.8 ± 0.1 μl/g/h (n=10).

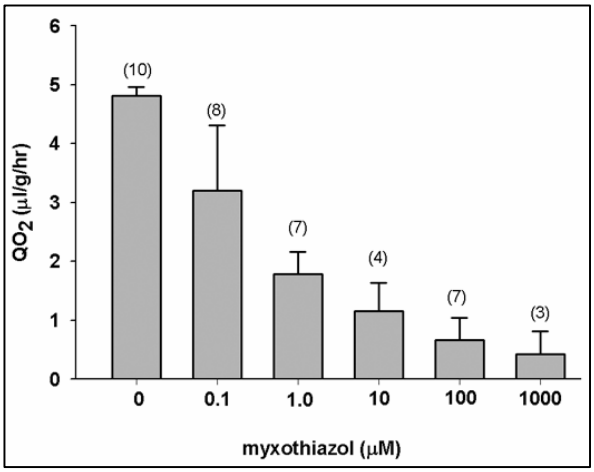

Figure 2.19 *The role of mitochondria in bovine lens QO_2. Lens respirometry was performed in 36 mmHg (5% O_2) at 37°C in the presence of various concentrations of the oxidative phosphorylation inhibitor myxothiazol. QO_2 was inhibited by myxothiazol in a dose dependent fashion. (n) = number of lenses.*

At 1 mM, myxothiazol caused a 91% decrease in QO_2 to 0.7 ± 0.4 µl/g/h (n=7). For comparison, under the same conditions, 3-NPA (0.5 mM), azide (5 mM) and cyanide (10 mM) caused a 66%, 79% and 90% decrease in QO_2, respectively (data not shown).

Myxothiazol treatment also produced a concomitant change in the intralenticular Po_2 profile (Figure 2.20).

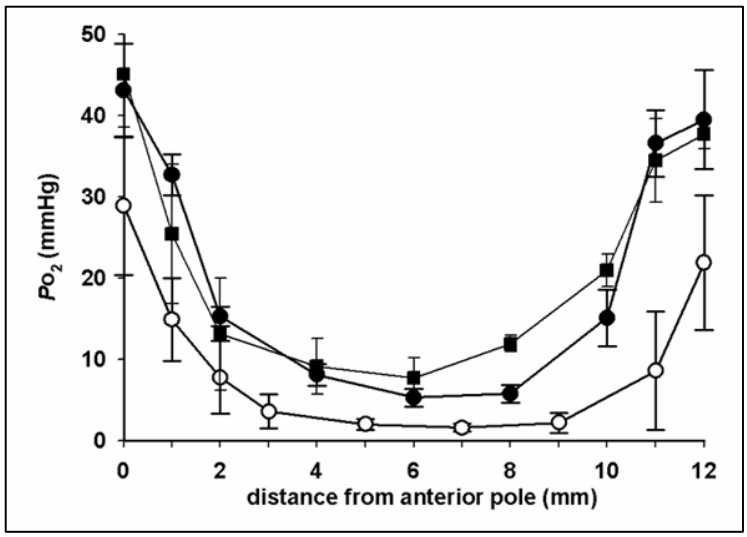

Figure 2.20 *Effect of mitochondrial inhibitors on bovine lens P_{O_2} profiles. Lenses were equilibrated in 36 mmHg (5% O_2) for 4 hours in the presence of 10 µM myxothiazol (filled circles, n=4) or 5 mM azide (filled squares, n=4) and profiles measured along the optic axis. Compared to control lenses (open circles, n=6), treated lenses have a higher P_{O_2} at all points within the lens.*

In lenses equilibrated in a Po_2 of 36 mmHg, treatment with 10 μM myxothiazol caused a generalised increase in Po_2 at all locations within the lens. In the centre of the lens, Po_2 increased from 1.6 ± 0.5 (n=8) to 5.3 ± 1.1 mmHg (n=4). Treatment with 3-NPA (0.5 mM) or azide (5 mM) resulted in similar increases in core Po_2 to 5.8 ± 0.53 (n=3) and 7.7 ± 2.5 (n=4), respectively. Significantly, treatment with either myxothiazol or azide also resulted in a change in shape of the Po_2 profile. In the presence of either inhibitor, Po_2 gradients in the outer few millimeters of the lens were markedly reduced, consistent with the inhibition of O_2 consumption in the mitochondria-containing DF. The implication of this finding for regional O_2 consumption will be discussed in the diffusion/consumption model in Figure 2.33.

The effect of age on lens QO_2

As discussed in §1.5, there is evidence in some tissues that with age, oxidative phosphorylation decreases with a concomitant fall in mitochondrial O_2 consumption. If mitochondria are the most important modulators of O_2 levels in the mammalian lens, then it may be that old lenses consume less O_2. This would have the effect of raising lens core Po_2. In fact, we would expect lens core Po_2 to increase with age even if total lens O_2 consumption remained constant throughout the lifespan, because of the increase in size of the lens with age. We examined lens O_2 consumption in guinea pig lenses (Figure 2.21). Guinea pigs were obtained at various ages across the lifespan: 6 weeks (adolescence), 4 months (early adulthood) and 2 years of age (elderly). After dissection, lenses were weighed and respirometry was performed on groups of isolated lenses after a 4-hour equilibration period in an environment of 36 mmHg (5% O_2). As expected, lens weight

increased with age, approximately doubling from 50 ± 3 mg (n=12) to 116 ± 6 mg (n=8) between 6 weeks and 2 years of age. The total amount of O_2 consumed by lenses did not change with age, being 0.7 ± 0.1, 0.7 ± 0.1 and 0.7 ± 0.2 µl/lens/h for 6 week (n=12), 4 month (n=12) and 2 year old (n=8) lenses respectively (Figure 2.21). There was a decrease in QO_2 on a per gram basis from 13.8 ± 0.7 (n=12, 6 weeks) to 7.8 ± 0.4 (n=8, 4 months) to 6.0 ± 1.0 µl/g/h (n=8, 2 years). However, regional studies and mathematical modelling (see later sections) indicate that most O_2 is consumed in the lens cortex. Therefore, the decrease in QO_2 on a per gram basis with age may not reflect a true decrease in lens QO_2 because the lens core (which probably consumes relatively little O_2) is included in the calculation. Overall, the data suggest that lens QO_2 did not decrease with age in the guinea pig. We were unable to measure Po_2 in guinea pig lenses due to the relatively large size of the optode (320 µm) compared to the size of the guinea pig lenses (approximately 3mm in diameter). However, the constancy of lens O_2 consumption and the increase in size with age suggest that lens core Po_2 would increase with age in the guinea pig lens. We will examine this issue in the human lens in the next chapter.

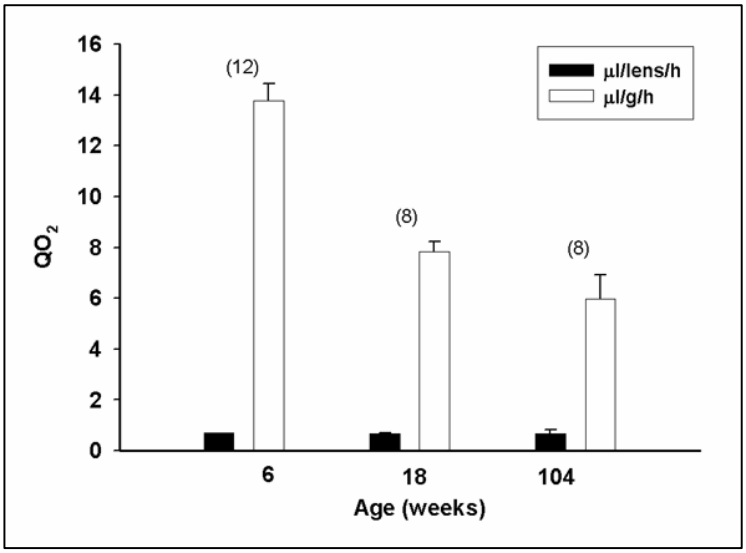

Figure 2.21 *Effect of age on guinea pig lens QO_2. Respirometry was performed in a Po_2 environment of 36 mmHg (5% O_2). 4 lenses were used for each respirometry measurement. 6 weeks of age is regarded as adolescence, 4 months as early adulthood and 2 years close to the end of the lifespan. Lens QO_2 did not decrease with age on a per lens basis. The apparent decrease in QO_2 when corrected for weight reflects the continued growth of the lens with age. (n) =number of lenses.*

Regional Analysis

The above data concerning the shape of the Po_2 profiles, the distribution of mitochondria and the mitochondria inhibition studies suggest O_2-consumption occurs mainly in the cortex, with a possible minor component in the mitochondria-free lens core. To determine directly the contribution of different regions of the bovine lens to the regulation of O_2 levels, QO_2 and Po_2 measurements were made by region with or without inhibitors of O_2 consumption. Respirometry was performed on three regions of the lens: the anterior capsule with epithelium, the central 1g of core (which corresponds to approximately 50% of the lens diameter) and the remaining cortex. Since bovine lens core QO_2 in a Po_2 environment of 36 mmHg (5% O_2) at 37°C was within the error of the instrument (0.1 ± 0.2 µl/h), respirometry was performed in a Po_2 environment of 150 mmHg (21% O_2). Where possible, all samples were equilibrated in this environment for four hours prior to respirometry.

Confocal microscopy of capsule samples treated in rhodamine 123 for 20 minutes at 37°C, confirmed that lens epithelial cells adhered to the capsule after dissection (Figure 2.22).

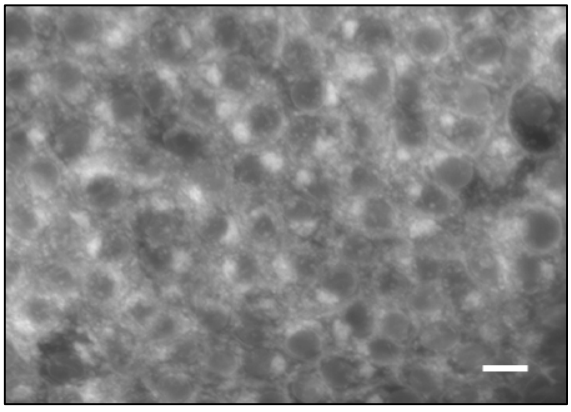

Figure 2.22 *Micrograph of anterior epithelium adherent to the bovine lens capsule. The anterior capsule was removed from the lens and placed in rhodamine 123 at 37°C for 30 min. After rinsing, the sample was mounted on a slide and viewed on a confocal microscope. The typical cobblestone appearance of the epithelium is seen in the figure Scale bar= 10 µm.*

QO_2 values of the regions of the lens are presented in Figure 2.23. Although the epithelium is at times assumed to be the epicentre of lens O_2 metabolism (Harding, 1991), it accounted for only ~3% of whole lens QO_2 values (0.4 ± 0.4 µl/g/h, n=5). This relatively low value was not due to loss of epithelial cells during dissection because rhodamine 123 staining indicated an intact epithelial layer (Figure 2.22). The cortical tissue disintegrated

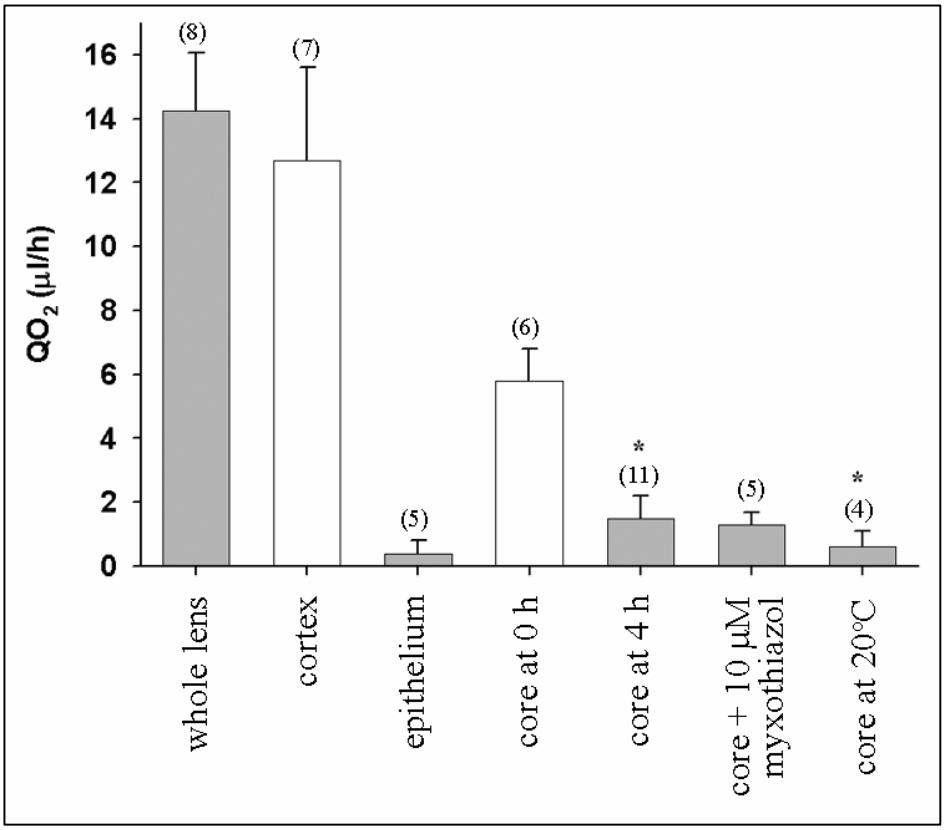

Figure 2.23 *QO_2 by region in the bovine lens. The QO_2 was measured immediately after dissection (open bars) or after a four hour equilibration period (closed bars). Measurements were made at 37°C in solutions containing Po_2 of 150 mmHg (21% O_2). Cortical samples deteriorated over the four hour equilibration period. Consequently, only an initial cortical measurement was possible. The QO_2 value of the isolated cortex was not significantly different from that of the whole lens, suggesting that much of the O_2 consumption of the intact tissue can be attributed to the outer fibre cell layers (DF). Note that the value for whole lens QO_2 reported here was higher than in Figure 2.13 because the unit used here is µl/h instead of µl/g/h. In contrast, epithelial O_2 consumption represented only a minor component (approximately 3%) of the total. The QO_2 values of equilibrated core samples were significantly lower than those measured immediately after dissection. Myxothiazol, an oxidative phosphorylation inhibitor, had no significant effect on QO_2 in the lens core. Lens core QO_2 decreased significantly at 20°C compared to 37°C. *=$p<0.05$, Student's t-test. (n) = number of lenses.*

during the four hour equilibration. Therefore, whole lenses had to be equilibrated first, then the cortex dissected immediately prior to measurement. QO_2 of the lens cortex was not significantly different from whole lens values, consistent with it being the primary site of lens O_2 consumption. Lens cores also consumed O_2. Unequilibrated core QO_2 was higher than equilibrated values (5.8 ± 1.0 (n=6) vs 1.5 ± 0.7 (n=11) µl/g/h respectively). The higher rate in unequilibrated cores probably reflects a mixture of true O_2 consumption, and an apparent O_2 consumption from the diffusion of O_2 into the hypoxic lens core (see Figure 2.6). As a control experiment, we confirmed that the QO_2 of mitochondria-free cores was not significantly changed by treatment with myxothiazol (10 µM), an inhibitor of oxidative phosphorylation (Figure 2.23). Cooling also significantly reduced core QO_2 from 1.5 ± 0.7 (n=11) µl/g/h at 37°C to 0.6 ± 0.5 (n=4) µl/g/h at 20°C. Therefore, similar to whole lens, the QO_2 in the mitochondria-free MF is also sensitive to temperature (see Figure 2.15).

It is expected that consumption of O_2 by the isolated lens core should lead to core Po_2 values lower than that of the bathing solution. To test this, Po_2 profiles were measured in lens cores equilibrated in a Po_2 environment of 150 mmHg (21% O_2) (Figure 2.24). The Po_2 profile was symmetrical, and Po_2 gradients extended to the lens centre. Although Po_2 gradients persisted in the isolated lens core, the Po_2 was higher than in the centre of whole lenses under the same conditions (approximately 50 mmHg (n=5) versus 30 mmHg (n=6), respectively, see Figures 2.9 and 2.10). This probably reflects the smaller size and the lower rate of O_2 consumption of the isolated core compared to the whole lens. Even after prolonged incubation (>8 h), the Po_2 within the sample did not rise to that of the bathing medium (data not shown).

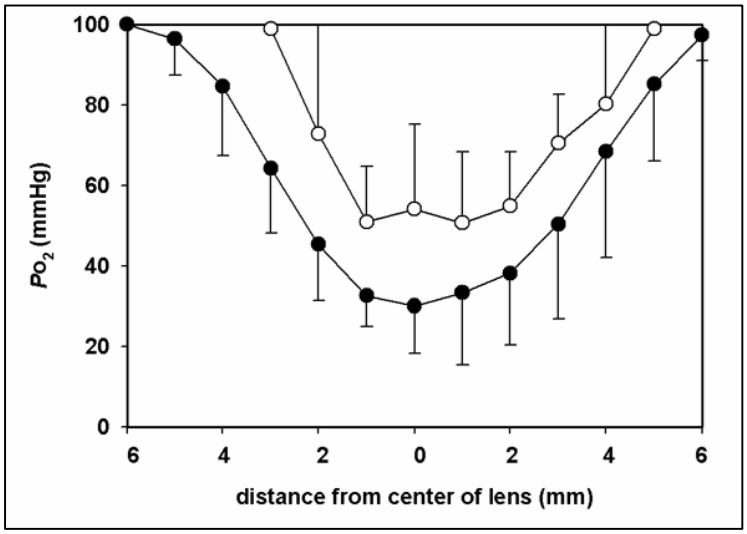

Figure 2.24 *P_{O2} profiles in the dissected core of the bovine lens. Bovine lenses were dissected to remove the mitochondria containing cortex leaving the central 1g of tissue. Isolated cores (open circles) were equilibrated with 150 mmHg (21% O_2). Data from intact lenses under the same conditions (from Figure 2.10) are shown for comparison (filled circles). A steep gradient persists within the dissected core. However, dissected lens core P_{O2} is higher than in the core of the whole lens (n=5).*

In summary, the steep Po_2 gradients in the outer cortex of the bovine lens suggest that the cortex was the primary site of lens O_2 consumption (Figure 2.9). The regional QO_2 measurements in the bovine lens confirmed that the cortex consumed more O_2 than the lens core (Figure 2.23). Most of the cortical O_2 consumption was probably due to mitochondrial O_2 consumption (Figure 2.19). However, several pieces of evidence point to O_2 consumption occurring in the lens core. In the intact lens, Po_2 gradients extended into the MF region (Figure 2.18). In addition, the isolated cores consumed O_2 (Figure 2.23) and maintained a Po_2 gradient (Figure 2.24). The contribution of the core to whole lens O_2 consumption is probably minor. According to the mitochondria-inhibition studies, the non-mitochondrial QO_2 was approximately 9% (Figure 2.19). Also of interest was that the epithelial layer was not a major contributor to lens O_2 consumption.

Non-mitochondrial O_2 consumption

We will now examine some candidate processes that could be involved in modulating O_2 levels in the mitochondria-free MF region. It should be kept in mind that such processes could also be involved in the mitochondria-rich DF as accessory O_2-consumers.

Ascorbate

Found in unusually high concentrations in some lenses (Garland, 1991), ascorbate is able to consume O_2 (Eaton, 1991). The role of ascorbate in lens QO_2 was investigated in the guinea pig, one of the few animals which cannot synthesize ascorbate. Guinea pigs were placed on an ascorbate-free (scorbutic) diet for four weeks with the aim of lowering lens ascorbate levels. While control animals on a normal diet gained weight over the four week period (from 806 ± 86 mg to 872 ± 88 mg, n=5), animals placed on the scorbutic diet lost ~15% body weight over the same time period (from 793 ± 73 mg to 679 ± 95 mg), consistent with previous reports (Giblin, et al., 1984;Reddy, et al., 1998) (Figure 2.25). One scorbutic guinea pig died before the completion of the experiment.

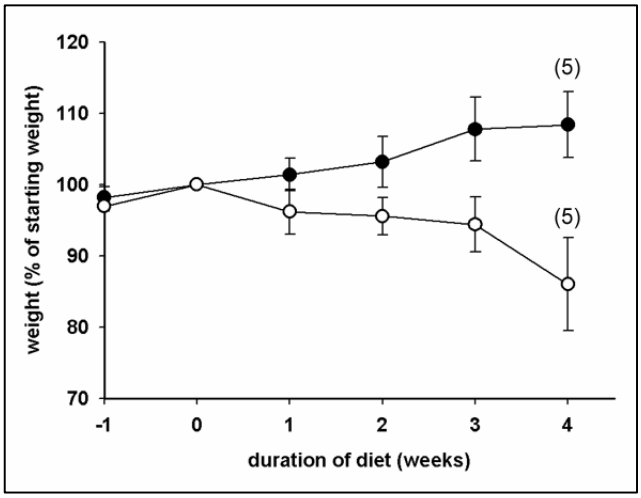

Figure 2.25 *Effect of an ascorbate-free diet on guinea pig weight. Guinea pigs were fed either a diet containing no ascorbate or a normal diet for four weeks and their weight monitored. While control animals (closed circles) on a normal diet continued to gain weight, the scorbutic animals (open circles) lost ~15% body weight by week 4. (n) = number of animals.*

After 4 weeks, animals were sacrificed and lenses weighed and photographed. The scorbutic lenses were transparent and the same size as control lenses (Figure 2.26).

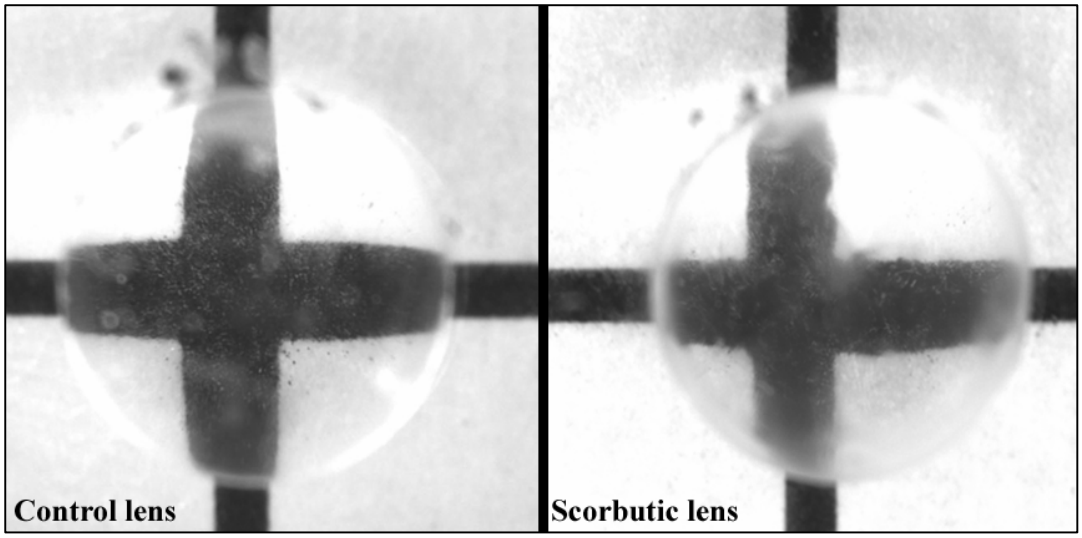

Figure 2.26 *Photographs of control and scorbutic guinea pig lenses. Guinea pigs were fed a normal or scorbutic diet for 4 weeks. An example of a scorbutic lens is shown (right) with a control lens (left) for comparison. The scorbutic lens is transparent and of normal size and shape.*

Weights of control and scorbutic lenses were not significantly different at 82.2 ± 4.9 and 82.6 ± 3.0 mg respectively (n=10 for each group). The tissue concentration of ascorbate was assessed by HPLC. Ascorbate levels were calculated assuming that the water content of the guinea pig lens is similar to that reported for the rat lens (i.e., 58%; (Duncan & Jacob, 1984)). Ascorbate concentrations were 696 ± 84 μM (n = 4) and 88 ± 21 μM (n = 3) in the control and scorbutic groups, respectively. Thus, the scorbutic diet led to an 87.4% reduction in lens ascorbate. This value was similar to previous reports of diet-induced lens ascorbate decreases of 77% (1.3 mM to 0.3 mM) (Yokoyama, et al., 1994) and 83% (1.03 mM to 0.18 mM) (Reddy, et al., 1998). These results suggest it is difficult to completely eliminate ascorbate from the lens. Measurements on pooled lenses indicated that QO_2 was unaffected by the reduction in ascorbate levels (Figure 2.27). QO_2 was 7.0 ± 0.8 μl/g/h (0.6

± 0.1 µl/lens/h) in the scorbutic group and 6.9 ± 2.6 µl/g/h (0.6 ± 0.2 µl/lens/h) in the control group (n=10 lenses in each group). Guinea pig lenses are small compared to the dimensions of the optode tip (approximately 2.5-3 mm vs 320 µm, respectively). Consequently, we were unable to make a series of Po_2 measurements in the guinea pig lenses.

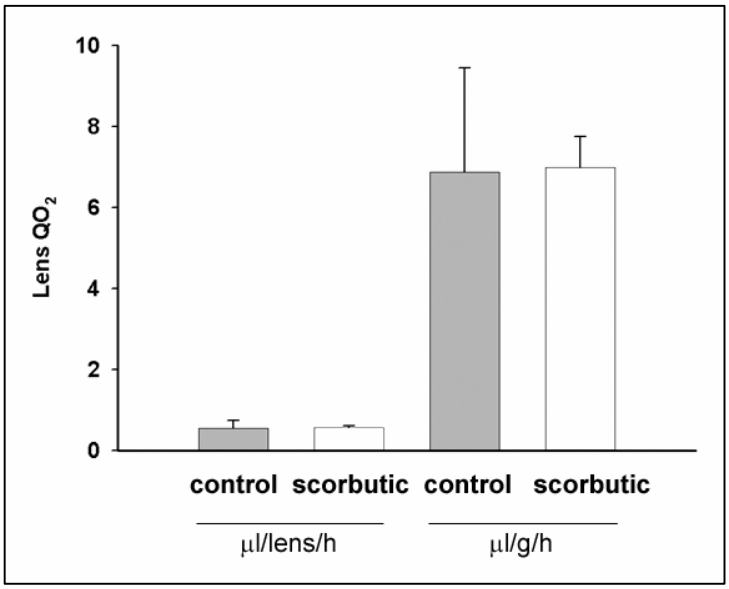

Figure 2.27 *The effect of ascorbate on QO_2 of the guinea pig lens. Guinea pigs were fed an ascorbate-free diet for 4 weeks. Respirometry was performed on isolated scorbutic and control lenses after equilibration in AAH at 37°C containing 5% O_2. QO_2 was unaffected despite having ascorbic acid levels below 13% of normal values (5 lenses were used in each respirometry measurement. 2 measurements were performed for each group).*

The concentration of ascorbate in the scorbutic guinea pig lenses (88 µM) was still nearly two orders of magnitude higher than the expected concentration of O_2 in the lens (1-2 µM, see §2.2). It is possible, therefore, that ascorbate-dependent O_2-consumption was still occurring in the lenses. Consequently, additional experiments were undertaken to assess the role of ascorbate in lens O_2-consumption. As O_2-consumption by ascorbate is metal-dependant (§1.5), we would expect to be able to inhibit ascorbate-related lens core O_2-consumption with metal-chelators. We undertook preliminary in vitro experiments on solutions of ascorbate. Ascorbate-dependent O_2-consumption varied with the amount of redox available metals (Figure 2.28A). The addition of increasing amounts of Cu^{2+} (1, 10 or 100 µM) to 100 µM ascorbate resulted in a higher QO_2. The consumption of O_2 was also

dependent on the concentration of ascorbate (Figure 2.28B). The addition of 10 µM Cu^{2+} to a solution of 2 mM ascorbate resulted in the rapid consumption of nearly all O_2, whereas lower concentrations (1 mM or 0.1 mM) did not lower Po_2 to zero. The O_2-consumption by ascorbate in the presence of Cu^{2+} was totally inhibited by the addition of the chelator ethylenediaminetetraacetic acid (EDTA) (1 mM) (Figure 2.28B). Interestingly, ascorbate-dependent O_2 consumption was dramatically reduced by adding dessicated bovine lens to the solution, showing that the bovine lens itself can act as a chelator.

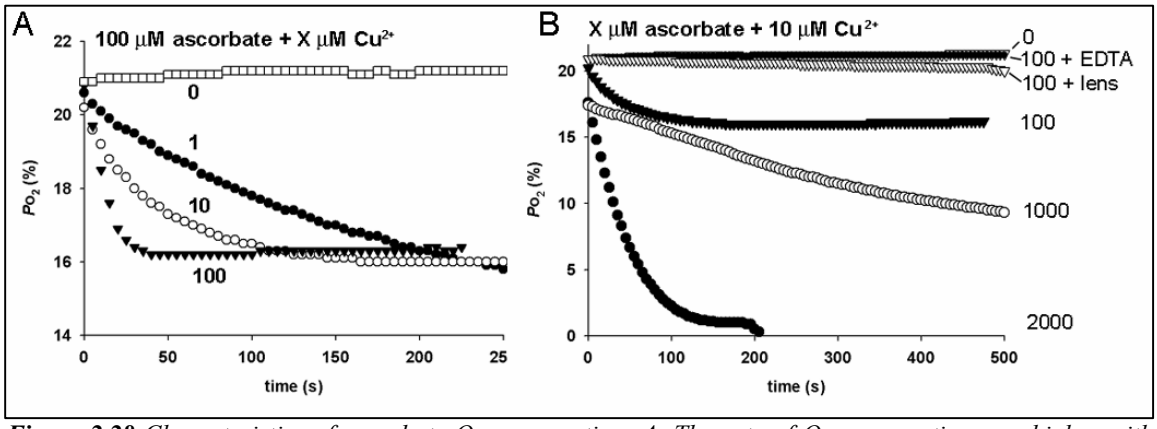

Figure 2.28 *Characteristics of ascorbate O_2 consumption.* ***A.*** *The rate of O_2 consumption was higher with increasing amounts of Cu^{2+} (1, 10 or 100 µM).* ***B.*** *Ascorbate levels (100, 1000 or 2000 µM) affect the amount of O_2 consumed. The O_2 consumption was inhibited by the addition of the metal-chelator EDTA (1 mM) or 1g of dried bovine lens core to the solution. This shows the lens has chelating properties.*

In light of these results, we incubated bovine lens cores for 4 hours in the presence of the metal-chelators EDTA and diethylenetriaminepentaacetic acid (DETAPAC) to assess whether chelation affected lens QO_2 (Figure 2.29). Neither EDTA (1 mM) nor DETAPAC (1 mM) had a significant effect on intact lens core QO_2. To counter the possibility that the chelators did not penetrate the relatively dense lens core, homogenised lens cores were also analysed. The lens core homogenate QO_2 was significantly higher than the intact core QO_2 (2.3 ± 0.9 µl/g/h (n=7) vs 1.5 ± 0.7 (n=11) µl/g/h, respectively, $p<0.05$). This may be due to

the homogenates having a massively larger surface area exposed to O_2. Although treatment of homogenates with 1 mM EDTA had no significant effect, 1 mM DETAPAC lowered core homogenate QO_2 from 2.3 ± 0.9 to 1.1 ± 0.7 µl/g/h (n=7 each group), a decrease of 52% ($p<0.05$). There is some evidence that DETAPAC is a superior chelator to EDTA (Fisher, et al., 2004), which may explain the difference in effect between the two compounds.

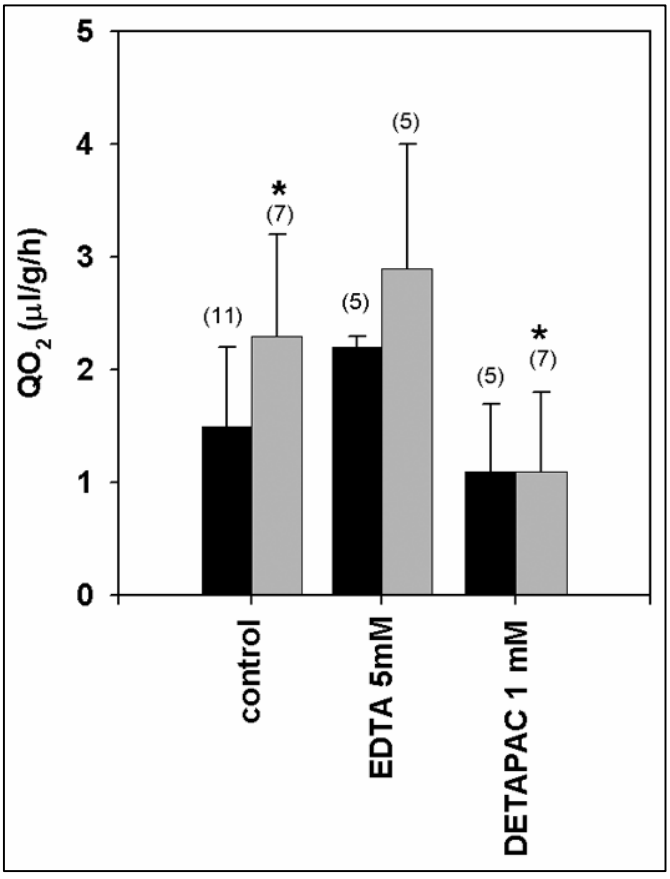

Figure 2.29 *Metal-chelator inhibition studies on bovine lens core QO_2. The central 1g of lens was dissected and equilibrated in Po_2 of 150 mmHg (21% O_2) and the presence or absence of metal chelators. QO_2 was measured on intact (black columns) or homogenised (grey columns) tissue. Homogenised control tissue (in 3ml of PBS) consumed more O_2 than the intact control core (*=$p<0.05$, Student's t-test). Although EDTA did not reduce QO_2, DETAPAC significantly reduced QO_2 of lens homogenates compared to controls (*=$p<0.05$, Student's t-test).*

The hypothesis that ascorbate consumes O_2 in the lens is contingent upon the lens being capable of metal-dependent O_2 consumption. However, it was demonstrated in Figure 2.28B that the lens can act as a chelator. Therefore, it was of interest to establish whether metal-dependent O_2 consumption is possible in the lens. To this end, O_2 consumption of

bovine lens homogenates was measured in the presence and absence of exogenous Cu^{2+} (Figure 2.30). The addition of Cu^{2+} (10 or 100 μM) to lens homogenates increased O_2 consumption. Although the concentrations of Cu^{2+} used here are higher than reported physiological levels (Garner, et al., 2000), these data show that metal-dependent O_2 consumption in the lens is indeed possible.

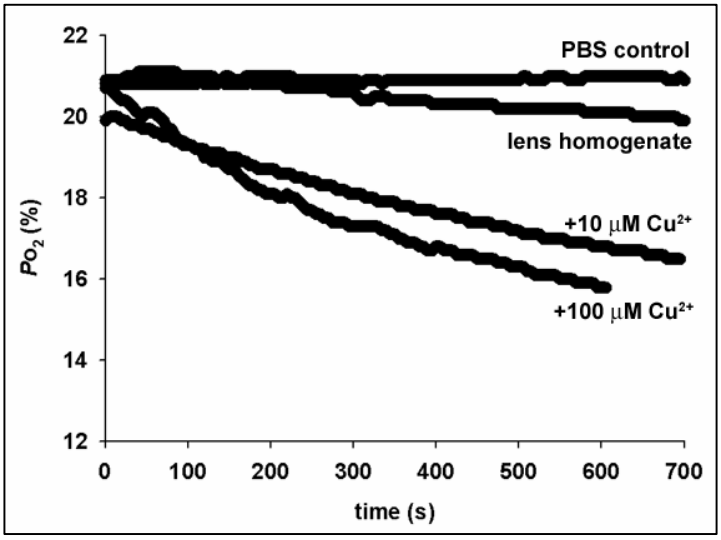

Figure 2.30 *Metal-induced O_2 consumption in the bovine lens. Respirometry was performed on lens core homogenates in the presence or absence of exogenous Cu^{2+}. The respirometry traces show that lens homogenates consume a small amount of O_2. However, the addition of Cu^{2+} increases the amount of O_2 consumed.*

In summary, a significant reduction in ascorbate was achieved in guinea pig lenses with no discernible effect on lens QO_2. However, a role for ascorbate could not be excluded on this basis as it was not possible to remove all the ascorbate from the lens. Even in the scorbutic lenses, there remained a nearly 100-fold higher concentration of ascorbate compared to the estimated concentration of O_2. Conversely, there is some indirect evidence to support the ascorbate hypothesis. Metal-dependent O_2 consumption in the lens is possible despite the ability of the lens substance to act as a chelator. Furthermore, the chelator DETAPAC significantly reduced core homogenate QO_2. On these grounds, it is plausible that ascorbate consumes O_2 in the lens. However, further experiments will be needed to test this hypothesis directly.

PMOR

Another possible non-mitochondrial O_2 consumer in the lens core is a trans-plasma membrane oxido-reductase (PMOR) system. As a screening test for whether such a system may operate in the lens, QO_2 was measured on intact and homogenised cores treated with the PMOR inhibitors capsaicin (200 µM) or NADH (1 mM) (Figure 2.31). These compounds did not significantly reduce QO_2 in either intact or homogenised samples, suggesting that a PMOR system is unlikely to make a major contribution to lens core QO_2.

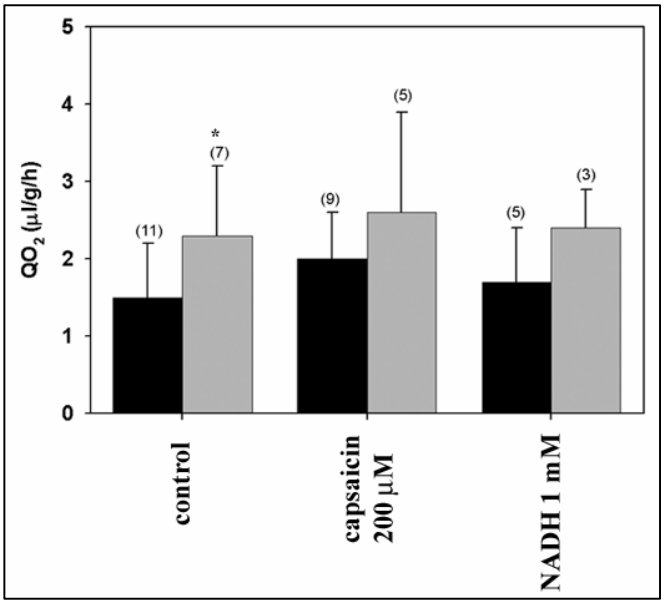

Figure 2.31 *PMOR inhibition studies on bovine lens core QO_2. The central 1g of lens was dissected and equilibrated in Po_2 of 150 mmHg (21% O_2) and the presence or absence of inhibitors of capsaicin and NADH, inhibitors of PMOR systems (see text). QO_2 was measured on intact (black columns) or homogenised (grey columns) tissue. Neither drug had a significant effect on QO_2. Control values from Figure 2.28 are included for comparison *=$p<0.05$ Student's t-test.*

Photo-oxidation

To analyse the role of light in modulating lens O_2 levels, bovine lenses were equilibrated and tested in the presence or absence of laboratory lighting. Lens QO_2 in a Po_2 environment of 36 mmHg (5% O_2) was not significantly lower in the dark (5.68 ± 1.83 µl/g/h (n=4) and 4.8 ± 0.1 µl/g/h (n=10), for dark and light, respectively). Neither did the

absence of light significantly affect Po_2 profiles (Figure 2.32). These data suggest that photo-oxidation is not an important modulator of tissue O_2 levels in the lens.

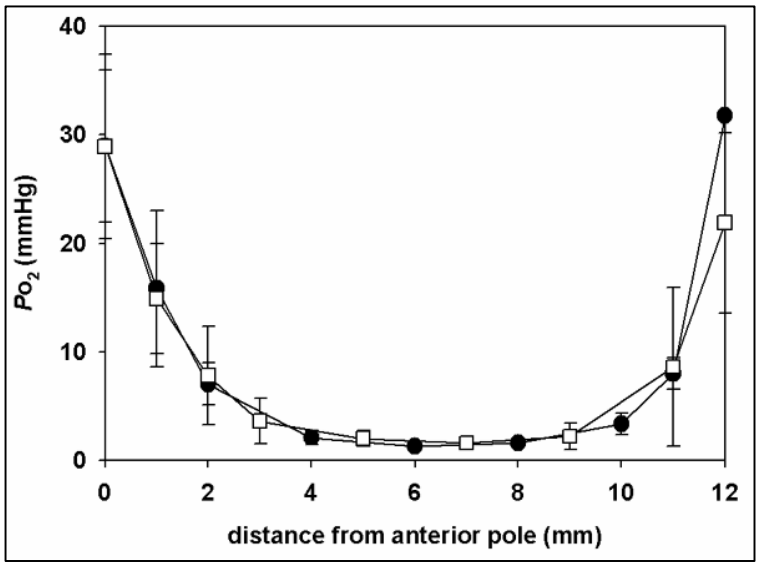

Figure 2.32 *Effect of light on Po_2 profiles in the bovine lens. Under physiological conditions (Po_2 of 36 mmHg or 5% O_2), lenses were equilibrated and tested in the light (open squares, n=6) or dark (closed circles n=4). The figure shows that the absence of light produced no significant change to the profiles.*

Mathematical modelling

A diffusion/consumption mathematical model (see Appendix to this chapter) was developed and applied to the data in collaboration with Huan Wang, Richard Mathias and Steven Bassnett. Modelling allowed the calculation of time (τ (s)) and length constants (λ (mm)) for O_2 consumption in various regions of the lens and an effective O_2 diffusion coefficient (D_{O_2} (cm^2/s)). To derive the model, assumptions had to be made regarding the relationship between lens anatomy and the optode Po_2 profiles. Passing the optode stepwise through the lens caused a slight distortion in the tissue, particularly on the far side of the preparation, where the tip of the optode had to penetrate the elastic capsule to exit the lens. As a result, the total distance travelled by the optode tip slightly exceeded (by 5-10%) the actual measured diameter of the lens. To graph the data as a function of distance (r cm)

from the lens centre required that the distance travelled by the optode be converted to the actual position (relative to the geometric centre) within the lens. The simplest assumption is that if the total distance moved by the optode was, for example, 1.1 times the lens diameter, then each step moved the optode into the lens a factor of 0.9 times the calibrated step size. The model assumes that O_2 enters the lens by simple diffusion, with an effective diffusion coefficient D_{O_2} (cm^2/s), which depends on diffusion through membranes and cytoplasm. For O_2, membranes are not a large diffusion barrier (see §2.1), so it is anticipated that D_{O_2} will have a value only somewhat less than that for diffusion in water. Once the O_2 enters the lens cells, it will be consumed by mitochondria or non-mitochondrial elements with time constants τ_{DF} (s) in the mitochondria-containing differentiating fibres (DF), and τ_{MF} (s) in the mitochondria-free mature fibres (MF) (see Figure 1.13, §1.7.1). The model predicts that P_{O_2} will decrease exponentially with distance into the lens, the length constants for the exponential decrease being $\lambda_{DF} = (D_{O_2}\tau_{DF})^{0.5}$ in the DF and $\lambda_{MF} = (D_{O_2}\tau_{MF})^{0.5}$ in the MF. It was also assumed that the P_{O_2} at the lens surface was the same as that in the bathing solution. With these assumptions, we were able to fit the empirical data with the diffusion/consumption model that calculated P_{O_2} as a function of distance from the lens centre.

The best fits of the model to empirically determined Po_2 profiles in 7 mmHg (1% O_2) and 36 mmHg (5% O_2) are shown in Figure 2.33. The curve fitting procedure provided estimates for the values of the length constants, which were λ_{DF} = 1.4 mm and λ_{MF} = 1.3 mm for the 7 mmHg data, and λ_{DF} = 0.8 mm and λ_{MF} = 0.9 mm for the 36 mmHg data. Given the standard deviations of the data and the assumptions intrinsic to the modelling

process, these values are probably not significantly different and we conclude that the length constants in all instances are about 1.0 mm. This conclusion was surprising, since, as previously described, the processes responsible for O_2 consumption in the DF and MF are probably different.

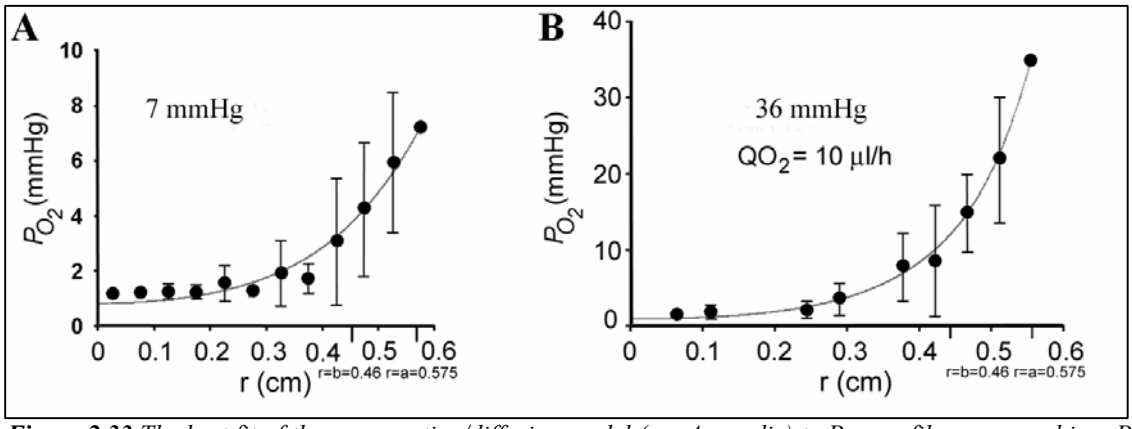

Figure 2.33 *The best fit of the consumption/diffusion model (see Appendix) to P_{O_2} profiles measured in a Po_2 of 7 mmHg (A) or 36 mmH g (B) (1% or 5% O_2, respectively). Radius of lens (MF + DF) is r=a cm. Radius of MF is r=b cm. The data were well fit by the two compartment (DF and MF) model. In both Po_2 environments, derived values for the length constants for O_2 consumption in the outer (mitochondria-rich) and central (mitochondria-free) regions of the lens were about 1 mm, which implies that the rates of O_2 consumption in these two domains are nearly the same. Based on measurements of QO_2 in Po_2 of 36 mmHg and the best fit values of length constants, the effective diffusion coefficient for O_2 in the lens is calculated to be 3 x 10^{-5} cm^2/s and the time constant for O_2 consumption within any lens cell is about 5 minutes.*

For lenses bathed in 36 mmHg, the rate of total lens O_2 consumption was also measured at QO_2 = 9.9 µl/hr (from Figure 2.13, units have been changed). This additional piece of information allowed calculation of the effective diffusion coefficient, which was D_{O_2} = 3 x 10^{-5} cm^2/s, a value slightly smaller than that of O_2 in water (4 x 10^{-5} cm^2/s). This agreement with expectations provided some degree of confidence that the model contained no absurdities. Based on a length constant of 1 mm and a diffusion coefficient of 3 x 10^{-5} cm^2/s, the time constant for O_2 consumption in normal lens cells is about 5 minutes. Importantly, the calculated time constants did not differ between differentiating fibres (DF) that contain mitochondria and mature fibres (MF) that do not.

To examine whether treatment with mitochondrial inhibitors had a different effect on O_2 consumption in distinct regions of the lens, the diffusion/consumption model was used to fit the azide data from Figure 2.19 and to calculate the proportional contribution of DF and MF cells to lens O_2 consumption (Figure 2.34). Under control conditions, τ_{DF} and τ_{MF} were very similar (Figure 2.32). However, in the presence of azide, they differed significantly, due to a striking increase in τ_{DF} (i.e. a reduction to near zero in the rate of O_2 consumption in DF cells).

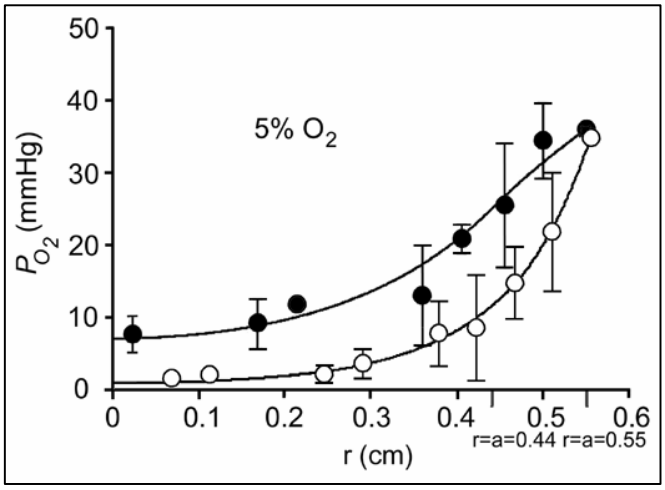

Figure 2.34 *The best fit of the diffusion/consumption model to Po_2 data of bovine lenses inhibited with azide. The best fit to the data from Figure 2.20 (closed circles) are presented. Control data and best fit from Figure 2.31B are shown for comparison (open circles). Azide inhibition caused a generalised increase in P_{O_2} and a shallower gradient in the superficial cell layers. This indicates a significant decrease in QO_2 in the outer shell of the mitochondria-rich DF layer.*

Under control conditions, approximately 80% of the total O_2 consumed by the lens occurred in the DF (Figure 2.35). The important contribution of the DF to lens O_2 consumption is due to two factors. First, because of the spherical geometry, about half the lens volume is contained in the outer shell of DF, even though this shell constitutes only the outer 20% of the radius. Second, the rate of consumption per cell is given by the concentration divided by the time constant, and the P_{O_2}

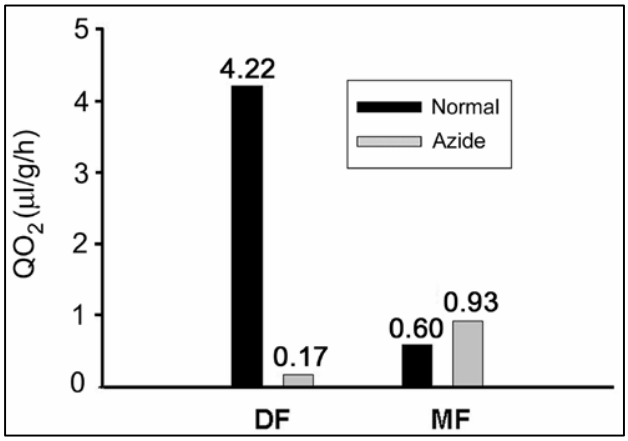

Figure 2.35 *The effect of mitochondrial inhibitors on calculated O_2 consumption time constants. The amount of O_2 consumed by the DF and MF cell layers in the presence or absence of azide was calculated using equation (10) (Appendix B). In the presence of azide, O_2 consumption by DF cells is dramatically reduced. In contrast, azide has little effect on O_2 consumption by the MF cells.*

in the DF is much higher than in the MF. Following treatment with azide, the calculated consumption of O_2 by the DF cell layer was drastically reduced. In contrast, azide treatment had little effect on O_2 consumption by MF cells. The model thus suggested that the ≈80% reduction in QO_2 observed by treating lenses with mitochondria-inhibitors could be attributed to the near complete inhibition of O_2 consumption in the outer DF layer (Figure 2.35). Thus the modelling studies are in accordance with the bovine lens regional QO_2 studies (Figure 2.23) in attributing most O_2 consumption in the lens to the outer cortex.

2.4 Discussion

The lens QO_2 results from bovine, guinea pig and rabbit lenses are consistent with other reports showing that the lens has a small rate of O_2 consumption. Lens QO_2 results from an extensive survey of the literature are presented in Table 2.3.

Table 2.3 Lens QO_2

SPECIES	QO_2 (µl/gwet/h)	COMMENT	REFERENCE
cow	**7.5 ± 1.8**	***P*o$_2$ of 150 mmHg (21% O_2)**	**Present study**
	4.8 ± 0.1	***P*o$_2$ of 36 mmHg (5% O_2), 37°C**	
	0.9 ± 0.5	***P*o$_2$ of 36 mmHg (5% O_2), 20°C**	
rabbit	**6.8 ± 1.3**	***P*o$_2$ of 36 mmHg (5% O_2)**	**Present study**
guinea pig	**6.0 ± 1.0**	***P*o$_2$ of 36 mmHg (5% O_2)**	**Present study**
rabbit	32.1	Barcroft differential, 30°C	(Field, 1937)
	47.4	37°C	
rabbit	(152-196)	Warburg apparatus, 37.5°C	Pignalosa, cited in (Ely, 1949)
rabbit	(17.4-130)	Warburg apparatus, 37.5°C	Kronfeld and Bothman, cited in (Ely, 1949)
rabbit	(39-113)	Warburg apparatus, 37.5°C	Schmerl, cited in (Ely, 1949)
rabbit	17.4	Warburg apparatus, 37.5°C	Schmerl, cited in (Ely, 1949)
rabbit	260	Warburg apparatus, 30°C	Mashimo, cited in (Ely, 1949)
rabbit	7.8		Hans, Hockwin and Kleifeld, cited in (Van Heyningen, 1965)
rabbit	8.8#		Hans, Hockwin and Kleifeld, cited in (Van Heyningen, 1965)
ox	(4-32)	not intact	(Griffiths, 1966)
rabbit	16.5±2.8	37°C	(Edelhauser, 1974)
	12.2±0.5	24°C	(Edelhauser, 1974)
rabbit	(46-49)	intact lens	(Talaat, et al., 1974)
	(317-346)	homogenate	
rat	31.4		Sippel cited in (Edelhauser, 1974)
trout	11.82		Olson cited in

			(Edelhauser, 1974)
trout	54±3		(Edelhauser, 1974)
toad	12.2	25°C	(Yorio, et al., 1979)

QO_2 stated as average ± SD (range). All measurements are in 21% O_2 and at 37°C unless otherwise indicated. # converted from 0.35 µmol/g/h assuming 1 µmol/ml = 25.1 µl/ml at 37°C, 21% O_2.

Early determinations of lens QO_2 were made using Warburg respirometers. This now outdated technique measured the change in volume of a known amount of air in order to calculate the O_2 consumption by the test sample. It is possible that these values are subject to high errors due to the relatively small amount of O_2 consumed by the lens. The wide range of values in the literature may also be explained by measurements being made under a variety of conditions. Generally, the lenses were not allowed to equilibrate with the test environment prior to the experiment. Another factor could be the difference in weights and sizes between lenses from different species. Larger lenses have a higher internal volume which may not participate in O_2 consumption and therefore act as "dead weight."

We measured lens bovine and rabbit Po_2 profiles in vitro. There are several advantages to this technique. Fresh bovine lenses are freely available, and their large size allows detailed mapping of the distribution of O_2 within the tissue. Control of the Po_2 of the solution bathing the lens allows the influence of external Po_2 on lens O_2 levels to be determined. In addition, the in vitro technique allows for lens dissection and the administration of toxic drugs, which would not be possible in vivo.

The data support a model whereby most of the O_2 entering the lens was consumed by mitochondria located superficially in the lens cortex. Steep Po_2 gradients existed over the region where the mitochondria were located. Furthermore, mitochondrial inhibition significantly reduced QO_2 and raised lens Po_2. The results of regional studies and modelling also supported the conclusion that the cortex was the key site for lens O_2 consumption.

However, a small contribution to lens O_2 consumption was non-mitochondrial in origin. This may be as high as 9% according to mitochondrial inhibition studies (Figure 2.18). Using respirometry, we found direct evidence that cores consumed O_2. The O_2 consumption was inhibited by metal-chelator DETAPAC. Indirect evidence also came from the existence of Po_2 gradients in the lens core (MF region) which does not contain mitochondria. Under physiological circumstances, it may be that mitochondrial O_2 consumption is the predominant O_2 consumer in the lens. Non-mitochondrial O_2 consumption may only become important when mitochondrial O_2-consumption has reached its maximal rate, has been inhibited, or has become otherwise dysfunctional.

We were unable to positively identify the putative non-mitochondrial O_2 consumer. We found no evidence of a role for PMOR or light in determining lens Po_2. However, the role of ascorbate deserves more attention. The findings that metal-dependent O_2-consumption is possible in the lens core and that core homogenate O_2-consumption could be inhibited by DETAPAC are consistent with a role for ascorbate in lens O_2-consumption. It is possible that the concentration of ascorbate remaining in scorbutic guinea pig lenses

was sufficient to consume O_2. Furthermore, if ascorbate only consumes O_2 in the MF, even total depletion of ascorbate would only cause about a 20% reduction in lens QO_2. Given that it was not possible to completely eliminate ascorbate from the lens, the lack of a marked inhibition of lens O_2 consumption in the scorbutic animals cannot be taken as definitive evidence against a role for ascorbate in lens O_2 consumption.

The data raise interesting questions about the role of mitochondria in lens physiology and in cataract formation. In the presence of mitochondrial inhibitors, bovine lens QO_2 was reduced by approximately 90%. This indicates that oxidative phosphorylation is the major consumer of O_2 in the bovine lens. However, oxidative phosphorylation is not the major producer of ATP (§2.1). In fact, numerous studies have indicated that lens ATP content is not significantly depleted following incubation in 100% N_2 or mitochondrial inhibitors (Kinoshita, et al., 1961;Trayhurn & Van Heyningen, 1971;Winkler & Riley, 1991). Similarly, amino acid transport (Kern, 1962), sodium content (Trayhurn & Van Heyningen, 1971) and lens clarity (Giblin, et al., 1988), are all preserved following short term incubation in 100% N_2. These data support the view that glycolysis is the major energy source for the lens and that mitochondrial respiration in the fibre cells is inconsequential with regard to lens energy requirements. It is believed that mitochondria and other organelles are eliminated from cells in the centre of the lens because they would constitute potential sources of light scattering (Bassnett, 2002). If mitochondria are not a significant source of ATP, and their presence may compromise lens transparency, why are they retained in the outer fibre layers? One possible explanation comes from the work of Eaton (1991). He pointed out that the best way to preserve food at room temperature in a

hydrated state for a prolonged period is to can it. In the canning process, food is sealed in airtight containers from which O_2 has been removed thereby preventing oxidation and spoilage during long term storage. This may be analogous to the situation in the lens nucleus where, in the absence of cell turnover or *de novo* protein synthesis, long term preservation of proteins and membranes is a prerequisite for maintaining tissue transparency. We propose, therefore, a novel accessory function for mitochondria in the lens: to maintain the oldest cells in the tissue (i.e. those in the lens core) in a perpetually hypoxic state. If this view is correct, it follows that conditions where mitochondrial metabolism is compromised might be associated with an unusually high incidence of cataract. There is some support for this hypothesis. Many inherited mitochondrial diseases are associated with an elevated risk of cataract (§1.8), although the mechanism leading to opacification is not understood.

As discussed in §1.8, in aged human lenses there is a barrier to the diffusion of small molecular weight molecules, such as the antioxidant GSH, into the lens core. Because the physical nature of the barrier has not yet been determined, this barrier may also apply to the diffusion of O_2. O_2 was found to move freely into the centre of the lens under a variety of conditions, such as the inhibition of lens O_2 consumption, high external Po_2 and, more dramatically, sub-physiological temperatures. The significance of this finding is twofold. Firstly, the barrier to diffusion of small molecular weight molecules such as the antioxidant GSH found in middle aged human lenses (Truscott, 2000) does not seem to apply to O_2. If old human lenses have a decreased ability to transport antioxidants into the lens core, yet O_2 is free to diffuse in, then this represents a condition of oxidative stress and a possible predisposition to cataract formation. In the next chapter, we will examine the diffusion of

O_2 in the human lens. Secondly, it raises the possibility that the centre of the lens could suffer oxidative stress from high O_2 levels if conditions allowed O_2 to enter the lens in vivo. Of particular relevance is vitrectomy surgery (detailed in Appendix A). As the vitreous humour is removed during vitrectomy, the eye is internally perfused with room temperature balanced salt solutions equilibrated with atmospheric levels of O_2 (Po_2 of 150 mmHg or 21% O_2). The operation uses perhaps 350-600 ml of balanced salt solution and lasts approximately 45-90 minutes (personal communication, Dr N.M.Holekamp, vitreo-retinal surgeon), representing a high O_2-flux during the procedure. When the bovine lens core was placed in solutions with a relatively high O_2 content at room temperature, the lens core was flooded with O_2 (Figure 2.15). The increase in the concentration of O_2 in the lens core at low temperature is actually higher than the P_{O_2} values alone indicate because the O_2 solubility coefficient (αo_2) decreases by 1-4% $°C^{-1}$ (Sidell, 1998), resulting in a 30% increase in the solubility of O_2 as the temperature drops from 37°C to 20°C. It may be that an intra-operative oxidative insult to the lens core is a contributing factor to the development of post-vitrectomy nuclear cataract. Vitrectomy is associated with a high incidence of cataract formation. In the six months that followed vitrectomy surgery, 21% of patients developed cataract (Novak, et al., 1984), and by 12 months this number rose to 63% (Van Effenterre, et al., 1992). At 2-10 years follow up, the incidence of cataract in operated eyes ranged from 51%-80% (Blankenship & Machemer, 1985;Blodi & Paluska, 1997;Cherfan, et al., 1991;Leaver, et al., 1979;Melberg & Thomas, 1995). In the next chapter, we will investigate the effect of temperature on O_2 levels in the human lens.

The presence of O_2 gradients in the lens extends the list of gradients known or inferred to exist in this tissue. Gradients of Na^+, K^+, pH, Ca^{2+}, HCO_3^- and lactate have been

reported previously (Bassnett, et al., 1987;Bassnett & Duncan, 1986;Duncan & Jacob, 1984;Paterson, 1969). O_2 gradients may play a role in the development and normal physiology of the lens. The possibility that hypoxia may be a trigger for the process of organelle loss in the lens will be discussed in Chapter 4.

Chapter 3:

The regulation of O_2 levels

in the human lens

3.1 Introduction

The aim of this chapter is to examine the regulation of tissue O_2 levels in human donor lenses. To our knowledge, there is only one report of human lens Po_2. Values of 0.8–4.0 mmHg were found in the anterior cortex during cataract surgery (Helbig *et al.*, 1993). There are no reports of human lens QO_2 values.

The use of human lenses from a donor program allows us to study the effect of age on O_2 levels. There is a decrease in mitochondrial oxidative phosphorylation and O_2 consumption with age seen in some tissues (Beckman & Ames, 1998; Hagen *et al.*, 1998). In Chapter 2, mitochondria were shown to be the major consumers of O_2 in the bovine lens. We therefore hypothesize that lens O_2 consumption declines with age. If so, one would expect that Po_2 in the centre of the lens would increase with age.

We will also investigate the effect of diabetes on O_2 measurements. Diabetes is associated with a high incidence of cataract formation (Klein *et al.*, 1998), which may be due to the formation of advanced glycation end products (AGE) (Zarina *et al.*, 2000). Since AGE can promote oxidative stress (Fu *et al.*, 1998), it is of interest to see how tissue O_2 levels in diabetic lenses compare to controls. If tissue O_2 levels are higher in diabetic lenses, then they may be susceptible to further oxidative damage in the presence of AGE.

Incubating bovine lenses at sub-physiological temperatures led to high tissue O_2 levels (Figure 2.15). If this phenomenon were to be found in the human lens, it would be relevant to the development of post-vitrectomy cataract. During the vitrectomy procedure,

O_2-rich solutions are introduced into the eye at room temperature. Hence, we will also measure human lens core Po_2 under these conditions.

3.2 Methods

Chemicals, gases and AAH solution. As described in §2.2.

Human donor lenses. The use of human lenses was approved by Washington University Human Studies Committee (04-0511). Human lenses were generously donated by patients who participated in an organ donor program and sourced with the kind help of the Heartland Lion's Eye Bank (St Louis, Missouri, USA). Some lenses used in preliminary experiments were sourced with the help of Professor David Beebe, Department of Ophthalmology, Washington University in St Louis, MO, USA. After death, the patients' corneas were usually harvested at the health care facility for use in transplant procedures. For some patients, the rest of the eye was also harvested and sent to the eye bank on ice where a technician dissected the lenses under sterile conditions and placed them in HL-1 medium (Washington University Tissue Culture Support Center) and transported to the laboratory on ice. Alternatively, the patient was sent to the mortuary where an eye bank technician performed the lens dissection. Consequently, it was difficult to obtain lenses less than 24 hours since death. The time between death and QO_2 measurement ranged from 12-60 hours and averaged 28.5 ± 12.0 hours (n=24). On arrival in the lab, the lenses were visually inspected and damaged lenses were excluded from the study. No lenses were found to contain cataracts on gross examination. The lenses were incubated for 4 hours at 37°C in AAH containing antibiotics (described in §2.2), and containing various Po_2. The average age of donor lenses used for QO_2 measurements was 55.5 ± 14.0 years (24 lens pairs) and

for Po_2 measurements was 59.3 ± 12.7 years (n=37 lenses). Basic information and medical history were available for most donors. All donors were Caucasian. Males were over-represented in the sample, accounting for 75% of donors (27 males vs 9 females).

***Po*$_2$ measurement and respirometry.** Po_2 was measured in vitro with the fluorescent optode as described (§2.2). The lenses were placed on a plastic stand in a custom built chamber containing AAH at 37°C and known Po_2. A small hole was made in the lens capsule with a 25G needle and the optode, mounted on a micromanipulator, was passed along the optic axis in increments. QO_2 was measured with the respirometer described in §2.2. Preliminary experiments revealed that human lens QO_2 was small, therefore respirometry was performed on lens pairs in 2 ml of AAH, and using the same conditions as during the equilibration period. Lenses were weighed after respirometry and QO_2 calculated as described (§2.2).

Mitochondrial mapping. Two techniques were used to visualize the distribution of mitochondria in human donor lenses. Living lenses were incubated at 37°C in AAH containing 100 nM of the mitochondria-specific rosamine-derivative dye Mito Tracker Deep Red 633 (M-22426, Molecular Probes, Eugene, OR, USA) for 30 minutes, rinsed in PBS and viewed on a confocal microscope. Mito Tracker is accumulated in active mitochondria (Poot *et al.*, 1996). Alternatively, immunoflourescence was performed on fixed tissue using a mouse anti-bovine IgG_{2a} antibody to cytochrome *c*-oxidase (complex IV or COX) of the mitochondrial respiratory chain (A-6431, Molecular Probes, Eugene, OR, USA) as described in §2.2. This antibody has human cross-reactivity and has been used in studies of human mitochondria (Kennaway *et al.*, 1990; Taanman *et al.*, 1996;

Marusich *et al.*, 1997). Human lens slices 100-150 μm thick were prepared. The slices were mounted on glass slides, coverslipped and viewed on a confocal microscope as described in Chapter 2.

Mitochondrial inhibition studies. The inhibitors used were described in §2.2. Preliminary experiments revealed that human lenses consume a relatively small amount of O_2. Hence, respirometry measurements were made on lens pairs. Therefore, the preparation of human lens samples for inhibition studies differed slightly from that used in Chapter 2. Baseline respirometry was performed on equilibrated human lens pairs. The lenses were then returned to AAH in the presence of a mitochondrial inhibitor for 4 hours, respirometry performed on the treated samples and compared to baseline measurements.

Statistics. Linear regression analysis was used to assess the statistical significance of the data. A p-value of <0.05 was regarded as significant. When two Po_2 values where obtained from the left and right lenses of the same patient, the average Po_2 value was used. This ensured that regression analysis was performed on data from independent samples.

3.3 Results

Human donor lens weight

Weights of human lens pairs were recorded for QO_2 calculations (Figure 3.1). Consistent with other reports (Bron, *et al.*, 1997), lens weight increased significantly ($p<0.0001$) with age by 3 mg/year (n=21 lens pairs).

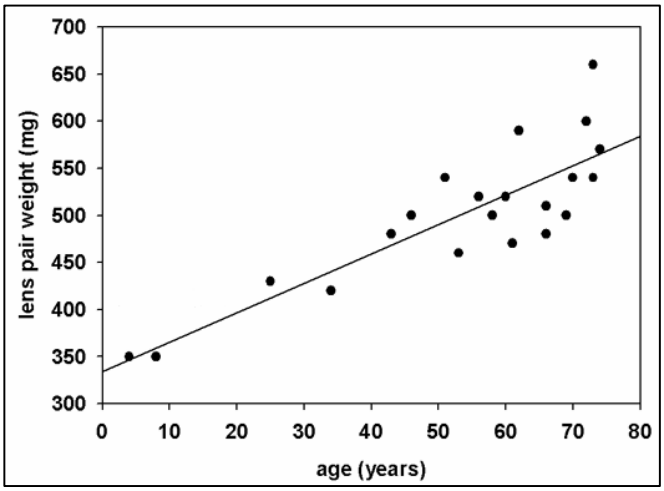

Figure 3.1 *Human lens weight. Human donor lenses were weighed as pairs. A linear regression line has been fitted to the data. Weight increased significantly ($p<0.0001$) by 3 mg/year (n=21 pairs).*

Po_2 profiles

Cataracts rarely develop simultaneously in both eyes of the same patient. In fact, the each eye may develop a different type of cataract. This suggests that the two lenses are not physiologically identical. Therefore, we measured the Po_2 in left and right lenses from the same patient. Lenses were incubated at 37°C in AAH equilibrated with various Po_2 values. Lens Po_2 profiles were measured using a fluorescent optode. Profiles were measured along the optic axis (anterior to posterior or vice versa in different lenses). Po_2 profiles were similar in both lenses from the same donor. An example of the Po_2 profiles of a 66-year-old lens pair is shown in Figure 3.2. The lens nucleus Po_2 values in left and right lenses from the same patient were similar (correlation coefficient = 0.89, n=11 lens pairs). In a Po_2 environment of 36 mmHg (5% O_2), the difference in lens nucleus Po_2 between the two lenses from the same donor was 2.4 ± 2.1 mmHg (20% of the average nucleus Po_2 value of ~12 mmHg) (n=11 lens pairs).

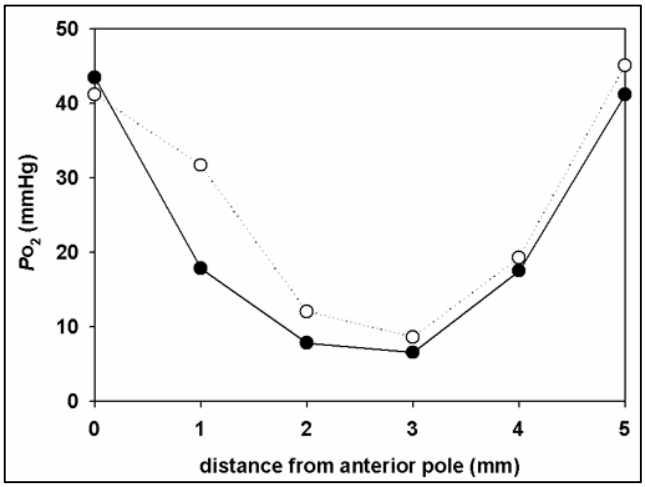

Figure 3.2 *Po_2 profiles in a human lens pair. The lenses from a 66-year-old patient were equilibrated with Po_2 of 36 mmHg (5% O_2). Each data set represents a profile from one lens. The profile shapes and Po_2 values were similar in both lenses.*

The effect of external Po_2 on human lens Po_2 profiles is shown in Figure 3.3. In a Po_2 environment of 7 mmHg (1% O_2), there was a symmetrical Po_2 profile with a gradient over the outer millimeter of cortex, resulting in a Po_2 of 1.2 ± 0.2 mmHg in the centre of the lens (n=6). Lens Po_2 profiles in a Po_2 environment of 36 mmHg (5% O_2) were also symmetrical. However, the gradient extended further into the lens and the Po_2 was higher throughout the core, with a central Po_2 of 12.4 ± 7.8 mmHg (n=29). In an environment of atmospheric levels of O_2 (Po_2 of 150 mmHg or 21% O_2), gradients extended to the centre of the lens and core Po_2 increased to 22.1 ± 17.1 mmHg (n=6). Lenses equilibrated with 100% O_2 saturated the optode signal (>100 mmHg) (n= 2, age 25 years).

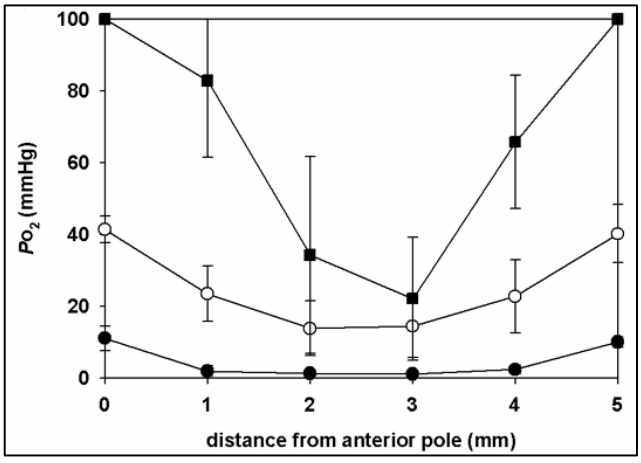

Figure 3.3 *Human donor lens Po_2 in vitro measured with a fluorescent optode. Po_2 profiles along the optic axis. Human donor lenses were equilibrated in a Po_2 environment of either 7 mmHg (1% O_2, closed circles, n=6), 36 mmHg (5% O_2, open circles, n=29) or 150 mmHg (21% O_2, closed squares, n=6). Profiles were symmetrical with cortical gradients and lens nucleus hypoxia under physiological conditions (Po_2 environment of <36 mmHg). Lens nucleus Po_2 rose with increasing external Po_2. Note that the optode signal saturates at 100 mmHg. Therefore, the outer data points for the profile in 21% O_2 are distorted.*

Symmetrical Po_2 profiles, cortical gradients and core hypoxia were also found in the rabbit and bovine lenses examined in the previous chapter (Figure 3.4). These features could, therefore, be general phenomena exhibited by all mammalian lenses.

In lenses from different species under the same conditions, core Po_2 appeared to inversely correlate with lens size. This may be because of the greater amount of tissue through which O_2 needs to diffuse to reach the lens core which increases the chance of the O_2 being consumed.

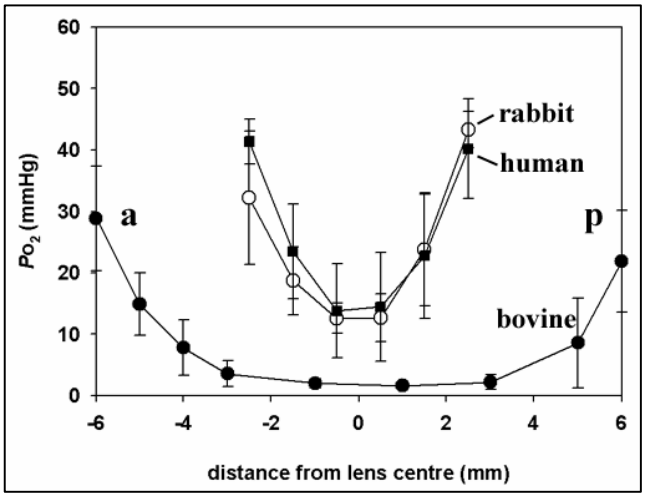

Figure 3.4 *Lens Po_2 profiles in three mammalian species. Bovine (closed circles), rabbit (open circles) and human (closed squares) lenses were equilibrated at 37°C in a Po_2 environment of 36 mmHg (5% O_2). Po_2 gradients were measured with a fluorescent optode from anterior (a) to posterior (p) along the optic axis. All species show symmetrical gradients and core hypoxia. Po_2 is lower in the larger (12 x 17 mm) bovine lens compared to the smaller rabbit and human lenses (both ~9 x 5 mm).*

Lens QO_2

Respirometry was performed on 24 lens pairs with an average age of 55.5 ±14.0 years, after equilibration in a Po_2 environment of 36 mmHg (5% O_2). QO_2 was 0.9 ± 0.4 µl/lens/h (or 3.4 ± 1.6 µl/g/h) (n=24 lens pairs). QO_2 of the capsule and adherent epithelium

in an environment of 36 mmHg was undetectable (n=2, age 47 years), suggesting that this is not the primary site of O_2 consumption by the human lens.

To examine whether lens Po_2 was determined primarily by lens QO_2, we measured both QO_2 and lens nucleus Po_2 of 22 lens pairs in an environment of 36 mmHg (5% O_2) (Figure 3.5). There was no statistically significant change in Po_2 with QO_2 per lens (Figure 3.5A) or per gram (Figure 3.5B), suggesting that other factors, such as lens size, may be involved in modulating lens nucleus Po_2.

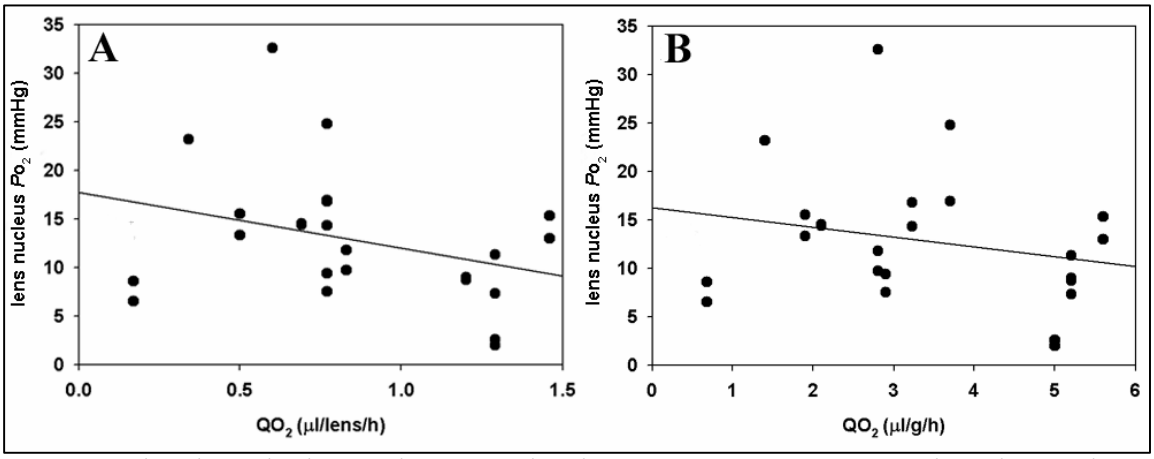

Figure 3.5 *The relationship between lens QO_2 and nucleus Po_2. Measurements were made on the same lenses in an environment of 36 mmHg (5% O_2). Although there was a trend to a lower core Po_2 as QO_2 increased per lens (A) or per gram (B), it did not reach statistical significance in either case (n=22 lens pairs).*

Lenses from all species examined in this thesis consumed O_2 (Figure 3.6). Although lens QO_2 is <1% of that of tissues such as myocardium and brain (Tune *et al.*, 2002; Van Lieshout *et al.*, 2003), it was sufficient to create steep Po_2 gradients in the lens due to O_2 only entering across the lens surface.

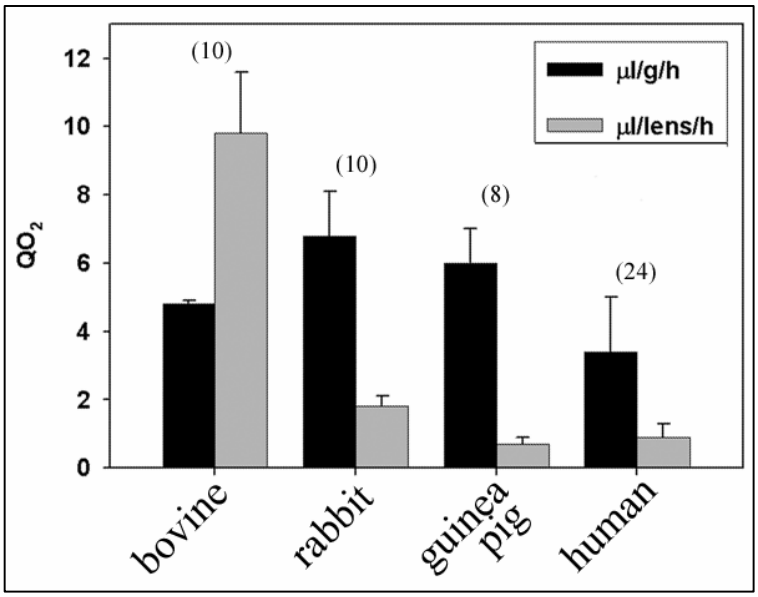

Figure 3.6 *QO_2 in adult mammalian lenses. There is a 10-fold difference in QO_2 when measured on a per lens basis. When corrected for weight, however, QO_2 was similar.*

The effect of age on O_2 measurements

Human lens QO_2 did not significantly change with age, either for QO_2 calculated on a per lens basis or corrected for weight (Figure 3.7A and B, respectively).

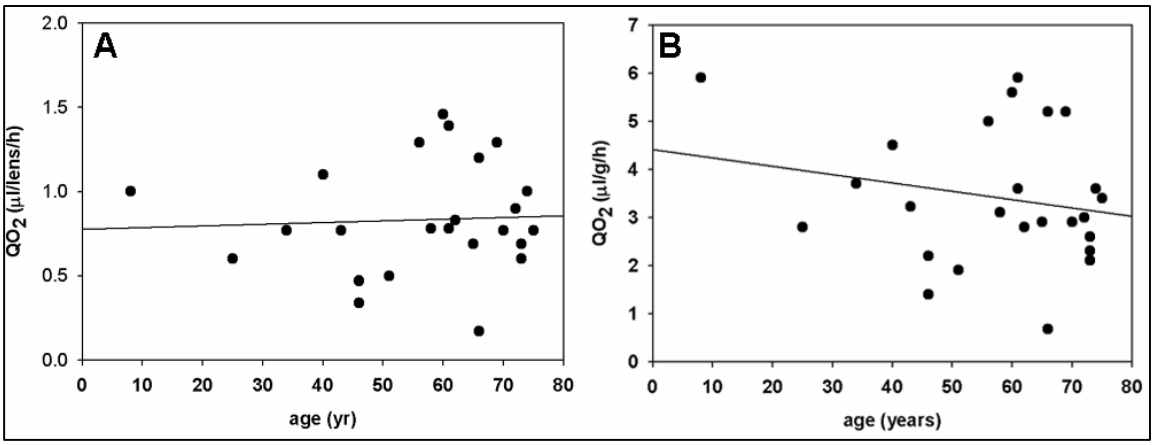

Figure 3.7 *The effect of age on human lens QO_2. Respirometry was performed on human donor lens pairs equilibrated at 37°C in a Po_2 environment of 36 mmHg (5% O_2) (n=24 lens pairs). There was no significant change in QO_2 with age measured either per lens **(A)** or per gram **(B)**.*

The effect of age on lens nucleus Po_2 is presented in Figure 3.8. The average age of lenses used for Po_2 measurements was 59.3 ± 12.7 years (n=37 lenses). There was a significant decrease in lens nucleus Po_2 (p=0.0462, n=18 patients) of 0.28 mmHg/year.

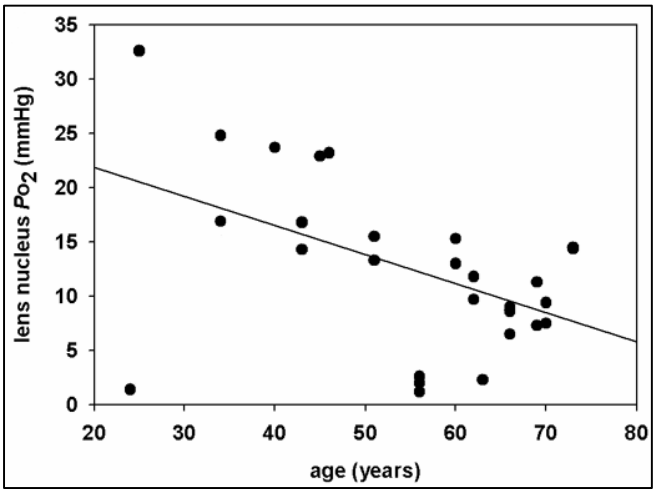

Figure 3.8 *The effect of age on lens nucleus Po_2. The Po_2 values from the geometric centre of the lenses equilibrated in a Po_2 environment of 36 mmHg (5% O_2) from Figure 3.3 are presented in the figure. A linear regression line has been fitted to the data. There was a statistically significant decrease in Po_2 of 0.28 mmHg/year (p=0.046). Note that for patients which had both left and right lens measurements, linear regression was performed using only the average Po_2 value. This provided 18 independent values for regression analysis.*

The effect of diabetes on O_2 measurements

Since diabetes is a cause of cataract, we were interested in the effect it has on lens O_2 levels. 6 out of 24 donors (25%) had a history of diabetes of unknown duration. In a Po_2 environment of 36 mmHg, diabetes had no significant effect on lens QO_2 or lens nucleus Po_2 compared to control lenses, being 0.9 ± 0.4 µl/lens/h (or 3.7 ± 1.5 µl/g/h) (n=6 lens pairs) and 12.5 ± 7.7 mmHg (n=7 lenses), respectively (Figure 3.9).

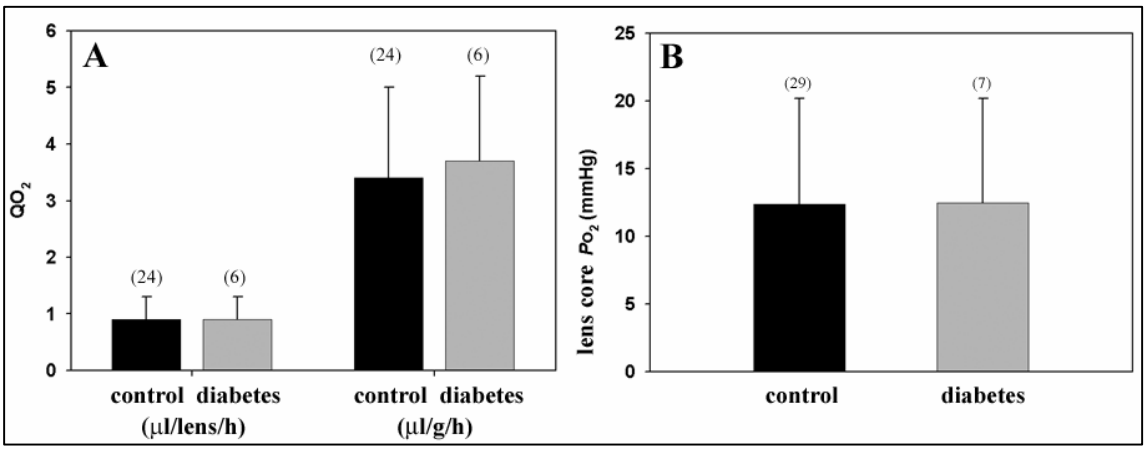

Figure 3.9 *The effect of diabetes on O_2 levels. Diabetes had no significant effect on lens QO_2* ***(A)*** *or lens core Po_2* ***(B)*** *in a Po_2 environment of 36 mmHg compared to control values.*

The effect of post-mortem time on O_2 measurements

The death of the patient could result in deterioration in the condition of the lens with time, possibly producing artefactually low QO_2 values, which could in turn affect tissue O_2 levels. The effect of time between death and experiment on QO_2 and lens nucleus Po_2 values is presented in Figure 3.10. Post-mortem time ranged from 12-60 hours and averaged 28.5 ± 12.0 hours (n=24). Although there appeared to be a trend to decreasing QO_2 values and increasing Po_2 values with increasing post-mortem time, this did not reach statistical significance.

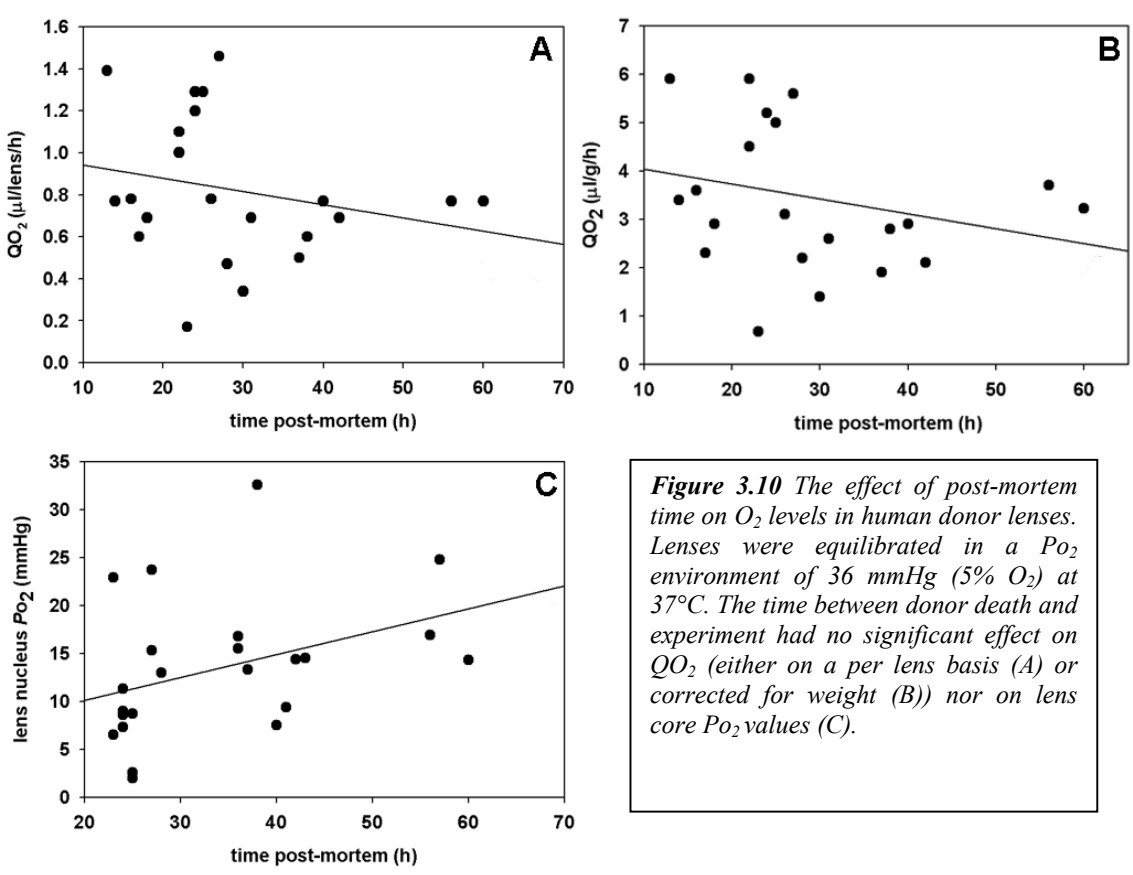

Figure 3.10 *The effect of post-mortem time on O_2 levels in human donor lenses. Lenses were equilibrated in a Po_2 environment of 36 mmHg (5% O_2) at 37°C. The time between donor death and experiment had no significant effect on QO_2 (either on a per lens basis (A) or corrected for weight (B)) nor on lens core Po_2 values (C).*

The role of mitochondria: mapping and inhibition studies

The role of mitochondria in shaping human lens O_2 levels was addressed by first establishing their distribution in the tissue. Preliminary experiments on living human lenses with rhodamine 123 revealed only a diffuse background fluorescence (data not shown). As an alternative, living lenses were treated with the vital mitochondria-specific dye Mito Tracker Deep Red 633 and viewed on a confocal microscope. Mitochondria were most abundant in the epithelial layer (Figure 3.11D). Elongated mitochondria were also found in the tips of the fibre cells under the epithelium (Figure 3.11D) and at the equator (data not shown). However, the quantity of mitochondria in the fibre cells of the human lens were

sparse compared to that found in the bovine lens with rhodamine 123 (Figure 2.16). Due to the possibility that mitochondria may have died in the post-mortem period, we employed a second technique to map the distribution of mitochondria. Fixed human lenses were sliced and processed for immunofluorescence using an antibody to cytochrome *c*-oxidase (COX or complex IV) of the mitochondrial respiratory chain. Slices were then viewed on a confocal microscope. Mitochondria were found in a continuous shell in the outermost cortex of the lens in all ages examined (ages 6, 27, 41, 53 and 60) (Figures 3.11 and 3.12). As with the bovine lens, the highest density of mitochondria was in the epithelium (Figure 3.11A). However, in the fibre cells, the mitochondria appeared as punctate structures, in contrast to the elongated mitochondria seen in the bovine lens (Figure 2.16). Another difference to the bovine lens was that the mitochondrial shell did not extend as deep into the human lens, being 95.8 ± 15.1 μm (n=5), 81 ± 11.2 μm (n=4) and 47.8 ± 1.6 μm (n=4) in the equatorial, anterior and posterior cortices respectively. If we assume average dimensions of 9 x 5 mm for the human lens, the mitochondrial depth is 2.2-2.6% of the human lens diameter, in contrast to ~9% in the bovine lens. The depth in the posterior cortex was significantly shallower than the anterior and equatorial cortices ($p<0.01$). As a control experiment, there were no structures detectable in slices that were not treated with the primary antibody (data not shown).

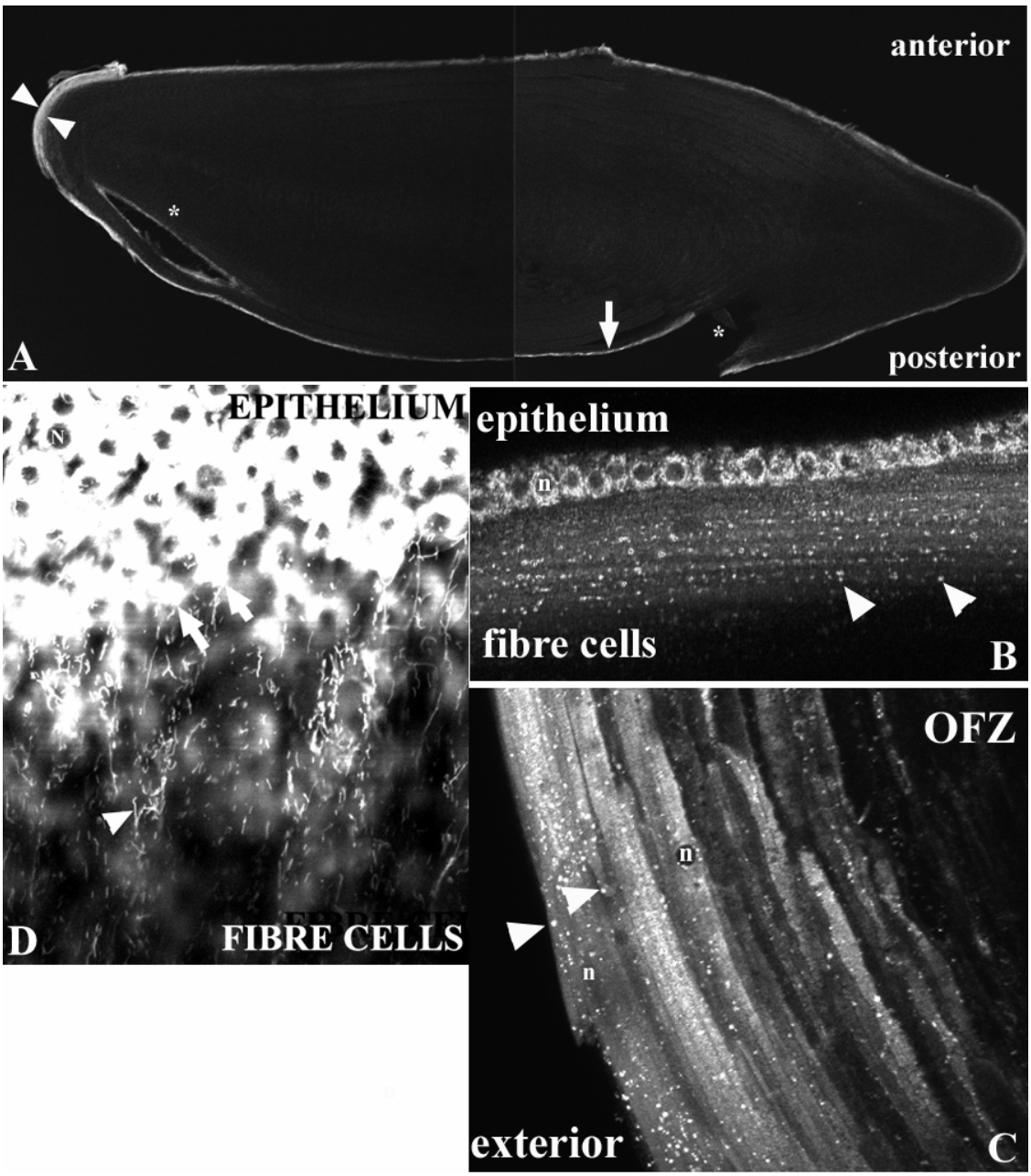

Figure 3.11 *Distribution of mitochondria in the human lens.* ***A-C.*** *Lenses were fixed, sliced and treated with an antibody to COX (complex IV) of the mitochondrial respiratory chain. The slices were then viewed on a confocal microscope.* ***A.*** *A collage of two micrographs of a 6-year-old lens at 2.5x magnification. There was a complete ring of mitochondria in the outer cortex of the lens, including the posterior pole (arrow). The mitochondria-containing cell layer depth was maximal at the equator (arrowheads). Tissue damage secondary to processing for histology is also evident (*).* ***B.*** *Anterior cortex of a 41-year-old lens. Mitochondria appeared as punctate structures (arrowheads). The epithelial cytoplasm had the highest density of mitochondria giving an outline of the cell nucleus (n)* ***C.*** *Mitochondria at the equator in a 6-year-old lens. Punctate mitochondria (arrowheads) and cell nuclei (n) were visible in the bow region. The mitochondria are absent in the organelle-free zone (OFZ).* ***D.*** *Mitochondria visualised with the vital dye MitoTracker Deep Red 633. Mitochondria were abundant in the cytoplasm of the epithelial cells (arrows), leaving a silhouette of the cell-nucleus (N). Sparse elongated mitochondria were also seen in the tips of the anterior fibre cells.*

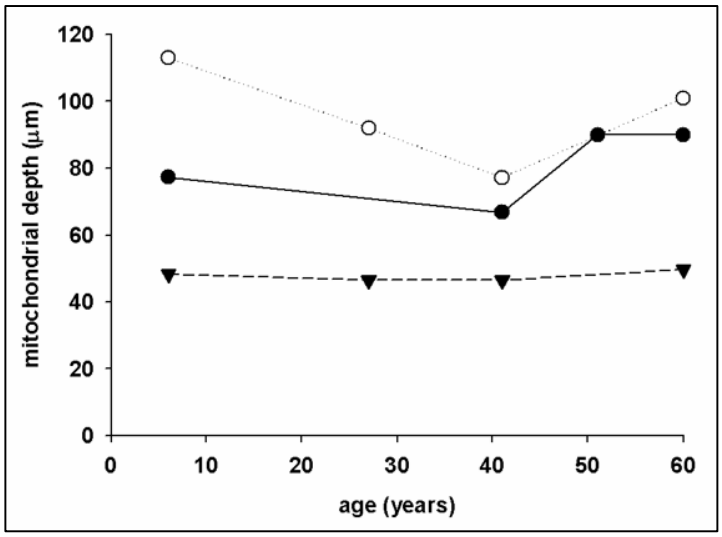

Figure 3.12 *Depth of the mitochondria-containing cell layer in the human lens. Mitochondria were visualized via immunofluorescence using an antibody to complex IV (COX). The maximum depth in the anterior (closed circles), posterior (closed triangles) and equatorial (open circles) cortices for various ages (6, 27, 41, 53 and 60 years) is presented in the graph. The cell layer extended deepest at the equator and was shallowest at the posterior cortex. There was no substantial change in depth with age. Note that the depths were significantly shallower than those found in the bovine lens (see §2.3).*

The contribution of mitochondrial O_2 consumption to human lens QO_2 consumption was investigated by treating lenses with the respiration inhibitors myxothiazol (10 µM), an inhibitor of the b-c_1 complex, or azide (5 mM), an inhibitor of cytochrome *c*-oxidase (complex IV). Lens pairs were equilibrated and tested at 37°C in a Po_2 environment of 36 mmHg (5% O_2). Neither mitochondrial inhibitor decreased QO_2 in the human lens. This is in contrast to the significant effect of the inhibitors on bovine lens QO_2 which was inhibited by >90% (Figure 2.19). Human lens QO_2 before and after treatment with myxothiazol was 0.6 ± 0.1 and 0.7 ± 0.1 µl/lens/h, respectively (or 2.5 ± 0.3 and 2.9 ± 0.8 µl/g/h, respectively) (n=3 lens pairs; age 46, 73 and 75 years). For azide, QO_2 before and after treatment was 0.9 ± 0.2 and 0.8 ± 0.2 µl/lens/h, respectively (or 3.9 ± 0.8 and 3.8 ± 0.8 µl/g/h, respectively) (n=3 lens pairs; age 56, 61 and 64 years). The azide data includes a 56-year old lens pair that was examined 12 hours post-mortem.

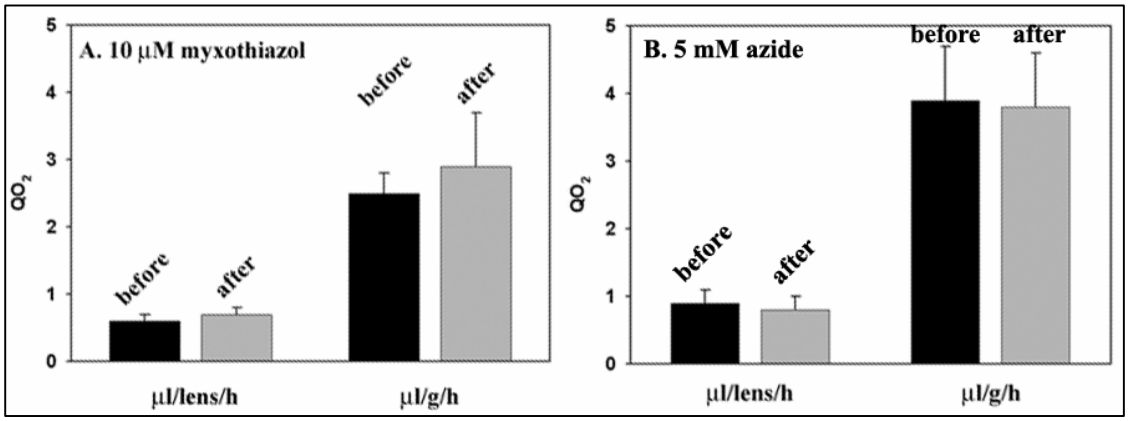

Figure 3.13 *Mitochondrial inhibition of human lens QO_2. Lens QO_2 was measured before and after incubation in 10 μM myxothiazol (3 lens pairs)* ***(A)*** *or 5 mM azide (3 lens pairs)* ***(B)****. In contrast to the bovine lens (Figure 2.19 and §2.3), neither drug had a significant effect on human lens QO_2.*

Non-mitochondrial O_2 consumption

Ascorbate, found in millimolar concentrations in the human lens (DL Garland, 1991), is capable of metal-catalysed O_2 consumption (§1.5.2). To assess the role of ascorbate, we examined whether O_2 consumption in the lens was metal-dependent by measuring lens homogenate QO_2 in the presence or absence of the metal-chelator DETAPAC (1 mM). Treatment decreased QO_2 by 50% from 6.8 ± 1.2 μl/g/h to 3.4 ± 1.1 μl/g/h (n=3 lenses each group). Therefore, the metal-dependence of human lens O_2 consumption is consistent with ascorbate-mediated O_2 consumption.

Effect of temperature on lens O_2 levels

Temperature was a significant factor in determining O_2 levels in the bovine lens. Decreasing temperature below physiological levels decreased bovine lens QO_2 (Figure 2.14) and concomitantly increased lens Po_2 (Figure 2.15). Due to the possible relevance of the effect of temperature on lens O_2 levels to post-vitrectomy cataract formation (§2.4), we sought to investigate O_2 levels in the human lens under conditions similar to those found during vitrectomy surgery. Human lenses were equilibrated in AAH containing

atmospheric levels of O_2 (Po_2 of 150 mmHg or 21% O_2). Lens nucleus Po_2 and temperature was monitored while the solution temperature was alternated between 37°C and room temperature (20°C) (Figure 3.14). At 37°C, core Po_2 was <10 mmHg. A decrease to room temperature (at time 0 in Figure 3.14A) caused the core Po_2 to rise to >100 mmHg in less than 30 minutes (Figure 3.14A). The rise in human nucleus Po_2 caused by a drop in temperature was more rapid than in the bovine lens, possibly due to the smaller dimensions of the human lens. Increasing the temperature to 37°C resulted in a drop in core Po_2, showing that the temperature effect was reversible and repeatable (Figure 3.14A). The increase in core Po_2 induced by a drop in temperature can be attenuated if the temperature decrease is minimized. For example, a reduction in solution temperature to 30°C resulted in a more modest rise in core Po_2 to approximately 40 mmHg (Figure 3.14B). This suggests that attempting to maintain the lens above room temperature may minimize lens Po_2 increases in vivo and hence possibly avoid additional oxidative stress.

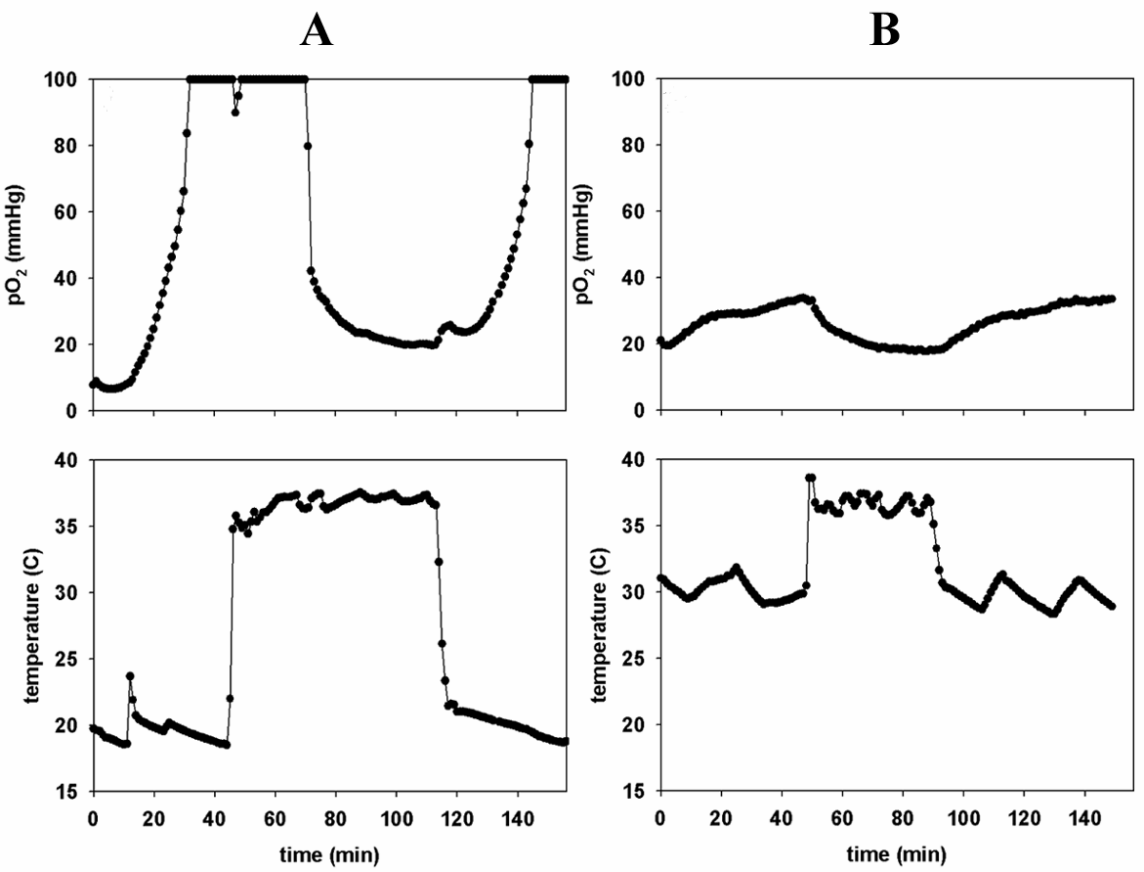

Figure 3.14 *Effect of temperature on Po_2 in the isolated human lens. Lenses were equilibrated in AAH containing atmospheric levels of O_2 (Po_2 of ~150 mmHg or 21% O_2). The Po_2 and temperature were monitored in the lens nucleus with an optode as the temperature of the bathing solution was varied. Lenses were incubated at 37°C prior to time 0.* ***A.*** *At time 0, temperature was decreased from 37°C to room temperature (~20°C) in a 45-year-old lens. At 37°C (prior to time 0), Po_2 in the lens nucleus was <10 mmHg. After changing to room temperature, Po_2 increased to >100 mmHg within 30 minutes. The effect is reversible.* ***B.*** *The lens core was maintained in a relatively hypoxic condition (<35 mmHg) provided the tissue temperature did not fall below ~30°C (69-year-old lens).*

3.4 Discussion

We hypothesized that human lens QO_2 decreased with age, leading to an increase in lens nucleus Po_2 in older lenses. In contrast to our prediction, however, lens QO_2 did not significantly change with age (Figure 3.7), and nucleus Po_2 decreased significantly with age (Figure 3.8). The decrease in Po_2 may be due to the increasing size of the lens which provides a longer distance over which O_2 has to travel to reach the lens centre.

According to inhibition studies, the role of mitochondria in lens QO_2 may be species dependent. Mitochondria were the main regulators of tissue Po_2 in the bovine lens, responsible for approximately 90% of O_2 consumption (Figure 2.18). Surprisingly, mitochondria appeared to play an insignificant role in human lens QO_2. This could be due to the inhibitors not penetrating into the human lens. Alternatively, the lack of effect of azide treatment on the human lens could be the reaction of azide with thiol groups. The human lens, unlike the bovine lens, contains millimolar concentrations of GSH (Giblin, 2000), which forms the basis of a very efficient thiol-based anti-oxidant system, as evidenced by the ability of monkey lenses to survive incubation in 1 mM H_2O_2 (Zigler, Jr. *et al.*, 1989). This provides a plausible mechanism for the inactivation of azide. To the best of our knowledge, it is unknown whether myxothiazol also reacts with thiol groups. In addition, the inhibitors used here (azide and myxothiazol) may not have an effect on human mitochondria. Azide is well known as a potentially lethal poison to humans (Chang & Lamm, 2003). However, this does not necessarily imply that azide inhibits human mitochondria. To the best of our knowledge, there is no data available on the effect of myxothiazol on human mitochondria. It may be that studies on isolated human mitochondria are needed in order to determine their role in human lens O_2 consumption. The variation of results between species may also be explained by differences in the physiology or quantity of mitochondria in the respective species. The mitochondrial contribution to lens QO_2 correlated with the depth of mitochondria. The mitochondrial depth in the bovine lens (approximately 500-760 μm or ~9% of lens diameter) was nearly an order of magnitude larger than in the human lens (approximately 50-100 μm or 2.2-2.6% of lens diameter). By inference, the bovine lens has a significantly higher number of

mitochondria than that found in the thin human layer which could consume O_2. Additionally, in the human, the mitochondrial morphology was punctate rather than elongated as in the bovine lens, which may reflect a functional difference. Although the correlations between the mitochondrial contribution to QO_2 and the depth or morphology were strong, it must be noted that mitochondrial function per se was not explicitly assessed in this thesis.

It may be that non-mitochondrial O_2 consumption is important in the human lens. Ascorbate, which is found in millimolar amounts in the human lens (see §1.5), may play a major role in this tissue. Another possible candidate is the non-phagocytic NADPH-oxidase system, which was recently identified in the human lens (Rao *et al.*, 2004). This enzyme consumes O_2 by the transfer of an electron from NADPH to produce $O_2^{\bullet-}$. Future studies will be needed to address these issues.

In isolated human lenses under conditions found during vitrectomy surgery (i.e., the lens is surrounded by room temperature O_2-rich solutions), lens core Po_2 rose nearly an order of magnitude within 25 minutes (Figure 3.14A). This time-frame makes it plausible that human lens core Po_2 may rise to similar levels during vitrectomy, which therefore represents an oxidative stress to the lens. This is an attractive explanation for the high incidence of nuclear cataract seen after vitrectomy. We have developed a clinical trial at Washington University in St Louis to test the hypothesis that the use of pre-warmed infusion solutions during the vitrectomy procedure may avoid an oxidative insult to the lens and hence decrease the incidence of post-vitrectomy cataract. According to our data,

warming the solutions to perhaps 30°C may be enough to avoid a flood of O_2 to the lens core (Figure 3.14B). The protocol for the study is presented at the end of the thesis.

Chapter 4:

Tissue O_2 levels in the developing chicken eye and their relation to organelle loss

4.1 Introduction

The lens is an apparently homogenous ball of cells and yet we know that specific genes are turned on and off at specific depths. One example of this is the gradient of protein concentration along the radius (Veretout & Tardieu, 1989). This in turn generates the graded internal refractive index found in the lens (Pierscionek & Chan, 1989). In addition, the outermost layers of the lens contain newly differentiating fibre cells that are elongating, moving across the capsule and commencing expression of high levels of crystallin proteins. As differentiation progresses, they become buried by younger fibre cells, detach from the capsule, and reach the sutures (Bassnett & Winzenburger, 2003). One plausible mechanism of coordinating the transcription of genes is the presence of a standing Po_2 gradient. In this chapter we investigate the role of O_2 gradients on one of the most dramatic events to occur during fibre cell differentiation: the loss of all intracellular organelles. At a well-defined depth, the organelles and nuclei vanish simultaneously (Bassnett, 1995;Bassnett & Beebe, 1992). The loss of organelles is thought to decrease light scatter. In chicken lenses, this process begins in the central lens fibres on embryonic day 12 (E12). Thereafter, the resulting organelle-free zone (OFZ) of the lens expands at a rate of 80 μm/day (Bassnett & Beebe, 1992), eventually encompassing most of the lens volume. Because the growth rate of the OFZ closely matches that of the embryonic lens, the border of the OFZ remains a fixed distance below the surface of the tissue. The depth at which the organelle-free zone border occurs is species dependent. For example, in embryonic chicken lenses, the OFZ border is located approximately 800 μm beneath the equatorial surface (Bassnett & Beebe, 1992). In the lens of the adult rhesus monkey, the organelle containing layer is approximately 150 μm thick at the equator (Bassnett, 1997),

while in the bovine lens, this region is more than 700 μm thick (§2.3). In each case however, the border is sharply defined. This implies that organelle breakdown is relatively rapid, and synchronized in a shell of fibre cells situated a specified distance below the lens surface.

The O_2 gradients within the lens demonstrated in previous chapters may provide the spatial cue necessary to coordinate the loss of organelles in the differentiating fibre cell population. During its lifetime, a lens cell experiences a predictable change in Po_2. Epithelial cells are exposed to an average Po_2 of 36 mmHg (Fitch, et al., 2000). However, MF are located in an environment of <2 mmHg (Figure 2.9). This requires a shift from aerobic to anaerobic metabolism. It is known that glycolysis is the major energy source in the lens. An interesting possibility is that genes not normally considered to be hypoxia-regulated may occur in the lens. The regulation of organelle-loss by an O_2 gradient would be an example of this. A possible mechanism by which hypoxia may regulate organelle-loss is through the link between apoptosis (programmed cell death) and hypoxia. Organelle loss has characteristics reminiscent of apoptosis (Appleby & Modak, 1977;Dahm, 1999;Ishizaki, et al., 1998;Modak & Bollum, 1972) and hypoxia is known to trigger apoptosis in a variety of cells (Banasiak, et al., 2000).

The hypothesis that hypoxia regulates organelle-loss predicts that elevated tissue O_2 levels in the lens would delay organelle loss. This hypothesis was tested in collaboration with Dr Steven Bassnett (Department of Ophthalmology, Washington University in St Louis, USA). Dr Bassnett incubated chicken embryos in normoxic (Po_2

of 150 mmHg or 21% O_2) and hyperoxic (Po_2 of 360 mmHg or 50% O_2: 50% N_2) conditions and carried out morphometric analysis of the lenses. Hyperoxic conditions not only resulted in larger lenses, but did in fact delay organelle loss and as a consequence increased the depth of the organelle-containing fibre cell layer in the outer cortex (Figure 4.1) Results in full can be found in (Bassnett & McNulty, 2003).

The study has two aspects: examining the effect of varying O_2 levels on the fate of organelles and measuring the fluctuations in Po_2 in the embryonic eye. The latter aspect is presented in detail in this chapter. Measuring Po_2 in the embryonic eye represents a technical challenge. Here, we couple the use of the hypoxia marker pimonidazole with a fluorescent optode to measure O_2 levels in and around the lens of the developing chicken eye under normoxic and hyperoxic conditions.

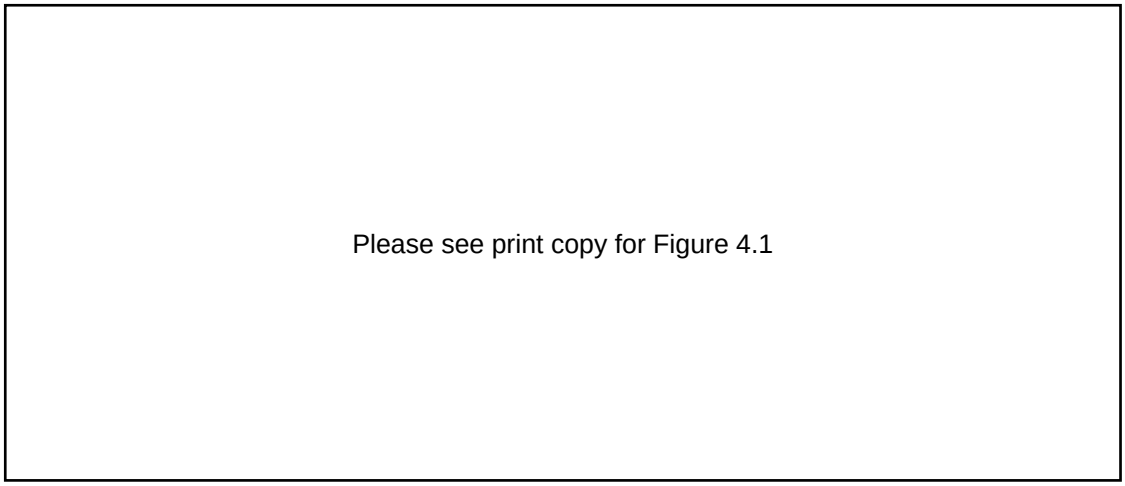

Figure 4.1 *Effect of hyperoxia on the morphometry of the embryonic chicken lens. Chicken eggs were placed in normoxic or hyperoxic conditions (see text for details). Lenses were fixed, sliced and dimensions of the whole lens and organelle containing zones measured.* ***A.*** *Diagram of lens slice and dimensions used in B and C.* ***B.*** *Effect of hyperoxia on lens cross-sectional area. Mid-sagittal slice area was measured in normoxic (closed circles) and hyperoxic (open circles) lenses. Hyperoxia resulted in larger lenses (n=at least 9 lenses for each data point).* ***C.*** *Effect of hyperoxia on organelle-containing fibre cell depth. Hyperoxia caused an increase in the depth of the organelle-containing fibre cells as indicated by the average of d1 and d2 from Figure A (n=at least 16 lenses for each data point). (*=P<0.05, Student's t-test). Data courtesy Dr S. Bassnett.*

4.2 Methods

Animals

White Leghorn chicken (*Gallus gallus*) eggs (CBT Farms, Chestertown, MD, USA) were incubated in a humidified forced draft incubator at 38^{o}C under normoxic conditions until the seventh day of embryonic development (E7). At this point, some eggs were transferred to hyperoxic conditions in an airtight Plexiglas chamber (Bellco glass Inc, Vineland, NJ, USA) located within the incubator. Humidified 50% O_2:50% N_2 was passed continually through the chamber (flow rate 50 ml/minute). Normoxic and

hyperoxic eggs were removed at various embryonic days from E9 and subjected to further analysis (chickens hatch on E21).

O_2 measurement

Po_2 measurement. Vitreous *P*o_2 at various days of embryonic development was measured using the optode system described in §1.6.2. To measure vitreous *P*o_2, the egg shell was windowed and the head of the embryo exposed. A hole was made in the posterior sclera with a 25G needle. The optode was guided through the hole into the eye via a micromanipulator to position the optode tip in the geometric centre of the vitreous. Stable measurements were usually obtained within 20 seconds. After *P*o_2 was measured in the central vitreous, the optode tip was advanced to a position immediately behind the lens, where a second measurement was made. To ensure readings were vitreal, eyes were dissected after sacrifice to verify that the optode had not pierced the lens or iris.

Visualising hypoxia. Lens hypoxia was visualised using the hypoxia marker pimonidazole (Hypoxyprobe-1; NPI, Inc., Belmont, MA, USA). Hypoxia markers (see §1.6.3), such as pimonidazole (Figure 1.11), bind covalently to tissue protein only in hypoxic conditions (<10 mmHg) (Gross, et al., 1995;Raleigh, et al., 1999). The distribution of bound pimonidazole can be visualised immunocytochemically.

Both normoxic and hyperoxic eggs were assayed. The eggs were windowed to expose the head of the embryo. An injection of 3µl of 10 mg/ml solution of pimonidazole hydrochloride (Hypoxyprobe-1; NPI, Inc., Belmont, MA, USA) was made into the left

vitreous humour. The right vitreous humour was injected with PBS and served as a control. The egg was resealed and placed in the incubator for one hour. Then embryos were decapitated and lenses removed through an incision in the posterior globe. Lenses were fixed for two hours at room temperature in 4% paraformaldehyde/PBS and processed for routine paraffin sections. This consisted of fixation for 24 hours in 10% neutral buffered formalin, followed by tissue dehydration in 95% ethanol for 4 hours and then xylene for 2 hours. Lenses were embedded in paraffin and 4 µm slices were cut and placed on glass slides. Immunocytochemistry was performed according to the instructions provided with the Hypoxyprobe-1 system. Briefly, following slicing and antigen-retrieval with pronase, sections were incubated with 1:50 dilution of Hypoxyprobe Mab1, an antibody that specifically recognizes protein adducts formed by pimonidazole under hypoxic conditions. Antibody distribution was visualised with a horseradish peroxidase-conjugated secondary antibody, with diaminobenzidine (DAB) as the chromogenic substrate.

To confirm that pimonidazole binds to the lens only under hypoxic conditions, isolated lenses were treated with pimonidazole in solutions of known Po_2. Normoxic embryos were sacrificed and lenses dissected from the eye by making an incision in the posterior sclera and removing them along with the vitreous humour. After careful dissection, the lenses were placed in PBS containing 10 mg/ml of pimonidazole. This solution was then gassed with known concentrations of O_2 for one hour. Lenses were then fixed and processed for immunocytochemistry as above. Negative controls included no pimonidazole or no primary antibody. After histology, lens slices were mounted on

slides for viewing on an inverted light microscope (model Axiovert 200M, Carl Zeiss Inc., Thornwood, NY, USA) and photographed using a Spot RT cooled CCD camera (Diagnostic Instruments Inc., Sterling Heights, MI, USA).

4.3 Results

An optode O_2 sensor was used to measure vitreous Po_2 in developing chicken embryos incubated under normoxic (Po_2 of 150 mmHg or 21% O_2) and hyperoxic conditions (Po_2 of 360 mmHg or 50% O_2) (Figure 4.2). At early stages (≤E9), due to the small size of the eye in relation to the probe, only a single measurement was made in the centre of the vitreous. From E10, however, eyes were large enough to allow separate Po_2 measurements in the mid- and anterior vitreous. Under normoxic conditions, Po_2 levels in the developing eye of young embryos (≤E8) were very low (<5 mmHg). Values rose from E6 to E9 and stabilised thereafter. From E9 to E20, Po_2 in the mid-vitreous was 10.4 ± 0.7 mmHg (mean ± SEM, n=11). Anterior vitreous was consistently lower than the mid-vitreous value. The average anterior vitreous Po_2 from E9 to E20 was 2.8 ± 0.3 mmHg (mean ± SEM, n=11).

We examined whether incubating eggs under hyperoxic conditions resulted in a significant increase in vitreous Po_2. Eggs were incubated under normoxic conditions until E7 and then switched to hyperoxic conditions until E13. Measurements were made at E13 in the mid-vitreous and anterior vitreous (Figure 4.2, triangles). Hyperoxia produced approximately a three-fold elevation in Po_2 throughout the vitreous. In E13 hyperoxic embryos, the mid-vitreous Po_2 was 29.6 ± 3.8 mmHg and the anterior vitreous Po_2 was

9.6 ± 1.9 mmHg (n=6). Both of these values were significantly higher than those of normoxic controls (P<0.001).

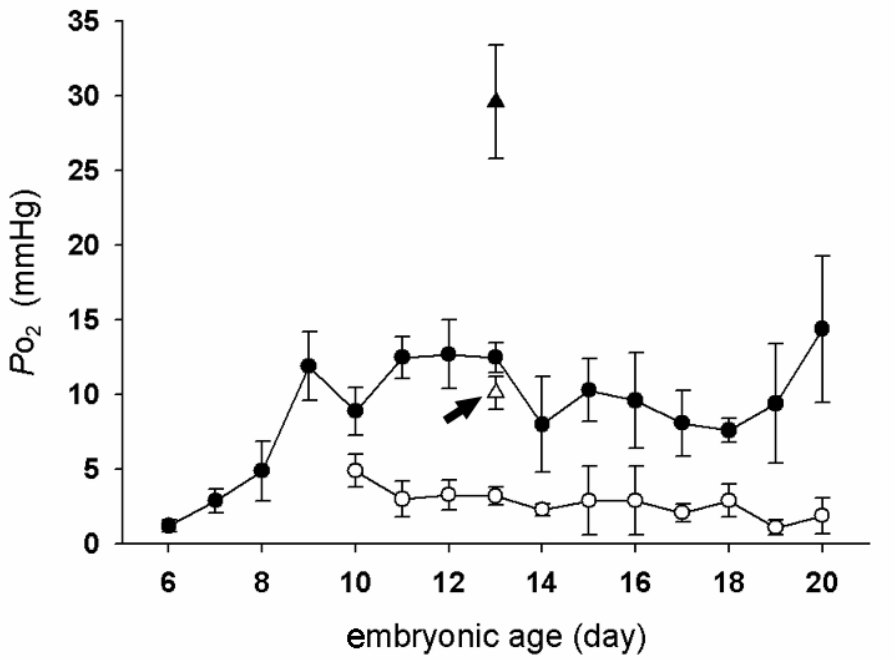

Figure 4.2 *Intraocular Po_2 in the embryonic chicken. An optode was used to measure in the anterior (open symbols) and mid-vitreous humour (filled symbols) of normoxic (exposed to Po_2 of 150 mmHg or 21% O_2) chicken embryos (circles). Each data point represents at least 6 eyes. The vitreous shows a Po_2 gradient from posterior to anterior with extremely low O_2 tension behind the lens. Other eggs were incubated from E7 to E13 in a hyperoxic atmosphere (Po_2 of 360 mmHg or 50% O_2: 50% N_2). Measurements made at E13 on those embryos (triangles), indicated that hyperoxia causes a significant increase in Po_2 in both the anterior (arrow) and mid-vitreous. The O_2 gradient from posterior to anterior also remains in hyperoxic conditions.*

The optode has a diameter of 320 μm and although this was sufficiently small to allow O_2 measurements in the vitreous humour it was too large for intra-lenticular measurements. We therefore utilised the bioreductive hypoxia marker, pimonidazole, for visualising tissue O_2 levels within the lens. Experiments on E17 lenses in vitro confirmed that, similar to other tissues, pimonidazole-protein adducts were only formed in the lens under hypoxic conditions (Figure 4.3). Following incubation in solutions equilibrated

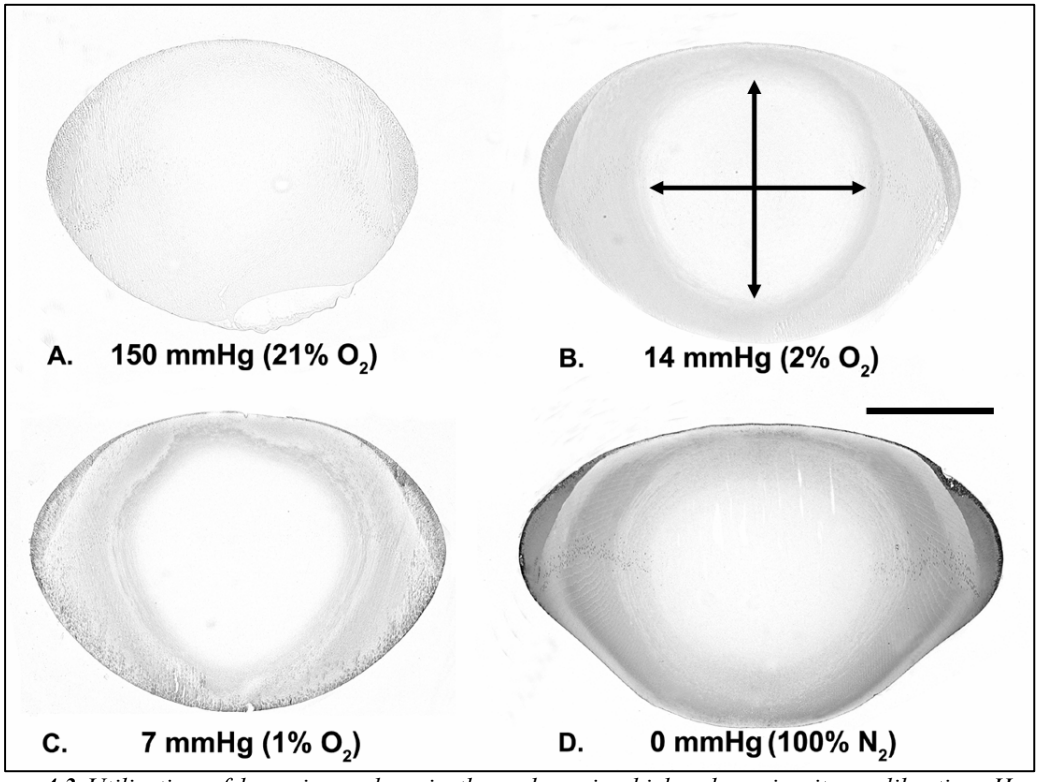

Figure 4.3 *Utilisation of hypoxia markers in the embryonic chicken lens: in vitro calibration. Hypoxia (<10 mmHg) was visualised using the bioreductive hypoxia marker, pimonidazole. For calibration purposes, E17 lenses were incubated in pimonidazole in vitro in PBS solution equilibrated with Po_2 of 150, 14, 7 or 0 mmHg. Formation of pimonidazole-protein adducts under hypoxic conditions was visualized immunocytochemically (see text for details). At 150 mmHg (A), no adducts were detected. However, adducts were detectable in lenses incubated in Po_2 ≤14 mmHg (B, C and D). Intense staining was present in lenses incubated in 100% N_2 (D). Staining was absent in the lens core, corresponding to the organelle-free zone (arrows, B). Scale bar= 250 µm.*

with atmospheric levels of O_2 (Po_2 of 150 mmHg or 21% O_2), no immuno-staining was observed (A). However, incubation with solutions equilibrated with Po_2 ≤14 mmHg (2% O_2) resulted in diffuse staining of the lens cortex (B, C and D). The most intense staining pattern was observed following incubation in solutions gassed with 100% N_2 (D). There was an absence of staining in the lens core. It is possible that the pimonidazole did not diffuse into the core region. However, the non-staining region corresponded in size and shape to the OFZ, suggesting that this region may lack the necessary bioreductive enzymes to metabolise pimonidazole.

Next, we examined lens O_2 levels in vivo by injecting pimonidazole into the vitreous humour of chicken embryos raised in normoxia. These in vivo experiments indicated that the lens existed in a chronically hypoxic state throughout embryonic development. Intra-vitreal injection of pimonidazole into E10 and E17 eyes, for example, resulted in adduct formation (Figure 4.4).

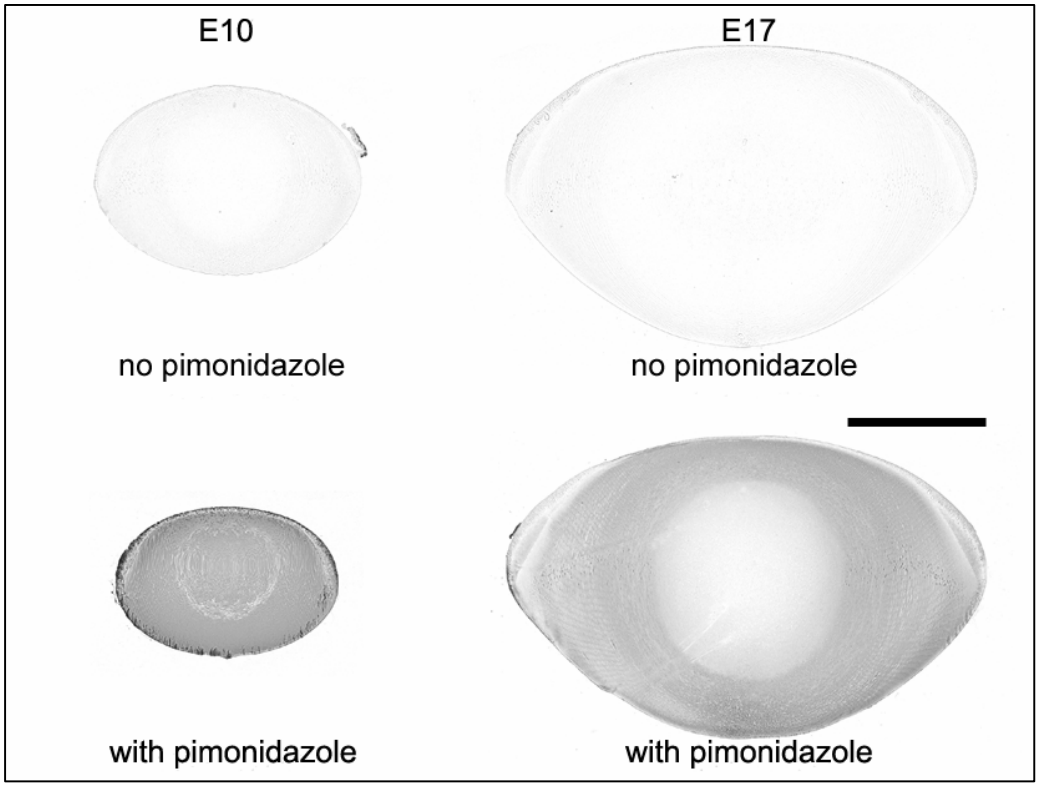

Figure 4.4 *In vivo hypoxia in the developing chicken lens. Hypoxia was visualised with the hypoxia marker pimonidazole. An injection of pimonidazole into the vitreous of embryos raised in normoxic conditions resulted in strong cortical immuno-staining throughout development. E10 and E17 samples are shown above. No immuno-staining was observed with a sham injection of PBS containing no pimonidazole, confirming the specificity of the pimonidazole antibody. Scale bar = 250 µm.*

In young embryos (<E13) adducts were present throughout the tissue. However, as with the in vitro experiments, at later stages (>E13), immuno-staining was restricted to the lens cortex, and pimonidazole adducts were not detected in the lens core (data for E13 not

shown). Control experiments confirmed that adduct formation was dependent on the presence of the pimonidazole (Figure 4.4).

We further examined whether incubation under hyperoxic conditions abolished pimonidazole staining in vivo. Despite the fact that hyperoxia caused an approximate doubling of intraocular Po_2 (Figure 4.2), no change in pimonidazole-adduct staining within the lens was observed in hyperoxic conditions (data not shown).

4.4 Discussion

A fluorescent optode was used to measure vitreous Po_2 in the developing chicken eye. Measurements revealed that Po_2 in the vitreous was low (<15 mmHg) throughout embryonic development. The Po_2 values recorded in the mid-vitreous were consistently higher than those measured immediately behind the lens. Although, to the best of our knowledge, these are the first Po_2 measurements in an embryonic eye, similar standing Po_2 gradients have been noted in the adult vitreous in other species (Table 1.3, §1.7.3). In rabbits, a vitreous Po_2 value of 2.1 mmHg was measured behind the lens and 20 mmHg adjacent to the retina (Ormerod, et al., 1987). In humans, values of 15.9 mmHg and 19.9 mmHg have been reported for the central vitreous and posterior vitreous respectively (Sakaue, et al., 1989;Sakaue, et al., 1989). These data likely reflect the fact that, in most vertebrates, the retina represents a source of O_2, and the lens a sink. The anterior lens, on the other hand, has a different source of O_2: namely, the vasculature of the iris (Helbig, et al., 1993;Hoper, et al., 1989) and possibly the ciliary body. After birth, diffusion through the cornea may also be a source of O_2 (Fitch, et al., 2000;Kwan, et al., 1972), but this is

probably less important in the embryonic eye. In adult humans, Po_2 values of 13.5 mmHg have been recorded in front of the pupil (Helbig, et al., 1993). Similar aqueous Po_2 values have been reported in rabbit and monkey eyes (Hoper, et al., 1989). As with the vitreous humour, standing gradients of Po_2 have been measured in the aqueous humour of immobilized eyes (Helbig, et al., 1993). However, these are likely to be dissipated by convective mixing in alert and active subjects (Maurice, 1998). Presumably, hyperoxic treatment resulted in an increase in aqueous humour Po_2. However, the relatively small size of the anterior segment compared with the diameter of the optode, and the leak of aqueous humour through any incision entering the anterior chamber, precluded direct measurement of aqueous Po_2 in the present study.

We attempted to measure Po_2 inside the lens. However, the optode would not enter the lens through the intact lens capsule and any attempt to make a hole in the capsule with a 25G needle resulted in extrusion of the lens contents. As an alternative, we used the hypoxia marker pimonidazole to visualize tissue hypoxia. As expected, pimonidazole adducts were produced in the lens in vitro under hypoxic conditions (Po_2 of 0-14 mmHg or 0-2% O_2). In young lenses (<E13), adducts were distributed throughout the lens, however, even in fully deoxygenated solutions, the cores of lenses from older embryos (≥E13) were not stained by the adduct-specific antibody. It is possible that pimonidazole did not enter the core of the lens. However, there was a remarkable concordance in the shape and size of the unstained region to the OFZ. Therefore, it may be that this region, which is known to lack stable mRNA and activity of other enzymes (Faulkner-Jones, et al., 2003;Hahn, et al., 1976;Ohrloff & Hockwin, 1983), also lacks the

endogenous bioreductase activity necessary to properly metabolise the marker. Another factor of relevance to pimonidazole binding in the lens is the presence of high levels of the anti-oxidant glutathione (GSH). This important molecule is found at high concentrations in the lens, ranging from 10-20 mM in the epithelium to 2 mM in the lens nucleus (Giblin, 2000). GSH may compete with protein-SH for binding of pimonidazole. Given the gradients of GSH in the lens, this would further complicate the interpretation of differential pimonidazole staining in the lens. In conclusion, it was not possible to quantify the pimonidazole staining as a function of Po_2. However, pimonidazole-protein adducts are generally considered to form only at Po_2 values of <10 mmHg (Varghese, et al., 1976). Our in vitro data were consistent with this (Figure 4.3). Thus, the present results indicate that the O_2 levels in the embryonic lens were below 10 mmHg by E10 and remained so throughout development. Quantitative in vivo optode measurements of Po_2 in the vitreous humour immediately behind the lens are consistent with this interpretation. The measured Po_2 in this region was ≤5 mmHg. Despite an approximately three-fold increase in Po_2 following incubation in hyperoxic conditions, the Po_2 in the vitreous bathing the posterior surface of the lens remained below the 10 mmHg threshold for pimonidazole-adduct formation. This most likely explains why lenses from both normoxic and hyperoxic embryos were stained similarly with the pimonidazole adduct-specific antibody.

The data were consistent with hypoxia being the trigger for organelle loss. The molecular mechanism responsible for organelle loss was not examined here. However, an increasing body of knowledge is accumulating concerning the actions of hypoxia on

cellular processes at the molecular level. For example, hypoxia is involved in controlling the expression of glycolytic enzymes and the formation of new blood vessels through activation of transcription factors such as hypoxia inducible factor (hif) which in turn controls *VEGF* expression (Bruick, 2003). This is a plausible starting point for studying the mechanism whereby hypoxia may trigger organelle loss.

Chapter 5:

Conclusions and

future directions

In this final chapter we will draw some general conclusions about O_2 levels in the mammalian lens by comparing the various species studied. We will also discuss ramifications of the data for our hypotheses regarding ageing, mitochondrial function and cataract. In addition, some ideas for future projects will be outlined.

The main aim of the thesis was to map in detail the distribution of O_2 in the lens in vitro and ascertain the mechanisms modulating the O_2 levels. Lenses are located in a low Po_2 environment (§1.7.3). Pimonidazole staining indicated that chicken lenses were chronically hypoxic (Figure 4.4). In larger lenses where optode measurements were feasible, we identified cortical O_2 gradients leading to symmetrical Po_2 profiles in the bovine, rabbit and human lens in vitro under physiological conditions (Figure 3.4). This suggests that these features are general phenomena exhibited by all mammalian lenses. The level of O_2 in the lens core was higher in human and rabbit lenses, compared to the bovine lens under the same conditions. The higher core Po_2 appeared to be inversely correlated with lens size, rather than a change in O_2 consumption by the different species (Figure 3.6). Studies in which temperature was altered showed that O_2 was freely diffusible in the lens (Figures 2.15 and 3.14). Therefore, O_2 consumption by the lens was probably the most important factor responsible for the creation of the O_2 gradients and lens core hypoxia. Interestingly, the role of mitochondria in lens QO_2 appeared to be species dependent. Although oxidative phosphorylation accounted for ~90% of QO_2 in the bovine lens according to inhibition studies (Figure 2.19), a role for this process in the human lens could not be identified (Figure 3.13). Further studies on isolated mitochondria from the human lens may be needed to investigate the role of mitochondria in lens O_2 consumption.

Since mitochondrial oxidative phosphorylation and O_2 consumption decreases with age in some tissues (§1.5), we hypothesised that lens QO_2 may also decrease with age, giving rise to higher core Po_2 values and hence vulnerability to oxidation. Contrary to this notion, however, we found that there was no significant change in QO_2 in old age in the human lens, nor in the guinea pig lens on a per lens basis (Figures 3.7 and 2.21, respectively). In the human lens, this may indicate that oxidative phosphorylation is not a major determinant of QO_2. In addition, older human lenses had a significantly lower nucleus Po_2 (Figure 3.8), possibly due to the continuous growth of the lens with age.

Although we did not directly examine cataractous lenses, the data also has ramifications for the theory of pathogenesis of ARNC. There are two main theories concerning the development of ARNC. The first proposes an extra-lenticular source of oxidants, such as H_2O_2, (Spector, 1984), and the other proposes the generation of oxidants within the lens nucleus itself (Garland, 1990; Truscott, 2000). The credibility of the latter hypothesis is contingent upon the presence of O_2 in the lens core. The data presented in thesis demonstrates that O_2 is present in the lens core under physiological conditions. Furthermore, the levels of O_2 can be increased under certain conditions, such as by decreasing the temperature or increasing external Po_2. The former finding may be relevant to the development of post-vitrectomy cataract. The latter finding is relevant to the development of nuclear cataracts in patients treated with hyperbaric O_2 therapy (Palmquist *et al.*, 1984). The presence of O_2 in the lens nucleus is a possible source of oxidative stress. The primary oxidative defence of the lens nucleus is GSH, which, if oxidised, must diffuse to the lens cortex to be reduced by GSH-reductase (Giblin, 2000). However, the transport of GSH to the lens core is compromised from middle age, resulting in a fall in lens core

GSH levels (Truscott, 2000). Therefore, if ageing is accompanied by constant (or possibly increased) O_2 levels, and falling anti-oxidant levels, then the lens core should become increasingly pro-oxidative. This may be a pre-condition for the subsequent formation of ARNC.

In §1.8, we raised the link between diseases caused by genetic defects in oxidative phosphorylation and early cataract formation. If human lens Po_2 is not primarily modulated by mitochondria, then it is likely that the cataract occurring with these diseases is not due to elevated O_2 levels in the lens core, but may instead be attributable to other causes, such as the production of ROS.

The role of mitochondria in ARNC deserves more attention. Recently, it was shown that the early accumulation of mtDNA mutations in mice, caused by an induced defect in mtDNA repair enzymes, was linked to early ageing (Trifunovic *et al.*, 2004). ARNC is also a disease of ageing. It would be of interest, therefore, to systematically study mitochondrial function and mtDNA mutations in ageing and cataractous human lenses. If this research were to reveal that mitochondrial dysfunction is also related to the formation of ARNC, then this would open the possibility of new treatment to prevent cataract formation. There are currently drugs being trialled in animals which modify mitochondrial dysfunction with ageing. Acetyl carnitine and lipoic acid, for example, have been used in old rats to reverse mitochondrial dysfunction with some success (Ames, 2004). Old rats treated with micronutrients showed improvement both in rat behavioural assessments and also at the level of functioning of the isolated mitochondria, effectively making old rats into young rats. Whether this treatment might also be of benefit to humans is an intriguing possibility.

Another challenge will be to measure human lens Po_2 in vivo. Polarography and fluorescence quenching are invasive techniques and would result in cataract formation in healthy subjects. Currently, there are no non-invasive techniques available to measure lens oximetry. One reason is because the extant non-invasive techniques which rely on luminescence cannot be accurately calibrated for the lens. Also, the lens lacks a blood supply and therefore the introduction of molecular probes into the tissue through the vasculature is not possible. Currently, therefore, measuring Po_2 with an optode during cataract surgery seems the only practicable approach.

We investigated the possibility that O_2 gradients may provide the spatial cue necessary to coordinate organelle loss in the embryonic chicken lens (Chapter 4). Hyperoxia delayed organelle loss consistent with the hypothesis that hypoxia is the trigger for organelle loss in the lens. Future studies will need to focus on the molecular basis of this phenomenon. The effects of O_2 gradients in the lens could be analysed with novel gene array technology to look at the effect of progressive hypoxia on the gene expression profiles of differentiating fibre cells. The effect of hypoxia on the expression of growth factors could underlie some of the changes found to occur in fibre cells as they differentiate and move further into the lens substance.

Possibly the most interesting and clinically relevant piece of data from the thesis was the finding that O_2 levels were very sensitive to temperature. Reducing the temperature below physiological levels resulted in decreased QO_2 and concomitantly raised core O_2 levels in both the bovine and human lens. We hypothesised that a similar rise in lens core

P_{O_2} may occur during vitrectomy, where O_2-rich solutions at room temperature are infused into the eye. This might be the explanation for the high rate of cataract formation caused by this procedure. We postulate that post-vitrectomy cataract may be prevented by simply warming the infusion solutions used during surgery. To test this, we have recently initiated a clinical study to compare the incidence of post-vitrectomy cataract in a control group receiving normal, room temperature solutions against an intervention group receiving warmed solutions. The study was approved by the Washington University Human Studies Committee in June, 2004. Although primarily a work of physiology, this thesis was undertaken with the hope that some progress might be made in understanding human cataract formation. Perhaps it is fitting, therefore, to conclude with an appendix containing the protocol for our study which may decrease the incidence of post-vitrectomy cataract.

Appendices

A. Protocol for clinical study at Washington University "The effect of pre-warmed infusion solutions on the incidence of post-vitrectomy cataract"

Aims

The purpose of this study is to determine whether pre-warming the infusion solution used during vitrectomy surgery reduces the incidence of post-vitrectomy cataract.

Background and Significance

Post-vitrectomy cataracts.

Vitrectomy is one of the most common procedures performed by vitreo-retinal surgeons and is indicated for several conditions including: diabetic retinopathy and retinal detachments. Although vitrectomy is an effective treatment, it is associated with an extremely high incidence of post-surgical cataracts. For example, within six months of vitrectomy 21% of patients develop cataract (Novak, et al., 1984) and, by 12 months, this number rises to 63% (Van Effenterre, et al., 1992). At 2-10 years follow up, the incidence of cataract in operated eyes ranges from 51%-80% (Blankenship & Machemer, 1985;Blodi & Paluska, 1997;Cherfan, et al., 1991;Leaver, et al., 1979;Melberg & Thomas, 1995). The successful treatment of post-vitrectomy cataracts requires further surgery with significant additional costs (fiscal and otherwise) to patients. For those patients for whom cataract surgery is contraindicated there is also the risk of permanent visual disability.

The most common type of cataract seen after vitrectomy is nuclear cataract (Blodi & Paluska, 1997;Cherfan, et al., 1991;Melberg & Thomas, 1995). It is generally accepted that nuclear cataract is the result of extensive oxidation of proteins and lipids in the lens core (Harding, 1991;Spector, 1984). Compelling evidence that molecular oxygen plays a

direct role in this process is provided by the observation that an extremely high proportion of patients receiving hyperbaric oxygen treatment develop nuclear cataract (Palmquist, et al., 1984).

Relationship between tissue temperature and oxygen concentration in the lens core.

The current study was prompted by our recent investigation of factors that influence the partial pressure of oxygen (P_{O2}) in bovine and human lenses in vitro (McNulty et al., submitted). Our measurements indicate that P_{O2} in the center of the lens is usually very low (<2 mmHg) as a result of oxygen consumption by cells in the superficial tissue layers. The maintenance of hypoxia in the lens core is probably essential for the long term transparency of the tissue (Eaton, 1981). In our studies we discovered that oxygen consumption in the lens has a high Q10. Thus, if the temperature of the lens is reduced from 37^{o}C to room temperature, oxygen consumption falls to a small fraction (<20%) of the normal rate. The effect of this decrease in oxygen consumption is that the core of the lens rapidly fills with oxygen (Figure A1.A). The increase in core P_{O2} occurs quite rapidly (within 20 minutes) in response to a decrease in tissue temperature. Interestingly, the temperature of the lens need not be maintained at precisely 37^{o}C in order to prevent oxygen entering the core. As shown in Figure A1.B, provided the lens temperature does not fall below 30^{o}C the lens core remains relatively hypoxic. At room temperature the P_{O2} in the center of the lens is significantly elevated (Figure A1.A) but the increase in oxygen *concentration* is probably even more marked, because oxygen solubility is increased by approximately 30% at the lower temperature. Thus, at room temperature, in the presence of oxygenated solutions, the concentration of oxygen in the lens core is increased by more than two orders of magnitude above the normal level.

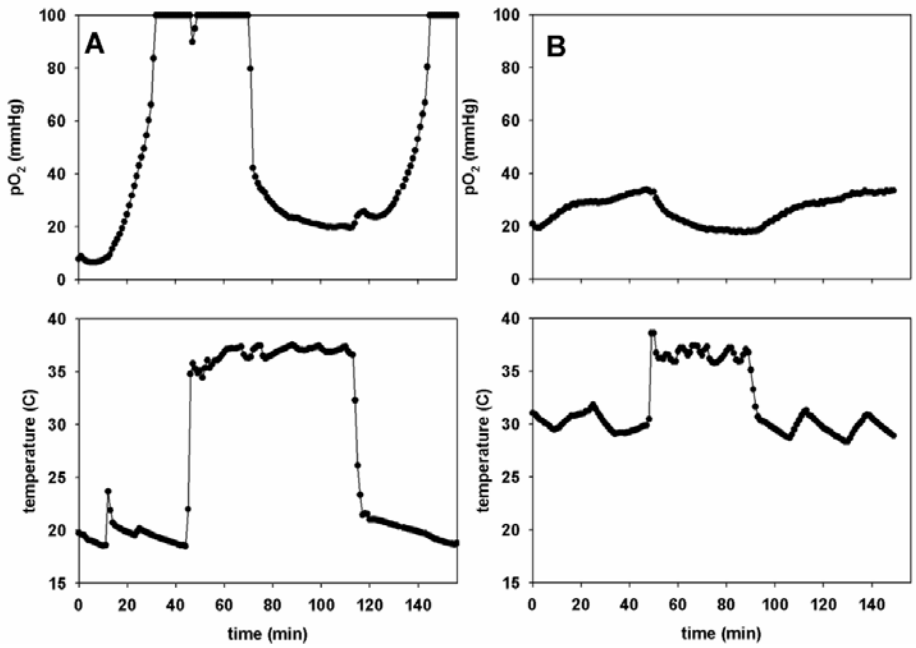

Figure A1 Effect of temperature on Po_2 in the nucleus of human donor lenses. *Isolated human lenses were incubated in solutions equilibrated with atmospheric oxygen (~150 mmHg or 21% O_2).* ***A.*** *The Po_2 and temperature were monitored in the lens center as the temperature of the bathing solution was alternated between 37°C and room temperature (20°C). At 37°C, Po_2 in the lens core is <10 mmHg. At room temperature, Po_2 increases to >100 mmHg. The effect is reversible.* ***B.*** *The lens core is maintained in a relatively hypoxic condition (<35 mmHg) provided the tissue temperature does not fall below 30°C.*

The standard vitrectomy procedure exposes the lens to cold, oxygenated solutions

During a typical vitrectomy procedure three probes (the vitrector, a light source, and an infusion canula) are inserted into the eye through small incisions in the sclera. The vitreous humor is removed using the vitrector, a miniature cutting and aspiration tool. The infusion line serves to keep the pressure in the eye constant during the procedure. As the vitreous is aspirated, a modified saline solution flows into the eye under slight positive pressure through the infusion canula. During the operation (which may take several hours), a total of approximately 400 ml of saline solution is infused into the eye and aspirated along with the vitreous. With regard to the current project, the salient feature of this procedure is

that the infusion solution is equilibrated with atmospheric oxygen (≈ 21%) and enters the eye at 17^{o}C (the temperature of the operating room).

From our in vitro experiments on human cadaveric lenses (see Figure. 1), we believe it is *very* likely that the lens core will be flooded with oxygen during the surgical procedure, due to the cooling of the lens in the presence of oxygenated solutions (we are not able to verify this directly in vivo because the oxygen measurement technique is invasive and would irreparably damage the lens).

We hypothesize that the introduction of high concentrations of oxygen into the previously hypoxic core of the lens is the direct cause of post-operative cataracts. We propose to test this hypothesis by pre-warming the infusion solution and establishing whether this relatively minor modification to the established vitrectomy procedure reduces the incidence of post-vitrectomy cataracts. It is important to emphasize that no appropriate animal model exists to study factors influencing the development of post-vitrectomy cataract. Indeed, cataracts do not even develop in all classes of patients. Only patients above the age of fifty are at significant risk of post-surgical nuclear cataracts.

Inclusion/Exclusion criteria.

Protocol inclusion criteria: Patients of 50 years of age or older with macular disease requiring vitrectomy.

Protocol exclusion criteria: Diabetes. Macular hole.

Treatment Plan/Method.

Selection of patients: 100 patients will be recruited from the practice of Dr Nancy Holekamp, MD. Adults requiring vitrectomy surgery and meeting the inclusion criteria will be asked if they would like to participate in the study. The alternative of having a standard vitrectomy procedure (using room temperature infusion solutions) will also be discussed. Counseling will be offered and a consent form signed.

Pre-operative arrangements: In addition to standard pre-operative screening, study participants will have their lenses photographed at the Center for Advanced Medicine by Rhonda Curtis, the Department's ophthalmic photographer. Patients will be randomized into the control or intervention groups.

Surgical procedure: The control group will have a vitrectomy employing room temperature infusion solution. This is the standard of care. The intervention group will have infusion solutions pre-warmed to 34^{o}C by passing them through a WarmFlo fluid warming device. In patients receiving warmed fluids, the temperature inside the eye will be measured once during the operation with an optode/thermocouple (OxyLab model 2.0/OT, 300 microns in diameter). This will take about 1 minute.

One safety concern in this study is the absolute need to avoid an overtemperature condition in the eye. It is essential that the delicate tissues of the retina not be exposed to solutions exceeding 37^{o}C. For this reason, we have elected to warm the solution using an FDA-approved fluid warming device (WarmFlo, model FW-538 and WF-100, Mallinckrodt, Inc., St Louis, MO). The fluid warmer utilizes a sterile, disposable, heat

exchange cassette. This particular instrument is widely used throughout the BJC hospital system for warming blood and I.V. solutions to help maintain normal body temperature of patients undergoing surgical procedures. The vitrectomy infusion solution will be fed through the fluid warmer, which will be positioned as close as possible to the patients' head. This will prevent excessive cooling of the solution as it flows through the line linking the fluid warmer to the eye. In preliminary experiments (see Figure A1.B), we established that it is not necessary to maintain the lens at precisely 37^{o}C in order to preserve hypoxia in the lens core. Therefore, as an additional safety measure, we will only pre-warm solutions to 34^{o}C. This should preserve hypoxia in the lens core but will allow a safety margin to guard against any small instrumental temperature fluctuations. Infusion solutions warmed to 34^{o}C have also been shown previously to have no deleterious effect on patient Electroretinograms (Horiguchi and Miyake, 1991). We should emphasize that the WarmFlo system is an accurate and reliable device and we do not anticipate any significant temperature fluctuations. Futhermore, the fluid warmer is also equipped with an audible over-temperature alarm. In the unlikely event that the alarm should sound, the fluid flow to the eye would be quickly turned off.

The proposed modification to the standard procedure is as follows:

The fluid warmer will be attached to a drip stand and placed near the head of the patient. The temperature will be set to 34°C. The operating room technician will attach the irrigation solution bottle to the sterile irrigation tubing as for a normal vitrectomy. The scrub nurse will attach the irrigation tubing to the proximal end of the sterile heat exchange unit. Then the distal end of the heat exchange unit will be attached to the standard 3-way tap and silicon tubing going to the eye. The irrigation tubing and heat exchange unit will be

primed with irrigation solution. The surgeon will proceed with the vitrectomy. This procedure protocol has been practiced by the research team and scrub nurse (Laurie Richards) in the Center for Advanced Medicine operating room in December 2003. The presence of the fluid warmer does not in any way impair the surgeon's access to the patient and therefore there is no additional surgical risk above and beyond that normally associated with the procedure. In patients receiving warmed fluids, the temperature inside the eye will be measured at an appropriate time with the OxyLab optode/thermocouple (hereafter referred to as the "optode"). A pre-sterilised optode will be opened by a technician and offered to the surgeon. The surgeon will hand back to the technician the distal end of the optode (which is now no longer sterile) to be inserted into the OxyLab monitor. The surgeon will insert the optode into the eye through one of the pre-existing portals for about 1 minute until a temperature reading is obtained. The optode will be removed, handed to the technician and the vitrectomy resumed. The procedure for using the optode, and the sterilization technique of the optode, has already been employed by Dr N.M Holekamp in a separate vitrectomy study approved by Washington University (#0170569). There are no changes in this study to the use and sterilization of the optode.

A second potential safety concern is the possibility that a warm eye may not tolerate the surgery as well as a cold eye. This is a difficult risk to quantify. World wide, the normal practice is to use room temperature solutions during the vitrectomy procedure. However, this is a matter of convenience rather than a scientifically validated choice. In fact, from day to day, the temperature of the infusion solutions presumably varies with the ambient temperature. Two studies using human patients have examined the effects of warmed infusion solutions on the electroretinogram (ERG) (Horiguchi and Miyaki, 1991; Miyake

and Horiguchi, 1998). The ERG measures the electrical currents produced by the retina upon stimulation by light and is a sensitive measure of retinal function. These studies showed that room temperature solutions adversely affect the ERG causing lower amplitude and peak delays. These changes largely reverse after five days. In contrast, treatment with pre-warmed (34^{o}C) infusion solutions had no deleterious effects on the ERG. Several animal studies have also examined the effects of introducing pre-warmed solutions into the eye. Perfusion of the rabbit eye at 36^{o}C for 60 minutes was not associated with retinal damage as assessed by light or electron microscopy (Faude, et al., 2001). In contrast, one study showed that at 37^{o}C the retina was more sensitive to phototoxicity than at 22^{o}C. However, as noted above, in human patients, introduction of warm infusion solutions did not have a detectable effect on the ERG suggesting that phototoxic damage to the retina was unlikely.

The standard of care involves careful post-operative monitoring with a full eye exam at 1 day, 1 week, 1, 3, 6 and 12 months. Should any adverse effect of treatment with pre-warmed infusion solutions be noted the study will immediately be suspended. It should also be noted that the recruitment rate for the study is likely to be slow. Dr. Holekamp currently sees approximately 2-4 patients per week that meet the inclusion criteria for the study. Thus, even if a high proportion of eligible patients agree to participate in the study, the rate at which surgeries will be performed will be relatively modest. Thus, we will have had a chance to examine the first few patients (and verify that there are no adverse effects of the treatment) before the modified procedure has been carried out on the bulk of the subjects.

Follow-up:

All patients will receive the normal post-operative follow-up of review by the surgeon at 1 day, 1 week, 1, 3, 6 and 12 months. Here visual acuity and indirect ophthalmoscopy will be performed. This is the normal standard of care. Additionally, for the purposes of our study, lenses will be photographed during the 3, 6, and 12 month visits by Rhonda Curtis, the Departments' ophthalmic photographer. The photographs will be used to document the incidence and progression of cataracts in each group.

Data Monitoring:

Dr Holekamp will monitor the study for any adverse and serious adverse events. All serious adverse events will be reported to the IRB: a) death – immediately; b) life-threatening within 7 calendar days; c) using an investigational device within 10 working days; d) all other SAEs within 15 calendar days using Form 6 (SAE report). Should there be a serious adverse event that occurs that increases the risks to the participants, the study will be stopped, an investigation will be conducted, and a findings report will be generated before the study is resumed. The safety of the intervention will be monitored by comparing the two groups' visual acuity and indirect ophthalmoscopy findings from the follow up visits.

B. Mathematical model of lens O_2 consumption and diffusion

This mathematical model was developed in collaboration with Huan Wang and Richard T Mathias from the Department of Physiology and Biophysics, State University of New York (SUNY), Stony Brook, New York and Steven Bassnett from the Department of Ophthalmology and Visual Sciences, Washington University in St Louis, Missouri, USA.

The purpose of this appendix is to derive an approximate model of steady state O_2 diffusion/consumption in the lens. This model can then be compared to the experimental data to obtain an estimate of the rate constants for O_2 consumption.

The rate of O_2 consumption is a saturable reaction, so if C is the concentration of O_2, then to a first approximation we can write

$$-\frac{dC}{dt} = \frac{V_{\max} C}{C + K} \qquad (1)$$

where V_{max} (M/s) is the max rate of consumption and K (M) is the effective dissociation constant for the reaction. There are generally several paths for O_2 consumption, so equation (1) is an effective reaction that embodies several different processes. Since equation (1) depends nonlinearly on C, it leads to differential equations that are intractable to analytic solution. However, as long as $C \ll K$, the equation is approximately linear. This assumption will clearly be valid in most regions of the lens, since the concentration of O_2 goes rapidly to near-zero as one looks from the surface into the lens. Moreover, when the concentration of O_2 in the bathing solution is not too high, this assumption will be valid everywhere. The linearized version of equation (1) is

$$-\frac{dC}{dt} \cong C/\tau, \ \ where\, \tau = K/V_{\max} \qquad (2)$$

The cellular structure and gross anatomy of the lens are shown in Figure A2. The lens is somewhat spherical in shape and comprises two functionally different domains of fibre cells. For the purposes of this analysis, we will assume the lens is indeed spherical with radius a (cm). If r (cm) is the distance from the lens centre, then the outer shell of differentiating fibres (DF) is located at $b \leq r \leq a$ where $b \cong 0.8a$. Thus mature fibres (MF) are at $0 \leq r \leq b$. With regard to this analysis, the relevant difference between MF and DF is that the DF contain mitochondria, which consume O_2, whereas the MF have no organelles (Bassnett, 2002).

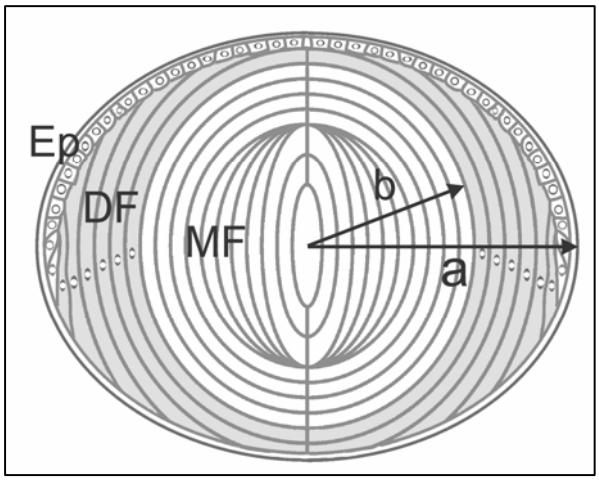

Figure A2 *Diagram of the cellular structure of the lens used for modelling. Anteriorly, the lens is bounded by an epithelium (Ep). The bulk of the tissue is composed of concentric layers of fiber cells. Differentiating fibers (DF, shaded region) near the surface contain a normal complement of organelles. Mature fibers (MF) located in the central region of the tissue do not contain organelles. The model calculations assume a spherical lens of radius a (cm) in which the border between DF and MF is located at a distance b (cm) from the centre.*

Thus, τ in equation (2) takes on two values in the lens.

$$\tau = \begin{cases} \tau_{MF} \quad (s) & 0 \leq r \leq b \\ \tau_{DF} \quad (s) & b \leq r \leq a \end{cases} \qquad (3)$$

Bi-domain equations have been previously used to analyse ionic current flow in lenses from various species (reviewed in (Mathias, et al., 1997)). In these equations, there are two paths for radial flow, intracellular (from cell-to-cell via gap junctions) and extracellular (along the narrow intercellular clefts). For ion flow, these bi-domain equations are required, since the permeability of plasma membranes for ions is very low, hence the two paths are truly separate. However, the diffusion coefficient of O_2 in water is about $4x10^{-5}$ cm^2/s, whereas in plasma membrane from erythrocytes the value is about $1x10^{-5}$ cm^2/s (Fischkoff & Vanderkooi, 1975), so membranes provide essentially no resistance to the diffusion of O_2 as they are very thin barriers (about 0.5% compared to cytoplasm). Hence, the concentration of O_2 in the intracellular and extracellular compartments of the lens will be essentially the same and a single effective value of D_{O2} should be close to $4x10^{-5}$ cm^2/s. In the text, we measure the partial pressure (Po_2), which is linearly proportional to C. Thus, at this stage we will use P_{O_2} instead of C.

Let Po_2 be our measure of the (extracellular and intracellular) concentration of O_2. The divergence in diffusion of O_2 must equal the rate of consumption, where diffusion depends on an effective diffusion coefficient D_{O_2} (cm^2/s) that incorporates the effects of membranes and cytoplasm. Other conditions are as follows: at the lens surface the value of $Po_2(a)$ equals the concentration of O_2 in the bathing solution, defined as $P_{O_2}(bath)$; at the lens centre the flux is zero; at the transition from DF to MF the concentration and flux of O_2 must be continuous. These physical requirements lead to the following differential equation and boundary conditions.

$$
\begin{aligned}
&D_{O2}\frac{1}{r^2}\frac{d}{dr}\left(r^2\frac{dP_{O2}}{dr}\right)=P_{O2}/\tau \\
&P_{O2}(a)=P_{O2}(bath) \\
&\frac{dP_{O2}(0)}{dr}=0 \\
&P_{O2}(b^-)=P_{O2}(b^+) \\
&\frac{dP_{O2}(b^-)}{dr}=\frac{dP_{O2}(b^+)}{dr}
\end{aligned}
\qquad (4)
$$

The solutions to equation (4) contain a common term, which we will call P_1:

$$
P_1=\frac{P_{O2}(bath)}{\cosh((a-b)/\lambda_{DF})\left[\tanh((a-b)/\lambda_{DF})+\frac{\lambda_{MF}}{\lambda_{DF}}\tanh(b/\lambda_{MF})\right]}
\qquad (5)
$$

where

$$
\begin{aligned}
\lambda_{DF}&=\sqrt{D_{O2}\tau_{DF}} \\
\lambda_{MF}&=\sqrt{D_{O2}\tau_{MF}}
\end{aligned}
\qquad (6)
$$

The P_{O2} profile is given by:

$$
P_{O2}(r)=P_1\begin{cases}\dfrac{\lambda_{MF}a\sinh(r/\lambda_{MF})}{\lambda_{DF}r\cosh(b/\lambda_{MF})} & 0\le r\le b \\ \dfrac{a\sinh((r-b)/\lambda_{DF})}{r}+\tanh(b/\lambda_{MF})\dfrac{\lambda_{MF}a\cosh((r-b)/\lambda_{DF})}{\lambda_{DF}r} & b\le r\le a\end{cases}
\qquad (7)
$$

At steady state there is a steep concentration gradient for O_2 in the lens, implying continuous diffusion and consumption. Total consumption (mmHg/s) within the volume of radius r must equal the rate of O_2 moving into the lens across the surface of area $4\pi r^2$:

$$
QO_2(r)=4\pi r^2 D_{O2}\frac{dP_{O2}(r)}{dr}
\qquad (8)
$$

Equation (8) can be evaluated using equation (7) at r = a to obtain total lens consumption:

$$QO_2(a) = 4\pi a D_{O2} P_{O2}(bath)\left[\frac{a}{\lambda_{DF}}\frac{1+\frac{\lambda_{MF}}{\lambda_{DF}}\tanh(b/\lambda_{MF})\tanh((a-b)/\lambda_{DF})}{\tanh((a-b)/\lambda_{DF})+\frac{\lambda_{MF}}{\lambda_{DF}}\tanh(b/\lambda_{MF})}-1\right] \quad (9)$$

Thus, we can curve-fit equation (7) to evaluate λ_{DF} and λ_{MF}, then use equation **(9)** with λ_{DF} and λ_{MF} fixed to determine D_{O_2}. Lastly, with D_{O_2}, λ_{DF} and λ_{MF} known, τ_{DF} and τ_{MF} can be determined from equation (6)**.** The results of this procedure are given in the discussion.

Once these parameters are determined, the relative O_2 consumption in the core of MF vs. the outer shell of DF can be calculated by evaluating equation (8) at r = b.

$$QO_2(b) = 4\pi b D_{O2} P_1 \frac{a}{\lambda_{DF}}\left(1-\frac{\tanh(b/\lambda_{MF})}{b/\lambda_{MF}}\right) \quad (10)$$

References

Alberts, ed. (1994). *Molecular Biology of the Cell*. Garland, New York.

Alder, VA & Cringle, SJ. (1985). The effect of the retinal circulation on vitreal oxygen tension. *Curr Eye Res* **4,** 121-129.

Alder, VA & Cringle, SJ. (1989). Intraretinal and preretinal PO2 response to acutely raised intraocular pressure in cats. *Am J Physiol* **256,** H1627-1634.

Alder, VA, Cringle, SJ & Constable, IJ. (1983). The retinal oxygen profile in cats. *Invest Ophthalmol Vis Sci* **24,** 30-36.

Alm, A & Bill, A. (1972). The oxygen supply to the retina. I. Effects of changes in intraocular and arterial blood pressures, and in arterial P O2 and P CO2 on the oxygen tension in the vitreous body of the cat. *Acta Physiol Scand* **84,** 261-274.

Ames, BN. (2004). Mitochondrial decay, a major cause of aging, can be delayed. *J Alzheimers Dis* **6,** 117-121.

Appleby, DW & Modak, SP. (1977). DNA degradation in terminally differentiating lens fiber cells from chick embryos. *Proc Natl Acad Sci U S A* **74,** 5579-5583.

AREDSresearchgroup. (2001). AREDS report No 9. *Arch Ophthalmol* **119,** 1439-1452.

Arteel, GE, Thurman, RG, Yates, JM & Raleigh, JA. (1995). Evidence that hypoxia markers detect oxygen gradients in liver: pimonidazole and retrograde perfusion of rat liver. *Br J Cancer* **72,** 889-895.

Bambot, SB, Lakowicz, JR & Rao, G. (1995). Potential applications of lifetime-based, phase-modulation fluorimetry in bioprocess and clinical monitoring. *Trends Biotechnol* **13,** 106-115.

Banasiak, KJ, Xia, Y & Haddad, GG. (2000). Mechanisms underlying hypoxia-induced neuronal apoptosis. *Prog Neurobiol* **62,** 215-249.

Bantseev, VL, Herbert, KL, Trevithick, JR & Sivak, JG. (1999). Mitochondria of rat lenses: distribution near and at the sutures. *Curr Eye Res* **19,** 506-516.

Barbazetto, IA, Liang, J, Chang, S, Zheng, L, Spector, A & Dillon, JP. (2004). Oxygen tension in the rabbit lens and vitreous before and after vitrectomy. *Exp Eye Res* **78,** 917-924.

Bardag-Gorce, F, French, BA, Li, J, Riley, NE, Yuan, QX, Valinluck, V, Fu, P, Ingelman-Sundberg, M, Yoon, S & French, SW. (2002). The importance of cycling of blood alcohol levels in the pathogenesis of experimental alcoholic liver disease in rats. *Gastroenterology* **123,** 325-335.

Barr, RE & Silver, IA. (1973). Effects of corneal environment on oxygen tension in the

anterior chambers of rabbits. *Invest Ophthalmol* **12,** 140-144.

Barron, SA, Heffner, RR, Jr. & Zwirecki, R. (1979). A familial mitochondrial myopathy with central defect in neural transmission. *Arch Neurol* **36,** 553-556.

Bassnett, S. (1990). Intracellular pH regulation in the embryonic chicken lens epithelium. *J Physiol* **431,** 445-464.

Bassnett, S. (1995). The fate of the Golgi apparatus and the endoplasmic reticulum during lens fiber cell differentiation. *Invest Ophthalmol Vis Sci* **36,** 1793-1803.

Bassnett, S. (1997). Fiber cell denucleation in the primate lens. *Invest Ophthalmol Vis Sci* **38,** 1678-1687.

Bassnett, S. (2002). Lens organelle degradation. *Exp Eye Res* **74,** 1-6.

Bassnett, S & Beebe, DC. (1992). Coincident loss of mitochondria and nuclei during lens fiber cell differentiation. *Dev Dyn* **194,** 85-93.

Bassnett, S, Croghan, PC & Duncan, G. (1987). Diffusion of lactate and its role in determining intracellular pH in the lens of the eye. *Experimental Eye Research* **44,** 143-147.

Bassnett, S & Duncan, G. (1986). Variation of pH with depth in the rat lens measured by double-barrelled ionsensitive microelectrodes. In *The lens: transparency and cataract*. ed. DUNCAN, G., pp. 77-86.

Bassnett, S & McNulty, R. (2003). The effect of elevated intraocular oxygen on organelle degradation in the embryonic chicken lens. *J Exp Biol* **206,** 4353-4361.

Bassnett, S & Winzenburger, PA. (2003). Morphometric analysis of fibre cell growth in the developing chicken lens. *Exp Eye Res* **76,** 291-302.

Bec, P & Arne, JL. (1976). [The measurement of the partial pressure of oxygen and carbon dioxide and pH of the aqueous humor in man. A preliminary study on 32 normal eyes]. *Arch Ophtalmol (Paris)* **36,** 227-230.

Becker B & Cotlier E (1962). Distribution of rubidium-86 accumulated in the rabbit lens. *Invest Ophthalmol* **1,** 642-5.

Beckman, A. (1998). The free radical theory of aging matures. *Physiol Rev* **78,** 547-581.

Beckman, KB & Ames, BN. (1998). Mitochondrial aging: open questions. *Ann N Y Acad Sci* **854,** 118-127.

Bennewith, KL, Raleigh, JA & Durand, RE. (2002). Orally administered pimonidazole to label hypoxic tumor cells. *Cancer Res* **62,** 6827-6830.

Berridge, M, Herst, P, Tan, A & Scarlett, D. (2002). The plasma membrane respirometry complex of mammalian cells: a model reconciling non-mitochondrial oxygen consumption, transplasma membrane electron transport and a cell surface NADH-oxidase. In *Oxidative Pathways in Chemistry, Biology and Medicine. The Society for Free Radical Research (Australasia).* University of Wollongong.

Bishop, PN, Takanosu, M, Le Goff, M & Mayne, R. (2002). The role of the posterior ciliary body in the biosynthesis of vitreous humour. *Eye* **16,** 454-460.

Blankenship, GW & Machemer, R. (1985). Long-term diabetic vitrectomy results. Report of 10 year follow-up. *Ophthalmology* **92,** 503-506.

Blodi, BA & Paluska, SA. (1997). Cataract after vitrectomy in young patients. *Ophthalmology* **104,** 1092-1095.

Bonanno, JA, Stickel, T, Nguyen, T, Biehl, T, Carter, D, Benjamin, WJ & Soni, PS. (2002). Estimation of human corneal oxygen consumption by noninvasive measurement of tear oxygen tension while wearing hydrogel lenses. *Invest Ophthalmol Vis Sci* **43,** 371-376.

Borchman, D, Giblin, FJ, Leverenz, VR, Reddy, VN, Lin, LR, Yappert, MC, Tang, D & Li, L. (2000). Impact of aging and hyperbaric oxygen in vivo on guinea pig lens lipids and nuclear light scatter. *Invest Ophthalmol Vis Sci* **41,** 3061-3073.

Boveris, A & Chance, B. (1973). The mitochondrial generation of hydrogen peroxide. General properties and effect of hyperbaric oxygen. *Biochem J* **134,** 707-716.

Brand, MD. (2000). Uncoupling to survive? The role of mitochondrial inefficiency in ageing. *Exp Gerontol* **35,** 811-820.

Braunwald, ed. (2001). *Harrison's principles of internal medicine*. McGraw-Hill medical Publishing, New York.

Brian, G & Taylor, H. (2001). Cataract blindness--challenges for the 21st century. *Bull World Health Organ* **79,** 249-256.

Briggs, R. (1973). Distribution and consumption of oxygen in the vitreous body of cats. In *Oxygen supply: theoretical and practical aspects of oxygen supply and microcirculation of tissue*. ed. Kessler, pp. 265-269. Urban and Schwarzenberg, Munich.

Brizel, DM, Scully, SP, Harrelson, JM, Layfield, LJ, Bean, JM, Prosnitz, LR & Dewhirst, MW. (1996). Tumor oxygenation predicts for the likelihood of distant metastases in human soft tissue sarcoma. *Cancer Res* **56,** 941-943.

Bron, T, Tripathi, R. (1997). *Wolff's anatomy of the eye and orbit*. Chapman and Hall, New York.

Bruick, RK. (2003). Oxygen sensing in the hypoxic response pathway: regulation of the hypoxia-inducible transcription factor. *Genes Dev* **17,** 2614-2623.

Brurberg, KG, Graff, BA & Rofstad, EK. (2003). Temporal heterogeneity in oxygen tension in human melanoma xenografts. *Br J Cancer* **89,** 350-356.

Burns, JJ. (1959). Biosynthesis of L-ascorbic acid; basic defect in scurvy. *Am J Med* **26,** 740-748.

Bussink, J, Kaanders, JH & van der Kogel, AJ. (2003). Tumor hypoxia at the micro-regional level: clinical relevance and predictive value of exogenous and endogenous hypoxic cell markers. *Radiother Oncol* **67,** 3-15.

Carr, AC & Frei, B. (1999). Toward a new recommended dietary allowance for vitamin C based on antioxidant and health effects in humans. *Am J Clin Nutr* **69,** 1086-1107.

Chamot, SR, Cranstoun, SD, Petrig, BL, Pournaras, CJ & Riva, CE. (2003). Blood pO2 and blood flow at the optic disc. *J Biomed Opt* **8,** 63-69.

Chance, B, Cohen, P, Jobsis, F & Schoener, B. (1962). Intracellular oxidation-reduction states in vivo. *Science* **137,** 499-508.

Chance, B, Sies, H & Boveris, A. (1979). Hydroperoxide metabolism in mammalian organs. *Physiol Rev* **59,** 527-605.

Chang, S & Lamm, SH. (2003). Human health effects of sodium azide exposure: a literature review and analysis. *Int J Toxicol* **22,** 175-186.

Chapman, JD, Baer, K & Lee, J. (1983). Characteristics of the metabolism-induced binding of misonidazole to hypoxic mammalian cells. *Cancer Res* **43,** 1523-1528.

Chen, K, Ng, CE, Zweier, JL, Kuppusamy, P, Glickson, JD & Swartz, HM. (1994). Measurement of the intracellular concentration of oxygen in a cell perfusion system. *Magn Reson Med* **31,** 668-672.

Cherfan, GM, Michels, RG, de Bustros, S, Enger, C & Glaser, BM. (1991). Nuclear sclerotic cataract after vitrectomy for idiopathic epiretinal membranes causing macular pucker. *Am J Ophthalmol* **111,** 434-438.

Chylack, LT, Jr. (1971). Control of glycolysis in the lens. *Exp Eye Res* **11,** 280-293.

Ciulla, TA, North, K, McCabe, O, Anthony, DC, Korson, MS & Petersen, RA. (1995). Bilateral infantile cataractogenesis in a patient with deficiency of complex I, a mitochondrial electron transport chain enzyme. *J Pediatr Ophthalmol Strabismus* **32,** 378-382.

Coles, CJ, Edmondson, DE & Singer, TP. (1979). Inactivation of succinate dehydrogenase

by 3-nitropropionate. *J Biol Chem* **254,** 5161-5167.

Corpechot, C, Barbu, V, Wendum, D, Chignard, N, Housset, C, Poupon, R & Rosmorduc, O. (2002). Hepatocyte growth factor and c-Met inhibition by hepatic cell hypoxia: a potential mechanism for liver regeneration failure in experimental cirrhosis. *Am J Pathol* **160,** 613-620.

Cruysberg, JR, Sengers, RC, Pinckers, A, Kubat, K & van Haelst, UJ. (1986). Features of a syndrome with congenital cataract and hypertrophic cardiomyopathy. *Am J Ophthalmol* **102,** 740-749.

Cursiefen, C, Kuchle, M, Scheurlen, W & Naumann, GO. (1998). Bilateral zonular cataract associated with the mitochondrial cytopathy of Pearson syndrome. *Am J Ophthalmol* **125,** 260-261.

Dahm, R. (1999). Lens fibre cell differentiation - A link with apoptosis? *Ophthalmic Res* **31,** 163-183.

Davies, MJ & Truscott, RJ. (2001). Photo-oxidation of proteins and its role in cataractogenesis. *J Photochem Photobiol B* **63,** 114-125.

de Juan, E, Jr., Hardy, M, Hatchell, DL & Hatchell, MC. (1986). The effect of intraocular silicone oil on anterior chamber oxygen pressure in cats. *Arch Ophthalmol* **104,** 1063-1064.

deHaan. (1922). La tension et la consummation d'oxygene dans l'humor aquese. *Arch Neerl Physiol* **7,** 245.

Dewhirst, MW, Klitzman, B, Braun, RD, Brizel, DM, Haroon, ZA & Secomb, TW. (2000). Review of methods used to study oxygen transport at the microcirculatory level. *Int J Cancer* **90,** 237-255.

Diddie, KR & Ernest, JT. (1977). The effect of photocoagulation on the choroidal vasculature and retinal oxygen tension. *Am J Ophthalmol* **84,** 62-66.

Dillon, B, Liang, Chang, Spector, Zheng, Merriam. (2003). oxygen tension in the rabbit vitreous and lens: changes with vitrectomy. Abstarct # 3501. In *Association for Research in Vision and Ophthalmology*.

Dillon, J. (1991). The photophysics and photobiology of the eye. *J Photochem Photobiol B* **10,** 23-40.

Djerassi, C & Hoffman, R. (2001). *Oxygen*. Wiley-VCH, Weinheim.

Drenckhahn, L. (1958). Der Sauerstoffdruck in der Vorderkammer des Auges und die Geschwindigkeit der Sauerstoffaufsattigung der Kammerwassers. *Graefes Arch Clin Exp Ophthalmol* **160,** 378.

Droge, W. (2002). Free radicals in the physiological control of cell function. *Physiol Rev* **82,** 47-95.

Duchen, MR. (1999). Contributions of mitochondria to animal physiology: from homeostatic sensor to calcium signalling and cell death. *J Physiol* **516 (Pt 1),** 1-17.

Duncan, G & Jacob, TJ. (1984). Influence of external calcium and glucose on internal total and ionized calcium in the rat lens. *J Physiol* **357,** 485-493.

Duncan, G & Jacob, TJ. (1984). Calcium and the physiology of cataract. In *Human Cataract Formation-Ciba Foundation Symposium 106*, pp. 132-148. Pitman, London.

Eaton, JW. (1991). Is the lens canned? *Free Radic Biol Med* **11,** 207-213.

Edelhauser, HF. (1974). Cornea and lens oxygen consumption in rabbit and trout: a comparative study. *Exp Eye Res* **19,** 317-322.

Ellozy, AR, Wang, RH & Dillon, J. (1994). Photolysis of intact young human, baboon and rhesus monkey lenses. *Photochem Photobiol* **59,** 474-478.

Ely. (1949). Metabolism of the crystalline lens. *American Journal of Ophthalmology* **32,** 220.

Emaus, RK, Grunwald, R & Lemasters, JJ. (1986). Rhodamine 123 as a probe of transmembrane potential in isolated rat-liver mitochondria: spectral and metabolic properties. *Biochim Biophys Acta* **850,** 436-448.

Enroth-Cugell, C, Goldstick, TK & Linsenmeier, RA. (1980). The contrast sensitivity of cat retinal ganglion cells at reduced oxygen tensions. *J Physiol* **304,** 59-81.

Ernest, JT. (1973). In vivo measurement of optic-disk oxygen tension. *Invest Ophthalmol* **12,** 927-931.

Ernest, JT. (1974). Autoregulation of optic-disk oxygen tension. *Invest Ophthalmol* **13,** 101-106.

Ernest, JT & Archer, DB. (1979). Vitreous body oxygen tension following experimental branch retinal vein obstruction. *Invest Ophthalmol Vis Sci* **18,** 1025-1029.

Ernest, JT, Goldstick, TK & Engerman, RL. (1983). Hyperglycemia impairs retinal oxygen autoregulation in normal and diabetic dogs. *Invest Ophthalmol Vis Sci* **24,** 985-989.

Fagerholm, PP, Philipson, BT & Lindstrom, B. (1981). Normal human lens - the distribution of protein. *Exp Eye Res* **33,** 615-620.

Fatt, I & Bieber, MT. (1968). The steady-state distribution of oxygen and carbon dioxide in the in vivo cornea. I. The open eye in air and the closed eye. *Exp Eye Res* **7,** 103-112.

Faulkner-Jones, B, Zandy, AJ & Bassnett, S. (2003). RNA stability in terminally differentiating fibre cells of the ocular lens. *Exp Eye Res* **77,** 463-476.

Field, T, Martin, Belding. (1937). Studies on the oxygen consumption of the rabbit lens and the effect of 2-4 dinitrophenol thereon. *American Journal of Physiology***,** 779-794.

Finsterer, J, Bittner, R, Bodingbauer, M, Eichberger, H, Stollberger, C & Blazek, G. (2000). Complex mitochondriopathy associated with 4 mtDNA transitions. *Eur Neurol* **44,** 37-41.

Fischkoff, S & Vanderkooi, JM. (1975). Oxygen diffusion in biological and artificial membranes determined by the fluorochrome pyrene. *J Gen Physiol* **65,** 663-676.

Fisher, AE, Maxwell, SC & Naughton, DP. (2004). Superoxide and hydrogen peroxide suppression by metal ions and their EDTA complexes. *Biochem Biophys Res Commun* **316,** 48-51.

Fitch, CL, Swedberg, SH & Livesey, JC. (2000). Measurement and manipulation of the partial pressure of oxygen in the rat anterior chamber. *Curr Eye Res* **20,** 121-126.

Franko, AJ. (1986). Misonidazole and other hypoxia markers: metabolism and applications. *Int J Radiat Oncol Biol Phys* **12,** 1195-1202.

Frei, B, England, L & Ames, BN. (1989). Ascorbate is an outstanding antioxidant in human blood plasma. *Proc Natl Acad Sci U S A* **86,** 6377-6381.

Fridovich, I. (2004). Mitochondria: are they the seat of senescence? *Aging Cell* **3,** 13-16.

Friedenwald, P. (1937). Circulation of the aqueous. *Arch Ophthalmol* **17,** 477-485.

Fritz, T, Wessel, K, Weidle, E, Lenz, G & Peiffer, J. (1988). [Anesthesia for eye operations in mitochondrial encephalomyelopathy]. *Klin Monatsbl Augenheilkd* **193,** 174-178.

Fu, S, Dean, R, Southan, M & Truscott, R. (1998). The hydroxyl radical in lens nuclear cataractogenesis. *J Biol Chem* **273,** 28603-28609.

Fu, S, Fu, MX, Baynes, JW, Thorpe, SR & Dean, RT. (1998). Presence of dopa and amino acid hydroperoxides in proteins modified with advanced glycation end products (AGEs): amino acid oxidation products as a possible source of oxidative stress induced by AGE proteins. *Biochem J* **330 (Pt 1),** 233-239.

Garland, D. (1990). Role of site-specific, metal-catalyzed oxidation in lens aging and cataract: a hypothesis. *Exp Eye Res* **50,** 677-682.

Garland, DL. (1991). Ascorbic acid and the eye. *Am J Clin Nutr* **54,** 1198S-1202S.

Garner, B, Roberg, K, Qian, M, Eaton, JW & Truscott, RJ. (2000). Distribution of ferritin and redox-active transition metals in normal and cataractous human lenses. *Exp Eye Res* **71,** 599-607.

Garner, MH & Spector, A. (1980). Selective oxidation of cysteine and methionine in normal and senile cataractous lenses. *Proc Natl Acad Sci U S A* **77,** 1274-1277.

Giblin, FJ. (2000). Glutathione: a vital lens antioxidant. *J Ocul Pharmacol Ther* **16,** 121-135.

Giblin, FJ, McCready, JP, Kodama, T & Reddy, VN. (1984). A direct correlation between the levels of ascorbic acid and H2O2 in aqueous humor. *Exp Eye Res* **38,** 87-93.

Giblin, FJ, Padgaonkar, VA, Leverenz, VR, Lin, LR, Lou, MF, Unakar, NJ, Dang, L, Dickerson, JE, Jr. & Reddy, VN. (1995). Nuclear light scattering, disulfide formation and membrane damage in lenses of older guinea pigs treated with hyperbaric oxygen. *Exp Eye Res* **60,** 219-235.

Giblin, FJ, Schrimscher, L, Chakrapani, B & Reddy, VN. (1988). Exposure of rabbit lens to hyperbaric oxygen in vitro: regional effects on GSH level. *Invest Ophthalmol Vis Sci* **29,** 1312-1319.

Glockner, JF, Chan, HC & Swartz, HM. (1991). In vivo oximetry using a nitroxide-liposome system. *Magn Reson Med* **20,** 123-133.

Goda, F, Liu, KJ, Walczak, T, O'Hara, JA, Jiang, J & Swartz, HM. (1995). In vivo oximetry using EPR and India ink. *Magn Reson Med* **33,** 237-245.

Goren, SB & Krause, AC. (1956). The effects of hypoxia and hyperoxia upon the oxygen tension in the vitreous humor of the cat. *Am J Ophthalmol* **42,** 764-769.

Griffiths, MH. (1966). The components of an alpha-glycerophosphate cycle and their relation to oxidative metabolism in the lens. *Biochem J* **99,** 12-21.

Griffiths, MH. (1966). The components of an alpha-glycerophosphate cycle and their relation to oxidative metabolism in the lens. *Biochem J* **99,** 12-21.

Groebe, K & Vaupel, P. (1988). Evaluation of oxygen diffusion distances in human breast cancer xenografts using tumor-specific in vivo data: role of various mechanisms in the development of tumor hypoxia. *Int J Radiat Oncol Biol Phys* **15,** 691-697.

Gross, MW, Karbach, U, Groebe, K, Franko, AJ & Mueller-Klieser, W. (1995). Calibration of misonidazole labeling by simultaneous measurement of oxygen tension and labeling density in multicellular spheroids. *Int J Cancer* **61,** 567-573.

Grote, J, Susskind, R & Vaupel, P. (1977). Oxygen diffusivity in tumor tissue (DS-carcinosarcoma) under temperature conditions within the range of 20--40 degrees C.

Pflugers Arch **372,** 37-42.

Hagen, TM, Wehr, CM & Ames, BN. (1998). Mitochondrial decay in aging. Reversal through supplementation of acetyl-L-carnitine and N-tert-butyl-alpha-phenyl-nitrone. *Ann N Y Acad Sci* **854,** 214-223.

Hahn, U, Swanson, AA & Hockwin, O. (1976). Age-related changes in the proteolytic enzymes of mammalian lens. *Albrecht Von Graefes Arch Klin Exp Ophthalmol* **199,** 197-206.

Hail, N, Jr. & Lotan, R. (2002). Examining the role of mitochondrial respiration in vanilloid-induced apoptosis. *J Natl Cancer Inst* **94,** 1281-1292.

Hale, LP, Braun, RD, Gwinn, WM, Greer, PK & Dewhirst, MW. (2002). Hypoxia in the thymus: role of oxygen tension in thymocyte survival. *Am J Physiol Heart Circ Physiol* **282,** H1467-1477.

Halliwell, B. (2001). Vitamin C and genomic stability. *Mutat Res* **475,** 29-35.

Hans, W, Hockwin, O & Kleifeld, O. (1955). Die bestimmung des sauerstoffverbrauches der linse auf polarographischem wege. *v Graefe's Arch Ophthal* **157,** 72-84.

Harding, J. (1991). *Cataract. Biochemistry, epidemiology and pharmacology*. Chapman and Hall, London.

Heald, L. (1956). Permeability of the cornea and the blood-aqueous barrier to oxygen. *Br J Ophthalmol* **40,** 705.

Helbig, H, Hinz, JP, Kellner, U & Foerster, MH. (1993). Oxygen in the anterior chamber of the human eye. *Ger J Ophthalmol* **2,** 161-164.

Helbig, H, Schlotzer-Schrehardt, U, Noske, W, Kellner, U, Foerster, MH & Naumann, GO. (1994). Anterior-chamber hypoxia and iris vasculopathy in pseudoexfoliation syndrome. *Ger J Ophthalmol* **3,** 148-153.

Himmelblau, D. (1964). Diffusion of dissolved gases in liquids. *Chemical Review* **64,** 527-550.

Hitchman, M. (1978). *Measurement of dissolved oxygen*. John Wiley and Sons, New York.

Hockwin, O. (1971). Age changes of lens metabolism. *Altern Entwickl Aging Dev* **1,** 95-129.

Hood, J & Hodges, RE. (1969). Ocular lesions in scurvy. *Am J Clin Nutr* **22,** 559-567.

Hoper, J, Funk, R, Zagorski, Z & Rohen, JW. (1989). Oxygen delivery to the anterior chamber of the eye--a novel function of the anterior iris surface. *Curr Eye Res* **8,** 649-659.

Howard-Flanders, P & Pirie, A. (1957). The effect of breathing oxygen on the radiosensitivity of the rabbit lens and the use of oxygen in x-ray therapy. *Radiat Res* **7,** 357-364.

Huang, E, Zhang, Meriam, Dillon. (2001). The diffusion of oxygen in the mammalian lens. *Investigative Ophthalmology and Visual Science, ARVO abstract #1538* **42,** S284.

Hulbert, AJ, Augee, ML & Raison, JK. (1976). The influence of thyroid hormones on the structure and function of mitochondrial membranes. *Biochim Biophys Acta* **455,** 597-601.

Isashiki, Y, Nakagawa, M, Ohba, N, Kamimura, K, Sakoda, Y, Higuchi, I, Izumo, S & Osame, M. (1998). Retinal manifestations in mitochondrial diseases associated with mitochondrial DNA mutation. *Acta Ophthalmol Scand* **76,** 6-13.

Ishizaki, Y, Jacobson, MD & Raff, MC. (1998). A role for caspases in lens fiber differentiation. *J Cell Biol* **140,** 153-158.

Jacobi, KW. (1965). [a Method for Continuous Oxygen Determination in the Aqueous Humor and Vitreous Humor of the Living Eye]. *Albrecht Von Graefes Arch Ophthalmol* **168,** 61-69.

Jacobi, KW. (1966). [Continuous measurement of oxygen partial pressure in the anterior chamber of the living rabbit eye]. *Albrecht Von Graefes Arch Klin Exp Ophthalmol* **169,** 350-356.

Jacobi, KW. (1968). [Measurements of the partial pressure of oxygen in the aqueous humor during exposure to different gas mixtures]. *Albrecht Von Graefes Arch Klin Exp Ophthalmol* **174,** 321-325.

Jacobi, KW & Driest, J. (1966). [Oxygen determinations in the vitreous body of the living eye]. *Ber Zusammenkunft Dtsch Ophthalmol Ges* **67,** 193-198.

Jaksch, M, Lochmuller, H, Schmitt, F, Volpel, B, Obermaier-Kusser, B & Horvath, R. (2001). A mutation in mt tRNALeu(UUR) causing a neuropsychiatric syndrome with depression and cataract. *Neurology* **57,** 1930-1931.

Javitt, JC, Wang, F & West, SK. (1996). Blindness due to cataract: epidemiology and prevention. *Annu Rev Public Health* **17,** 159-177.

Jiang, J, Nakashima, T, Liu, KJ, Goda, F, Shima, T & Swartz, HM. (1996). Measurement of PO2 in liver using EPR oximetry. *J Appl Physiol* **80,** 552-558.

Kaanders, JH, Wijffels, KI, Marres, HA, Ljungkvist, AS, Pop, LA, van den Hoogen, FJ, de Wilde, PC, Bussink, J, Raleigh, JA & van der Kogel, AJ. (2002). Pimonidazole binding and tumor vascularity predict for treatment outcome in head and neck cancer. *Cancer Res* **62,** 7066-7074.

Kannan, R, Stolz, A, Ji, Q, Prasad, PD & Ganapathy, V. (2001). Vitamin C transport in human lens epithelial cells: evidence for the presence of SVCT2. *Exp Eye Res* **73,** 159-165.

Kaufman, A, ed. (2003). *Adler's physiology of the eye*. 10th Ed. Mosby, St Louis.

Kennaway, NG, Carrero-Valenzuela, RD, Ewart, G, Balan, VK, Lightowlers, R, Zhang, YZ, Powell, BR, Capaldi, RA & Buist, NR. (1990). Isoforms of mammalian cytochrome c oxidase: correlation with human cytochrome c oxidase deficiency. *Pediatr Res* **28,** 529-535.

Kern, HL. (1962). Accumulation of amino acids by calf lens. *Invest Ophthalmol* **1,** 368-376.

Kessler, A, ed. (1973). *Oxygen supply: theoretical and practical aspects of oxygen supply and microcirculation of tissue*. Urban and Schwarzenberg, Munich.

Kinoshita, JH, Kern, HL & Merola, LO. (1961). Factors affecting the cation transport of calf lens. *Biochim Biophys Acta* **47,** 458-466.

Kleifeld, N. (1959). Der Sauerstoffgehalt des menschlichen Kammerwassers. *Klin Monatsbl Augenheilkd* **135,** 224-226.

Klein, BE, Klein, R & Lee, KE. (1998). Diabetes, cardiovascular disease, selected cardiovascular disease risk factors, and the 5-year incidence of age-related cataract and progression of lens opacities: the Beaver Dam Eye Study. *Am J Ophthalmol* **126,** 782-790.

Koskela, TK, Reiss, GR, Brubaker, RF & Ellefson, RD. (1989). Is the high concentration of ascorbic acid in the eye an adaptation to intense solar irradiation? *Invest Ophthalmol Vis Sci* **30,** 2265-2267.

Kuchle, M, Brenner, PM, Engelhardt, A & Naumann, GO. (1990). [Ocular changes in MELAS syndrome]. *Klin Monatsbl Augenheilkd* **197,** 258-264.

Kwan, M, Niinikoski, J & Hunt, TK. (1972). In vivo measurements of oxygen tension in the cornea, aqueous humor, and anterior lens of the open eye. *Invest Ophthalmol* **11,** 108-114.

Lakowicz, JR, Szmacinski, H, Nowaczyk, K, Berndt, KW & Johnson, M. (1992). Fluorescence lifetime imaging. *Anal Biochem* **202,** 316-330.

Landers, MB, 3rd, Stefansson, E & Wolbarsht, ML. (1982). Panretinal photocoagulation and retinal oxygenation. *Retina* **2,** 167-175.

Lane, N. (2002). *Oxygen. The molecule that made the world*. Oxford University Press, New York.

Leary, SC, Battersby, BJ, Hansford, RG & Moyes, CD. (1998). Interactions between

bioenergetics and mitochondrial biogenesis. *Biochim Biophys Acta* **1365,** 522-530.

Leaver, PK, Grey, RH & Garner, A. (1979). Silicone oil injection in the treatment of massive preretinal retraction. II. Late complications in 93 eyes. *Br J Ophthalmol* **63,** 361-367.

Liang, WJ, Johnson, D & Jarvis, SM. (2001). Vitamin C transport systems of mammalian cells. *Mol Membr Biol* **18,** 87-95.

Lide, D, ed. (1993). *Handbook of chemistry and physics*. CRC Press, Boca Raton.

Linke, W. (1965). *Inorganic and metal-organic compounds*. American Chemical Society, Washington DC.

Linsenmeier, RA, Goldstick, TK, Blum, RS & Enroth-Cugell, C. (1981). Estimation of retinal oxygen transients from measurements made in the vitreous humor. *Exp Eye Res* **32,** 369-379.

Linsenmeier, RA & Padnick-Silver, L. (2000). Metabolic dependence of photoreceptors on the choroid in the normal and detached retina. *Invest Ophthalmol Vis Sci* **41,** 3117-3123.

Linsenmeier, RA & Yancey, CM. (1989). Effects of hyperoxia on the oxygen distribution in the intact cat retina. *Invest Ophthalmol Vis Sci* **30,** 612-618.

Liu, KJ, Gast, P, Moussavi, M, Norby, SW, Vahidi, N, Walczak, T, Wu, M & Swartz, HM. (1993). Lithium phthalocyanine: a probe for electron paramagnetic resonance oximetry in viable biological systems. *Proc Natl Acad Sci U S A* **90,** 5438-5442.

Los, LI, Van Der Worp, RJ, Van Luyn, MJ & Hooymans, JM. (2004). Presence of Collagen IV in the Ciliary Zonules of the Human Eye: An Immunohistochemical Study by LM and TEM. *J Histochem Cytochem* **52,** 789-795.

Ly, JD & Lawen, A. (2003). Transplasma membrane electron transport: enzymes involved and biological function. *Redox Rep* **8,** 3-21.

Maeda, N & Tano, Y. (1996). Intraocular oxygen tension in eyes with proliferative diabetic retinopathy with and without vitreous. *Graefes Arch Clin Exp Ophthalmol* **234 Suppl 1,** S66-69.

Marcantonio, JM, Duncan, G, Davies, PD & Bushell, AR. (1980). Classification of human senile cataracts by nuclear colour and sodium content. *Exp Eye Res* **31,** 227-237.

Marusich, MF, Robinson, BH, Taanman, JW, Kim, SJ, Schillace, R, Smith, JL & Capaldi, RA. (1997). Expression of mtDNA and nDNA encoded respiratory chain proteins in chemically and genetically-derived Rho0 human fibroblasts: a comparison of subunit proteins in normal fibroblasts treated with ethidium bromide and fibroblasts from a patient with mtDNA depletion syndrome. *Biochim Biophys Acta* **1362,** 145-159.

Mathias, RT, Rae, JL & Baldo, GJ. (1997). Physiological properties of the normal lens. *Physiol Rev* **77,** 21-50.

Maurice, DM. (1998). The Von Sallmann Lecture 1996: an ophthalmological explanation of REM sleep. *Exp Eye Res* **66,** 139-145.

McCarty, C. (1999). The epidemiology of cataract in Australia. *American Journal of Ophthalmology* **128,** 446-465.

McLaren, JW, Dinslage, S, Dillon, JP, Roberts, JE & Brubaker, RF. (1998). Measuring oxygen tension in the anterior chamber of rabbits. *Invest Ophthalmol Vis Sci* **39,** 1899-1909.

McNamara, M & Augusteyn, RC. (1984). The effects of hydrogen peroxide on lens proteins: a possible model for nuclear cataract. *Exp Eye Res* **38,** 45-56.

McNeil, JJ, Robman, L, Tikellis, G, Sinclair, MI, McCarty, CA & Taylor, HR. (2004). Vitamin E supplementation and cataract: randomized controlled trial. *Ophthalmology* **111,** 75-84.

Melberg, NS & Thomas, MA. (1995). Nuclear sclerotic cataract after vitrectomy in patients younger than 50 years of age. *Ophthalmology* **102,** 1466-1471.

Minassian, DC & Mehra, V. (1990). 3.8 million blinded by cataract each year: projections from the first epidemiological study of incidence of cataract blindness in India. *Br J Ophthalmol* **74,** 341-343.

Miyazawa. (1981). Experimental study on the partial pressure of oxygen in the vitreous body. *Folia Ophthalmol Japan* **32,** 2027-2036.

Modak, SP & Bollum, FJ. (1972). Detection and measurement of single-strand breaks in nuclear DNA in fixed lens sections. *Exp Cell Res* **75,** 307-313.

Moffat, BA, Landman, KA, Truscott, RJ, Sweeney, MH & Pope, JM. (1999). Age-related changes in the kinetics of water transport in normal human lenses. *Exp Eye Res* **69,** 663-669.

Molnar, I, Poitry, S, Tsacopoulos, M, Gilodi, N & Leuenberger, PM. (1985). Effect of laser photocoagulation on oxygenation of the retina in miniature pigs. *Invest Ophthalmol Vis Sci* **26,** 1410-1414.

Mosewich, RK, Donat, JR, DiMauro, S, Ciafaloni, E, Shanske, S, Erasmus, M & George, D. (1993). The syndrome of mitochondrial encephalomyopathy, lactic acidosis, and strokelike episodes presenting without stroke. *Arch Neurol* **50,** 275-278.

Mueller-Klieser, W, Schlenger, KH, Walenta, S, Gross, M, Karbach, U, Hoeckel, M &

Vaupel, P. (1991). Pathophysiological approaches to identifying tumor hypoxia in patients. *Radiother Oncol* **20 Suppl 1,** 21-28.

Nishikimi, M & Yagi, K. (1991). Molecular basis for the deficiency in humans of gulonolactone oxidase, a key enzyme for ascorbic acid biosynthesis. *Am J Clin Nutr* **54,** 1203S-1208S.

Nordsmark, M, Loncaster, J, Chou, SC, Havsteen, H, Lindegaard, JC, Davidson, SE, Varia, M, West, C, Hunter, R, Overgaard, J & Raleigh, JA. (2001). Invasive oxygen measurements and pimonidazole labeling in human cervix carcinoma. *Int J Radiat Oncol Biol Phys* **49,** 581-586.

North, K, Korson, MS, Krawiecki, N, Shoffner, JM & Holm, IA. (1996). Oxidative phosphorylation defect associated with primary adrenal insufficiency. *J Pediatr* **128,** 688-692.

Novak, MA, Rice, TA, Michels, RG & Auer, C. (1984). The crystalline lens after vitrectomy for diabetic retinopathy. *Ophthalmology* **91,** 1480-1484.

Ohrloff, C & Hockwin, O. (1983). Lens metabolism and aging: enzyme activities and enzyme alterations in lenses of different species during the process of aging. *J Gerontol* **38,** 271-277.

O'Riordan, TC, Buckley, D, Ogurtsov, V, O'Connor, R & Papkovsky, DB. (2000). A cell viability assay based on monitoring respiration by optical oxygen sensing. *Anal Biochem* **278,** 221-227.

Ormerod, LD, Edelstein, MA, Schmidt, GJ, Juarez, RS, Finegold, SM & Smith, RE. (1987). The intraocular environment and experimental anaerobic bacterial endophthalmitis. *Arch Ophthalmol* **105,** 1571-1575.

Padgaonkar, VA, Lin, LR, Leverenz, VR, Rinke, A, Reddy, VN & Giblin, FJ. (1999). Hyperbaric oxygen in vivo accelerates the loss of cytoskeletal proteins and MIP26 in guinea pig lens nucleus. *Exp Eye Res* **68,** 493-504.

Pakalnis, VA, Wolbarsht, ML & Landers, MB, 3rd. (1988). Phenylephrine-induced anterior chamber hypoxia. *Ann Ophthalmol* **20,** 267-270.

Palmquist, BM, Philipson, B & Barr, PO. (1984). Nuclear cataract and myopia during hyperbaric oxygen therapy. *Br J Ophthalmol* **68,** 113-117.

Parliament, MB, Wiebe, LI & Franko, AJ. (1992). Nitroimidazole adducts as markers for tissue hypoxia: mechanistic studies in aerobic normal tissues and tumour cells. *Br J Cancer* **66,** 1103-1108.

Paterson, CA. (1969). Distribution of sodium and potassium in ox lenses. *Experimental Eye Research* **8,** 442.

Pepin, B, Mikol, J, Goldstein, B, Aron, JJ & Lebuisson, DA. (1980). Familial mitochondrial myopathy with cataract. *J Neurol Sci* **45,** 191-203.

Pierscionek BK & Chan DY (1989). Refractive index gradient of human lenses. *Optom Vis Sci* **66,** 822-9.

Pitkanen, S, Merante, F, McLeod, DR, Applegarth, D, Tong, T & Robinson, BH. (1996). Familial cardiomyopathy with cataracts and lactic acidosis: a defect in complex I (NADH-dehydrogenase) of the mitochondria respiratory chain. *Pediatr Res* **39,** 513-521.

Poot M, Zhang YZ, Kramer JA, Wells KS, Jones LJ, Hanzel DK, et al. (1996). Analysis of mitochondrial morphology and function with novel fixable fluorescent stains. *J Histochem Cytochem* **44,** 1363-72.

Pournaras, CJ, Riva, CE, Tsacopoulos, M & Strommer, K. (1989). Diffusion of O2 in the retina of anesthetized miniature pigs in normoxia and hyperoxia. *Exp Eye Res* **49,** 347-360.

Raleigh, JA, Chou, SC, Arteel, GE & Horsman, MR. (1999). Comparisons among pimonidazole binding, oxygen electrode measurements, and radiation response in C3H mouse tumors. *Radiat Res* **151,** 580-589.

Raleigh, JA, Chou, SC, Bono, EL, Thrall, DE & Varia, MA. (2001). Semiquantitative immunohistochemical analysis for hypoxia in human tumors. *Int J Radiat Oncol Biol Phys* **49,** 569-574.

Rao, PV, Maddala, R, John, F & Zigler, JS, Jr. (2004). Expression of nonphagocytic NADPH oxidase system in the ocular lens. *Mol Vis* **10,** 112-121.

Reddy, VN, Giblin, FJ, Lin, LR & Chakrapani, B. (1998). The effect of aqueous humor ascorbate on ultraviolet-B-induced DNA damage in lens epithelium. *Invest Ophthalmol Vis Sci* **39,** 344-350.

Reiss, GR, Werness, PG, Zollman, PE & Brubaker, RF. (1986). Ascorbic acid levels in the aqueous humor of nocturnal and diurnal mammals. *Arch Ophthalmol* **104,** 753-755.

Retsky, KL, Freeman, MW & Frei, B. (1993). Ascorbic acid oxidation product(s) protect human low density lipoprotein against atherogenic modification. Anti- rather than prooxidant activity of vitamin C in the presence of transition metal ions. *J Biol Chem* **268,** 1304-1309.

Roberts, H, Atherton, Dillon. (1992). A non-invasive method to detect oxygen tension in the lens. *Investigative Ophthalmoogy and Visual Science. ARVO abstract #537* **33,** S799.

Roetman, EL. (1974). Oxygen gradients in the anterior chamber of anesthetized rabbits. *Invest Ophthalmol* **13,** 386-389.

Rolfe, DF & Brown, GC. (1997). Cellular energy utilization and molecular origin of standard metabolic rate in mammals. *Physiol Rev* **77,** 731-758.

Rubin, ML. (1993). *Optics for clinicians*. Triad Publishing Company, Gainesville.

Rummelt, V, Folberg, R, Ionasescu, V, Yi, H & Moore, KC. (1993). Ocular pathology of MELAS syndrome with mitochondrial DNA nucleotide 3243 point mutation. *Ophthalmology* **100,** 1757-1766.

Sakaue, H, Negi, A & Honda, Y. (1989). Comparative study of vitreous oxygen tension in human and rabbit eyes. *Invest Ophthalmol Vis Sci* **30,** 1933-1937.

Sakaue, H, Tsukahara, Y, Negi, A, Ogino, N & Honda, Y. (1989). Measurement of vitreous oxygen tension in human eyes. *Jpn J Ophthalmol* **33,** 199-203.

Sastre, J, Pallardo, FV & Vina, J. (2000). Mitochondrial oxidative stress plays a key role in aging and apoptosis. *IUBMB Life* **49,** 427-435.

Seddon, BM, Honess, DJ, Vojnovic, B, Tozer, GM & Workman, P. (2001). Measurement of tumor oxygenation: in vivo comparison of a luminescence fiber-optic sensor and a polarographic electrode in the p22 tumor. *Radiat Res* **155,** 837-846.

Sengers, RC, Stadhouders, AM, van Lakwijk-Vondrovicova, E, Kubat, K & Ruitenbeek, W. (1985). Hypertrophic cardiomyopathy associated with a mitochondrial myopathy of voluntary muscles and congenital cataract. *Br Heart J* **54,** 543-547.

Sengers, RC, Trijbels, JM, Willems, JL, Daniels, O & Stadhouders, AM. (1975). Congenital cataract and mitochondrial myopathy of skeletal and heart muscle associated with lactic acidosis after exercise. *J Pediatr* **86,** 873-880.

Servidei, S, Zeviani, M, Manfredi, G, Ricci, E, Silvestri, G, Bertini, E, Gellera, C, Di Mauro, S, Di Donato, S & Tonali, P. (1991). Dominantly inherited mitochondrial myopathy with multiple deletions of mitochondrial DNA: clinical, morphologic, and biochemical studies. *Neurology* **41,** 1053-1059.

Severinghaus, JW. (2002). Priestley, the furious free thinker of the enlightenment, and Scheele, the taciturn apothecary of Uppsala. *Acta Anaesthesiol Scand* **46,** 2-9.

Shen, J, Khan, N, Lewis, LD, Armand, R, Grinberg, O, Demidenko, E & Swartz, H. (2003). Oxygen consumption rates and oxygen concentration in molt-4 cells and their mtDNA depleted (rho0) mutants. *Biophys J* **84,** 1291-1298.

Shonat, RD & Kight, AC. (2003). Oxygen tension imaging in the mouse retina. *Ann Biomed Eng* **31,** 1084-1096.

Shoubridge, EA. (2001). Nuclear genetic defects of oxidative phosphorylation. *Hum Mol Genet* **10,** 2277-2284.

Sidell, BD. (1998). Intracellular oxygen diffusion: the roles of myoglobin and lipid at cold body temperature. *J Exp Biol* **201 (Pt 8),** 1119-1128.

Silver, IA. (1973). The oxygen micro-electrode. *Adv Exp Med Biol* **37A,** 7-15.

Simpson, W, ed. (1989). *The Oxford English dictionary*, vol. XVIII. Clarendon Press, Oxford.

Smirnoff, N. (2000). Ascorbate biosynthesis and function in photoprotection. *Philos Trans R Soc Lond B Biol Sci* **355,** 1455-1464.

Sohal, RS, Ku, HH, Agarwal, S, Forster, MJ & Lal, H. (1994). Oxidative damage, mitochondrial oxidant generation and antioxidant defenses during aging and in response to food restriction in the mouse. *Mech Ageing Dev* **74,** 121-133.

Spector, A. (1984). Oxidation and cataract. *Ciba Found Symp* **106,** 48-64.

Spector, A & Garner, WH. (1981). Hydrogen peroxide and human cataract. *Exp Eye Res* **33,** 673-681.

Sperduto, RD, Hu, TS, Milton, RC, Zhao, JL, Everett, DF, Cheng, QF, Blot, WJ, Bing, L, Taylor, PR, Li, JY & et al. (1993). The Linxian cataract studies. Two nutrition intervention trials. *Arch Ophthalmol* **111,** 1246-1253.

Stefansson, E. (1988). Retinal oxygen tension is higher in light than dark. *Pediatr Res* **23,** 5-8.

Stefansson, E, Foulks, GN & Hamilton, RC. (1987). The effect of corneal contact lenses on the oxygen tension in the anterior chamber of the rabbit eye. *Invest Ophthalmol Vis Sci* **28,** 1716-1719.

Stefansson, E, Hatchell, DL, Fisher, BL, Sutherland, FS & Machemer, R. (1986). Panretinal photocoagulation and retinal oxygenation in normal and diabetic cats. *Am J Ophthalmol* **101,** 657-664.

Stefansson, E, Landers, MB, 3rd & Wolbarsht, ML. (1982). Vitrectomy, lensectomy, and ocular oxygenation. *Retina* **2,** 159-166.

Stefansson, E, Novack, RL & Hatchell, DL. (1990). Vitrectomy prevents retinal hypoxia in branch retinal vein occlusion. *Invest Ophthalmol Vis Sci* **31,** 284-289.

Stefansson, E, Peterson, JI & Wang, YH. (1989). Intraocular oxygen tension measured with a fiber-optic sensor in normal and diabetic dogs. *Am J Physiol* **256,** H1127-1133.

Stefansson, E, Robinson, D, Wolbarsht, ML, Landers, MB, 3rd & Walsh, A. (1983). Effect of epinephrine on PO2 in anterior chamber. *Arch Ophthalmol* **101,** 636-639.

Stryer. (1995). *Biochemistry*. WH Freeman, New York.

Subczynski, WK, Lukiewicz, S & Hyde, JS. (1986). Murine in vivo L-band ESR spin-label oximetry with a loop-gap resonator. *Magn Reson Med* **3,** 747-754.

Swartz, HM. (2002). Measuring real levels of oxygen in vivo: opportunities and challenges. *Biochem Soc Trans* **30,** 248-252.

Swartz, HM & Clarkson, RB. (1998). The measurement of oxygen in vivo using EPR techniques. *Phys Med Biol* **43,** 1957-1975.

Swartz, HM & Dunn, JF. (2003). Measurements of oxygen in tissues: overview and perspectives on methods. *Adv Exp Med Biol* **530,** 1-12.

Sweeney, MH & Truscott, RJ. (1998). An impediment to glutathione diffusion in older normal human lenses: a possible precondition for nuclear cataract. *Exp Eye Res* **67,** 587-595.

Szent-Gyorgi. (1928). observations on the function of peroxidase systems and the chemistry of the adrenal cortex:description of a new carbohydrate derivate. *Biochem J* **22,** 1387-1409.

Taanman, JW, Burton, MD, Marusich, MF, Kennaway, NG & Capaldi, RA. (1996). Subunit specific monoclonal antibodies show different steady-state levels of various cytochrome-c oxidase subunits in chronic progressive external ophthalmoplegia. *Biochim Biophys Acta* **1315,** 199-207.

Talaat, M, Hamdy, H, el-Bagoury, IM, Abdel-Rahman, YM, Makarem, F & el-Shewy, TM. (1974). The effect of short- and long-acting barbiturates on the oxygen uptake of the intact lens and its homogenate. *Exp Eye Res* **18,** 381-382.

Taylor, A & Hobbs, M. (2001). 2001 assessment of nutritional influences on risk for cataract. *Nutrition* **17,** 845-857.

Thierbach, G & Reichenbach, H. (1981). Myxothiazol, a new inhibitor of the cytochrome b-c1 segment of th respiratory chain. *Biochim Biophys Acta* **638,** 282-289.

Thylefors, N, Pararajasegaram, Dadzie. (1995). Global data on blindness. *Bull World Health Organ* **73,** 115-121.

Toppet, M, Telerman-Toppet, N, Szliwowski, HB, Vainsel, M & Coers, C. (1977). Oculocraniosomatic neuromuscular disease with hypoparathyroidism. *Am J Dis Child* **131,** 437-441.

Toth, I, Rogers, JT, McPhee, JA, Elliott, SM, Abramson, SL & Bridges, KR. (1995). Ascorbic acid enhances iron-induced ferritin translation in human leukemia and hepatoma

cells. *J Biol Chem* **270,** 2846-2852.

Trayhurn, P & Van Heyningen, R. (1971). Aerobic metabolism in the bovine lens. *Exp Eye Res* **12,** 315-327.

Trifunovic, A, Wredenberg, A, Falkenberg, M, Spelbrink, JN, Rovio, AT, Bruder, CE, Bohlooly, YM, Gidlof, S, Oldfors, A, Wibom, R, Tornell, J, Jacobs, HT & Larsson, NG. (2004). Premature ageing in mice expressing defective mitochondrial DNA polymerase. *Nature* **429,** 417-423.

Truscott, RJ. (2000). Age-related nuclear cataract: a lens transport problem. *Ophthalmic Res* **32,** 185-194.

Truscott, RJ. (2003). Human cataract: the mechanisms responsible; light and butterfly eyes. *Int J Biochem Cell Biol* **35,** 1500-1504.

Truscott, RJ & Augusteyn, RC. (1977). Oxidative changes in human lens proteins during senile nuclear cataract formation. *Biochim Biophys Acta* **492,** 43-52.

Truscott, RJ & Augusteyn, RC. (1977). The state of sulphydryl groups in normal and cataractous human lenses. *Exp Eye Res* **25,** 139-148.

Tsacopoulos, M, Baker, R & Levy, S. (1976). Studies on retinal oxygenation. *Adv Exp Med Biol* **75,** 413-416.

Tune, JD, Richmond, KN, Gorman, MW & Feigl, EO. (2002). Control of coronary blood flow during exercise. *Exp Biol Med (Maywood)* **227,** 238-250.

Uyama, C. (1973). Diffusion model of a cat eye. In *Oxygen supply: theoretical and practical aspects of oxygen supply and microcirculation of tissue*. ed. Kessler, pp. 64. Urban and Schwarzenberg, Munich.

Valsson, J, Laxdal, T, Jonsson, A, Jansson, KK & Helgason, H. (1988). Congenital cardiomyopathy and cataracts with lactic acidosis. *Am J Cardiol* **61,** 193-194.

Van Effenterre, G, Ameline, B, Campinchi, F, Quesnot, S, Le Mer, Y & Haut, J. (1992). [Is vitrectomy cataractogenic? Study of changes of the crystalline lens after surgery of retinal detachment]. *J Fr Ophtalmol* **15,** 449-454.

van Ekeren, GJ, Stadhouders, AM, Egberink, GJ, Sengers, RC, Daniels, O & Kubat, K. (1987). Hereditary mitochondrial hypertrophic cardiomyopathy with mitochondrial myopathy of skeletal muscle, congenital cataract and lactic acidosis. *Virchows Arch A Pathol Anat Histopathol* **412,** 47-52.

van Ekeren, GJ, Stadhouders, AM, Smeitink, JA & Sengers, RC. (1993). A retrospective study of patients with the hereditary syndrome of congenital cataract, mitochondrial myopathy of heart and skeletal muscle and lactic acidosis. *Eur J Pediatr* **152,** 255-259.

Van Heyningen, R. (1965). The metabolism of glucose by the rabbit lens in the presence and absence of oxygen. *Biochem J* **96,** 419-431.

van Heyningen, R & Linklater, J. (1975). The metabolism of the bovine lens in air and nitrogen. *Exp Eye Res* **20,** 393-396.

Van Lieshout, JJ, Wieling, W, Karemaker, JM & Secher, NH. (2003). Syncope, cerebral perfusion, and oxygenation. *J Appl Physiol* **94,** 833-848.

Van Os-Corby, DJ & Chapman, JD. (1986). In vitro binding of 14C-misonidazole to hepatocytes and hepatoma cells. *Int J Radiat Oncol Biol Phys* **12,** 1251-1254.

Van Os-Corby, DJ, Koch, CJ & Chapman, JD. (1987). Is misonidazole binding to mouse tissues a measure of cellular pO2? *Biochem Pharmacol* **36,** 3487-3494.

Vanderkooi, JM, Erecinska, M & Silver, IA. (1991). Oxygen in mammalian tissue: methods of measurement and affinities of various reactions. *Am J Physiol* **260,** C1131-1150.

Vanderkooi, JM, Maniara, G, Green, TJ & Wilson, DF. (1987). An optical method for measurement of dioxygen concentration based upon quenching of phosphorescence. *J Biol Chem* **262,** 5476-5482.

Vanderkooi, JM, Maniara, G, Green, TJ & Wilson, DF. (1987). An optical method for measurement of dioxygen concentration based upon quenching of phosphorescence. *J Biol Chem* **262,** 5476-5482.

Varghese, AJ, Gulyas, S & Mohindra, JK. (1976). Hypoxia-dependent reduction of 1-(2-nitro-1-imidazolyl)-3-methoxy-2-propanol by Chinese hamster ovary cells and KHT tumor cells in vitro and in vivo. *Cancer Res* **36,** 3761-3765.

Varma SD, Chakrapani B & Reddy VN (1970). Intraocular transport of myoinositol. II. Accumulation in the rabbit lens in vitro. *Invest Ophthalmol* **9,** 794-800.

Veretout F & Tardieu A (1989). The protein concentration gradient within eye lens might originate from constant osmotic pressure coupled to differential interactive properties of crystallins. *Eur Biophys J* **17,** 61-8.

Wang, U, Coleman, Minang. (1991). A two-dimensional fluorescence lifetime imaging system using a gated image intensifier. *Applied Spectroscopy* **45,** 360-366.

Wegener, JK & Moller, PM. (1971). Oxygen tension in the anterior chamber of the rabbit eye. *Acta Ophthalmol (Copenh)* **49,** 577-584.

West, SK & Valmadrid, CT. (1995). Epidemiology of risk factors for age-related cataract. *Surv Ophthalmol* **39,** 323-334.

WHO/PBL/97.61. (1997). Global initiative for the elimination of avoidable blindness. An informal consultation. (Unpublished document). World Health Organisation, Geneva.

Wilson, CA, Berkowitz, BA, McCuen, BW, 2nd & Charles, HC. (1992). Measurement of preretinal oxygen tension in the vitrectomized human eye using fluorine-19 magnetic resonance spectroscopy. *Arch Ophthalmol* **110,** 1098-1100.

Wilson, DF. (1993). Measuring oxygen using oxygen dependent quenching of phosphorescence: a status report. *Adv Exp Med Biol* **333,** 225-232.

Winkler, BS & Riley, MV. (1991). Relative contributions of epithelial cells and fibers to rabbit lens ATP content and glycolysis. *Invest Ophthalmol Vis Sci* **32,** 2593-2598.

Wolff, SP & Spector, A. (1987). Pro-oxidant activation of ocular reductants. 2. Lens epithelial cell cytotoxicity of a dietary quinone is associated with a stable free radical formed with glutathione in vitro. *Exp Eye Res* **45,** 791-803.

Wolvetang, EJ, Larm, JA, Moutsoulas, P & Lawen, A. (1996). Apoptosis induced by inhibitors of the plasma membrane NADH-oxidase involves Bcl-2 and calcineurin. *Cell Growth Differ* **7,** 1315-1325.

Yokoyama, T, Sasaki, H, Giblin, FJ & Reddy, VN. (1994). A physiological level of ascorbate inhibits galactose cataract in guinea pigs by decreasing polyol accumulation in the lens epithelium: a dehydroascorbate-linked mechanism. *Exp Eye Res* **58,** 207-218.

Yorio, T, Cruz, E & Bentley, PJ. (1979). Aerobic and anaerobic metabolism of the crystalline lens of a poikilotherm; the toad Bufo marinus. *Comp Biochem Physiol B* **62,** 123-126.

Yu, C, Alder. (1990). The response of rat vitreal oxygen tension to stepwise increases in inspired percentage oxygen. *Investigative Ophthalmology and Visual Sciences* **31,** 2493-2499.

Zarina, S, Zhao, HR & Abraham, EC. (2000). Advanced glycation end products in human senile and diabetic cataractous lenses. *Mol Cell Biochem* **210,** 29-34.

Zhao, Y, Richman, A, Storey, C, Radford, NB & Pantano, P. (1999). In situ fiber-optic oxygen consumption measurements from a working mouse heart. *Anal Chem* **71,** 3887-3893.

Zigler JS, Jr., Lucas VA & Du XY (1989). Rhesus monkey lens as an in vitro model for studying oxidative stress. *Invest Ophthalmol Vis Sci* **30,** 2195-9.

Zintz, R & Villiger, W. (1967). [Electron microscopic findings in 3 cases of chronic progressive ocular muscular dystrophy]. *Ophthalmologica* **153,** 439-459.

Zweier, JL & Kuppusamy, P. (1988). Electron paramagnetic resonance measurements of free radicals in the intact beating heart: a technique for detection and characterization of free radicals in whole biological tissues. *Proc Natl Acad Sci U S A* **85,** 5703-5707.